Thesis presented to the Instituto Tecnológico de Aeronáutica, in partial fulfillment of the requirements for the degree of Doctor of Science in the Graduate Program of Physics, Field of Nuclear Physics.

Abigail Rodrigues Castro

0^- BOUND STATE WITH DRESSED QUARK PROPAGATORS IN MINKOWSKI SPACE

Thesis approved in its final version by signatories below:

Prof. Dr. Wayne Leonardo Silva de Paula

Advisor

Profa. Dra. Emília Villani

Pro-Rector of Graduate Courses

Campo Montenegro
São José dos Campos, SP - Brazil
2023

Cataloging-in Publication Data
Documentation and Information Division

Castro, Abigail Rodrigues
0^- BOUND STATE WITH DRESSED QUARK PROPAGATORS IN MINKOWSKI SPACE / Abigail Rodrigues Castro.
São José dos Campos, 2023.
135f.

Thesis of Doctor of Science – Course of Physics. Area of Nuclear Physics – Instituto Tecnológico de Aeronáutica, 2023. Advisor: Prof. Dr. Wayne Leonardo Silva de Paula.

1. Matéria de Quarks. 2. Espaço de Minkowski. 3. Propagadores. 4. Equação de Bethe-Salpeter. 5. Cromodinâmica Quântica. 6. Física de Partículas. 7. Física. I. Instituto Tecnológico de Aeronáutica. II. Title.

BIBLIOGRAPHIC REFERENCE

CASTRO, Abigail Rodrigues. 0^- **BOUND STATE WITH DRESSED QUARK PROPAGATORS IN MINKOWSKI SPACE**. 2023. 135f. Thesis of Doctor of Science – Instituto Tecnológico de Aeronáutica, São José dos Campos.

CESSION OF RIGHTS

AUTHOR'S NAME: Abigail Rodrigues Castro
PUBLICATION TITLE: 0^- BOUND STATE WITH DRESSED QUARK PROPAGATORS IN MINKOWSKI SPACE.
PUBLICATION KIND/YEAR: Thesis / 2023

Abigail Rodrigues Castro
Av. Avião Regente, 25
12227-150 – São José dos Campos–SP

0^- BOUND STATE WITH DRESSED QUARK PROPAGATORS IN MINKOWSKI SPACE

Abigail Rodrigues Castro

Thesis Committee Composition:

Prof. Dr.	Brett Vern Carlson	Presidente	-	ITA
Prof. Dr.	Wayne Leonardo Silva de Paula	Advisor	-	ITA
Prof. Dr.	Franciole da Cunha Marinho	Membro Interno	-	ITA
Prof. Dr.	Jaume Carbonell	Membro Externo	-	CNRS/IJCLab
Prof. Dr.	Dyana Cristine Duarte	Membro Externo	-	UFSM

ITA

To my sisters,

Adália, Karoliny and Karina.

Acknowledgments

In those four years of doctoral work, I had many challenges. Coming to the end of this journey makes my heart forever grateful to all of whom stayed with me and helped me to achieve such an important step in my career.

My special gratitude to God, whom I believe gives and bless us with everything. Particularly, I dedicated this outcome to my father, who passed away in the first year of my doctoral studies. He was the major champion of my dreams and my studies in physics, he always was proud of me. As well as to my mother, whom always takes care of me in her mindful and sincere ways, her faithful love and trust give me peace.

Then, I would like to thank my Advisor Wayne. His gentle and patient guidance was crucial to the development of this work and also gave me encouragement to always have a more positive outlook in the entire process. I hope to always follow his example in my professional conduct in the years to come.

I am thankful for always having the companionship of my sisters, friends and cats. Also, I am grateful for having my colleagues and professors collaborations in my studies and work. I would like to thank CAPES for the financial support provided and ITA for having me in its graduate program in Physics.

"He existed before anything else, and he holds all creation together."
— Colossians 1:17

Resumo

Este trabalho analisa o efeito de vestir o propagador de quarks na formação do estado ligado no espaço de Minkowski. A equação de Bethe-Salpeter é resolvida, para um estado ligado de férmion-antifermion 0^- interagindo através de uma troca de bósons vetoriais na aproximação tipo escada, usando um propagador de quark vestido com uma função de massa fenomenológica ajustada aos cálculos QCD da rede. O modelo desenvolvido contém três escalas gluônicas: a massa efetiva do glúon $\sim \Lambda_{QCD}$, o tamanho do vértice quark-gluon estendido ~ 2 fm, e a vestimenta do propagador de quarks. Quantidades estáticas e dinâmicas que caracterizam o estado ligado são calculadas e os efeitos dessas escalas na dinâmica do sistema ligado são discutidos. Em especial, para o caso do quark com massa "bare" leve, uma mudança de hierarquia entre a constante de acoplamento do modelo de massa vestida do quark e do caso de massa fixa é vista conforme o valor da massa de estado ligado M varia. O aumento mais lento da constante de acoplamento do modelo de massa vestida quando comparado com o aumento da constante de acoplamento do modelo de massa fixa, de acordo com que a "binding" cresce, reflete a interação entre as três escalas gluônicas. As amplitudes da frente de luz e as distribuições longitudinal e transversal do momento de valência são analisadas para duas massas de estado ligado diferentes, $M = 653$ MeV e $M = 447$ MeV, com ou sem efeitos de vestimenta. Mostra-se que, no modelo de quarks vestidos, essas distribuições de momento decaem mais lentamente para momentos transversais altos quando comparadas ao modelo de massa de quark fixa igual à massa infravermelha de 344 MeV. Em particular, para os dois modelos é observado que a componente de spin alinhado da função de onda de valência é suprimida em relação a componente anti-alinhada.

Abstract

This work analyzes the effect of dressing the quark propagator in the bound state formation in Minkowski space. The Bethe-Salpeter equation is solved, for a 0^- fermion-antifermion bound state interacting through a vector boson exchange in the ladder approximation, using a dressed quark propagator with a phenomenological running mass function fitted to Lattice QCD calculations. The developed model contains three gluonic scales: the effective gluon mass $\sim \Lambda_{QCD}$, the size of the extended quark-gluon vertex ~ 2 fm, and the dressing of the quark propagator. Static and dynamical quantities that characterize the bound state are calculated and the effects of those scales in the dynamics of the bound system are discussed. In special, for the light quark mass case, a change of hierarchy between the coupling constant of the running quark mass model and of the fixed mass case is seen as the value of bound state mass M varies. The running mass coupling constant slower increase when compared with the increase of the fixed mass model coupling constant with the binding growth reflects the interplay between the three gluonic scales. The light-front amplitudes and the longitudinal and transverse valence momentum distributions are analyzed for two different bound state masses, $M = 653$ MeV and $M = 447$ MeV, with or without dressing effects. It is shown that, in the quark dressing model, those momentum distributions decay slower for high transverse momentum when compared to the case of an undressed one with a fixed quark mass equal to the Infrared mass of 344 MeV. In particular, either for the fixed mass model or running mass function model, the aligned spin component of the valence wave function is suppressed with respect to the anti-aligned one.

List of Figures

List of Tables

List of Abbreviations and Acronyms

BS	Bethe-Salpeter
DS	Dyson-Schwinger
DCSB	Dynamical Chiral Symmetry Breaking
GPDs	Generalized Parton Distributions
IR	Infrared
LF	Light-Front
LHS	Left-Hand Side
LQCD	Lattice Quantum Chromodynamics
NIR	Nakanishi Integral Representation
NWF	Nakanishi Weight Function
PDFs	Parton Momentum Distributions Functions
PTIR	Perturbation Theory Integral Representation
QCD	Quantum Chromodynamics
QED	Quantum Electrodynamics
QFT	Quantum Field Theory
RHS	Right-Hand Side
SM	Standard Model
TMDs	Transverse Momentum Distributions

Contents

1 Introduction

In 1935, Hideki Yukawa predicted the existence of mesons as mediator particles that are responsible for the strong interactions between hadrons (YUKAWA, 1935). Nonetheless, only in 1947 and 1950 that the charged and neutral pion, the mesons foretold by Yukawa, was experimentally first seen (LATTES *et al.*, 1947; BJORKLUND *et al.*, 1950; STEINBERGER *et al.*, 1950).

Hadrons are by concept non-elementary particles. In this aspect, the pion is a hadronic particle composed by a quark and anti-quark bound states. On the other hand, it is also accepted that the pion is a Nambu-Goldstone boson, which means that pion comes into existence by the spontaneous breaking of the chiral symmetry (NAMBU, 1960; GOLDSTONE, 1961). The chiral symmetry is the invariance under parity transformation and when it is dynamically broken the result is the manifestations of non-vanishing masses of nonpertubative origin (HORN; ROBERTS, 2016).

In particular, quarks and gluons are the building blocks of the baryonic matter. They carry color fundamental degrees of freedom, where the color confinement reflects the fact we didn't detect isolated colored particles in nature. This leads to an indirect measurement of quark mass since they are confined to other particles. Quarks are fermions and six types of them are known: up, charm, top, down, strange, and bottom. Their characteristics are given by their mass, electric charge, baryonic number, strangeness number, and charm number. By the number of quarks, one can classify the hadrons as baryons (three valence quarks) and mesons (a valence quark and an antiquark) (BELYAEV; ROSS, 2021).

The hadronic matter and its phenomena can be understood in the framework of the Standard Model. Within it, Quantum Chromodynamics (QCD) describes the interactions between quarks and gluons and is a tool to explain interesting phenomena, e.g. asymptotic freedom, confinement, and chiral symmetry breaking. To understand better hadrons as protons or pions, we need to understand quarks and gluons dynamics. In fact, efforts have been made to obtain a three-dimensional tomograph, in terms of QCD's quarks and gluons, of the hadron's structure. This 3D image can be obtained by such observables as the Generalized Parton Distributions (GPDs) and Transverse-Momentum Distributions (TMDs) (ACCARDI *et al.*, 2023), which are experimentally probed by Deeply

Virtual Compton Scattering (DVCS) and Semi-Inclusive Deep Inelastic Scattering (SIDIS) (FANELLI *et al.*, 2016; BACCHETTA, 2016; PASQUINI, 2020; KAUR *et al.*, 2020). In special, a new generation of colliders are being made with the purpose to access the inner structure of hadrons (ARBUZOV *et al.*, 2021; KHALEK *et al.*, 2022; CHAPON *et al.*, 2022).

A phenomenological study of quarks and gluons bound-states in the Minkowski space is necessary for a better understanding of the structure of the hadrons. One way to do that is through the Bethe-Salpeter (BS) formalism. The BS approach is a tool to study the properties of the relativistic few-body systems (SALPETER; BETHE, 1951). In special, as it is developed in the Minkowski space, it gives a suitable framework to study the hadronic phenomena (CARBONELL; KARMANOV, 2010; CARBONELL; KARMANOV, 2016; CASTRO *et al.*, 2019).

In literature, this formalism has been applied with success for the description of a two-scalar bound-state (KUSAKA *et al.*, 1997; CARBONELL; KARMANOV, 2010; FREDERICO *et al.*, 2014; GUTIERREZ *et al.*, 2016; PIMENTEL; PAULA, 2016), two fermions bound-state (CARBONELL; KARMANOV, 2010; PAULA *et al.*, 2016; SALMÈ *et al.*, 2017), scalar-fermion bound-state (NORONHA *et al.*, 2023). Additionally, pion observables were obtained within the BS framework,i.e. electromagnetic form-factors (YDREFORS *et al.*, 2021), the light-front momentum distributions (PAULA *et al.*, 2021), the parton distribution functions (PAULA *et al.*, 2022) and the unpolarized transverse-momentum dependent distribution functions (YDREFORS *et al.*, 2023).

Moreover, to solve the BS equation one can use the Nakanishi Integral Representation (NIR) to the components of the BS amplitude, which gives them an explicit analytical structure in terms of the external momenta, allowing the treatment of singularities and making easier to do the projection onto the Light-Front (NAKANISHI, 1963; NAKANISHI, 1969; BAKKER *et al.*, 2014). Thus, by solving the Bethe-Salpeter Equation one can obtain the light-front amplitudes, that enable the calculation of hadron observables (BRODSKY, 1998).

To better understand the structure of a bound system of quark and antiquark in Minkowski space, we developed a model to a 0^- bound state based on the BS approach considering dressed quark propagators, an extended quark-gluon vertex and an effective gluon mass. In solving the BS equation for a dressed quark propagator, it is possible to compute pion observables as, for example, the time- and space-like electromagnetic form factors, parton distribution functions, and transverse momentum distributions, directly in Minkowski space. In this thesis, using a dressed quark propagator, it is presented the relation between the binding and the coupling constant, the Light-Front amplitudes, and longitudinal and transverse light-front momentum distributions.

This thesis has the following organization:

- Chapter 2: an overview of selected topics of quantum field theory, which presents key concepts used in this thesis;
- Chapter 3: through the BS approach for the study of a pseudoscalar bound-system with dressed quark propagators in Minkowski space, it is presented the analytical steps to obtain a set of coupled equations that are suitable for numerical implementation. The dressed quark propagator is expressed using the Källén-Lehmann Representation and the components of the BS amplitude are represented by Nakanishi Integral representation.
- Chapter 4: by using a phenomenological mass function compatible with Lattice QCD computations, we obtain the full set of coefficients that will be used in the numerical implementation in order to solve the BS equation. Also, it is presented the necessary expressions to calculate the valence probability and the light-front momentum distributions.
- Chapter 5: the BS equation is solved and the numerical results are presented. At first, it is analyzed the relation between the binding and the coupling constant in the case of a heavy quark mass. Then, the Light-Front amplitudes and longitudinal and transverse light-front momentum distributions are shown to the case considering a light quark constituent for a system-mass range $3m_\pi < M < 5m_\pi$.
- Chapter 6: conclusions and future perspectives are discussed.

2 Selected topics in quantum field theory

The physics pertaining to the nuclear matter and the hadronic regime is very extensive. It has a multitude of topics and problems to discuss and solve. In this chapter, we will focus on doing some overview about those which are connected with our main study: bound state formation within strong interactions. First, we will discuss the theoretical framework where the electro-weak and strong interactions are described, called Standard Model. It will follow a description of the Bethe-Salpeter approach to describe and calculate the observables of a bound state of particles. Then we will discuss about mass generation through the study of the Dyson-Schwinger equation, in special we will consider about the pion's position in this context. To finish, we will consider the spectral representation methods necessary to solve the Bethe-Salpeter equation in Minkowski space, in special the Nakanishi Integral Representation.

2.1 Standard Model

In Particle Physics, the Standard Model (SM) is known for explaining some of the fundamental interactions of nature. Nowadays, we consider as the fundamental building blocks of nature: gravity, strong interaction, weak interaction, and electromagnetism. Each of them has its own mediator particle. The carrier of the electromagnetic interaction is the photon, a massless particle. The weak interactions are mediated by W^+, W^- and Z^0 bosons, with average mass of $m_W = 80.376 \pm 0.033$ GeV, $m_Z = 91.1876 \pm 0.0021$ GeV, respectively (WORKMAN *et al.*, 2022). The strong interaction has as carriers the gluons, which are massless particles (BELYAEV; ROSS, 2021).

Besides, theoretically, the gravitational interaction has as its mediator particle the massless graviton. Apart from those mediator particles, we have the Higgs boson, responsible for generating the masses of the elementary particles and experimentally discovered in 2012 (AAD *et al.*, 2012; CHATRCHYAN *et al.*, 2012). The gravitational force is the only one outside the scope of the Standard Model. Quantum Chromodynamics (QCD) is the theory that describes the strong force and Quantum Electro-Weak Theory describes the electro-weak forces. Together they form the theoretical framework of the Standard Model

of particle physics, its fundamental interactions are enumerated in Table 2.1 (BELYAEV; ROSS, 2021).

TABLE 2.1 – The fundamental interactions described by the Standard Model of physics.

interaction	coupling by	mediator boson
EM	electric charge	photon
Weak	weak charge	$W^{\pm}$,Z^0
Strong	color charge	gluons

The term elementary particles encompasses two groups: fermions and bosons. Fermions obey the Fermi-Dirac statistics, quarks and leptons are fermionic particles, and they have half-integer spin. Particles that have integer spin are called bosons, they obey the Bose–Einstein statistics. Quarks interact via strong forces and the leptons (electrons, muons, and neutrinos) do not. Example of bosonic particles are W^+, W^- and gluons, with spin-1, and Higgs boson, a spin-0 particle (BRAIBANT *et al.*, 2012; MARTIN; SHAW, 2019).

The historical development of SM began with the discovery of electrons, photons, protons, and neutrons. Probing and explaining the atom was the focus of the last century. Both experimental and theoretical developments were made, thus enabling the discovery of radioactivity, atomic nuclei, antimatter, and a multitude of quantum phenomena. In the first half of the twentieth century the main topic was the characterization of, then known, elementary constituents of matter and the nature of space-time. Quantum Electrodynamics emerged as a product of the work of Julian Schwinger, Shin'ichirō Tomonaga, Freeman Dyson and Richard Feynman (SCHWEBER, 1994; GLASHOW, 2018).

Between the decades of 1920 and 1930, there were superior achievements in the description of particles with Quantum Field Theory (QFT). It made possible to specify the particles by characteristics such as mass, spin, statistics, charge, and magnetic moment, and predict physical phenomena such as Compton and Bremsstrahlung scattering, and even some particle's prediction as the muon (SCHWEBER, 1994; GLASHOW, 2018). At the end of the 1940s, Schwinger and Tomonaga developed the QED using variational differentiation while Feynman used functional integration (TOMONAGA, 1946; SCHWINGER, 1948a; SCHWINGER, 1948b; TOMONAGA; OPPENHEIMER, 1948; FEYNMAN, 1949a; FEYNMAN, 1949b), and Dyson proved that both approaches are equivalent (DYSON, 1949b).

The strong sector of the Standard Model describes the interactions of quarks, antiquarks and gluons, making up fundamental constituents of the baryonic matter, such as protons and neutrons, and mesons such as the pions. Quarks are found in six varieties: up (u), down (d), strange (s), charm (c), bottom (b) e top (t). They carry three colors: red, blue, and green. Besides, in Nature, we observe eight types of gluons that carry both

color and anti-color numbers. The theoretical framework of this sector is given by the gauge theory of interactions Quantum Chromodynamics (QCD), formulated in the 1970s by works of Murray Gell-Mann, Harald Fritzsch, David J. Gross, Frank Wilczek, Hugh David Politzer (FRITZSCH *et al.*, 1973; MARCIANO; PAGELS, 1978; GROSS; WILCZEK, 1973; POLITZER, 1973).

2.2 Bethe-Salpeter Equation

The hadronic matter is made up of relativistic bound states of quarks interacting through the exchange of gluons. E. Salpeter and H. Bethe developed a covariant relativistic description of a bound state, thus providing the methodology known as Bethe-Salpeter (BS) equations to investigate the hadronic matter (SALPETER; BETHE, 1951).

The bound state can be represented by the pole of the four-point Green function. Let us consider a four-point Green's function that describes all possible interaction and self-interaction of two particles interacting through a scalar particle [1]

$$G(x_1, x_2; y_1, y_2) = \langle 0|T\{\phi_1(x_1)\phi_2(x_2)\phi_1^\dagger(y_1)\phi_2^\dagger(y_2)|0\rangle\,, \tag{2.1}$$

where T is the time-order operator. Such function is composed by three terms that represent the contribution of the free propagation of the two particles, the infinite sum of irreducible graphs and the infinite sum of reducible graphs, which it can be obtained by iterations of irreducible ones. Thus, one can write

$$\begin{aligned} G(x_1, x_2; y_1, y_2) &= G_0(x_1, x_2; y_1, y_2) + \int d^4z_1 d^4z_2 d^4z_1' d^4z_2'\, G_0(x_1, x_2; z_1, z_2) \\ &\quad \times I(z_1, z_2; z_1', z_2') G(z_1', z_2'; y_1, y_2)\,, \end{aligned} \tag{2.2}$$

with $I(z_1, z_2; z_1', z_2')$ representing the interaction kernel that contains all the irreducible diagrams of two particles. The $G_0(x_1, x_2; y_1, y_2)$ corresponds a Green's function of two non-interacting particles and it is given in terms of the particles propagators as follows

$$G_0(x_1, x_2; y_1, y_2) = \Delta(x_1 - y_1)\Delta(x_2 - y_2)\,. \tag{2.3}$$

where $\Delta_i(x_i - y_i) = \langle 0|T\{\phi_i(x_i)\phi_i^\dagger(y_i)\}|0\rangle$. One can diagrammatically express equation (2.2) as in Fig. 2.1. By considering that $IG = TG_0$, where the integral equation determining T is given by $T = I + IG_0T$, the Green's function present in equation (2.2) can

[1] For a more detailed derivation of the Bethe-Salpeter equation one can review the work of Gómez (GÓMEZ, 2016).

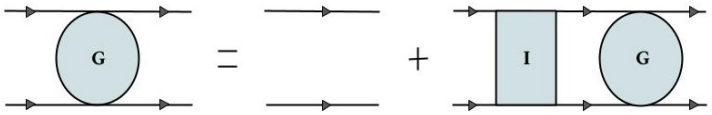

FIGURE 2.1 – Pictorical representation of four-point Green's function integral equation.

be expressed as $G = G_0 + G_0 I G_0$.

The four-point Green's function G can be written in the momentum space. In order to do that we will use a Fourier transform. First let us consider the global and relative coordinates:

$$\begin{aligned} x &= x_1 - x_2\,;\; X = \eta_1 x_1 + \eta_2 x_2 \\ y &= y_1 - y_2\,;\; Y = \eta_1 y_1 + \eta_2 y_2 \end{aligned} \tag{2.4}$$

with $\eta_1 + \eta_2 = 1$. Having those, we can write the a Fourier transform of a function $F(x_1, x_2; y_1, y_2) = F(x, y, X - Y)$ as

$$F(p_1, p_2; q_1, q_2) = (2\pi)^4 \delta(P - Q)\tilde{F}(k, p; P) \tag{2.5}$$

with

$$\tilde{F}(k, q; P) = \int d^4x \int d^4y \int d^4Z\; e^{-iP\cdot Z} e^{-ik\cdot x} e^{-iq\cdot y} F(x, y; Z) \tag{2.6}$$

wherein $P = p_1 + p_2$, $Q = q_1 + q_2$, $k = \eta_1 k_1 - \eta_2 k_2$, $q = \eta_1 q_1 - \eta_2 q_2$ are the conjugate momenta of $Z = X - Y$, x and y.

In special, in order to apply equation (2.5) in (2.2), we need to consider the two terms of the four-point Green's function. The Fourier transformation of the first term G_0, after considering the free propagators as

$$\Delta(x_1 - x_2) = \frac{1}{(2\pi)^4} \int dp \Delta(p) e^{p\cdot(x_1 - x_2)}\;, \tag{2.7}$$

and using delta functions, is given by

$$F_1 = (2\pi)^4 \delta^{(4)}(k - q) G_0(k, q; P)\,. \tag{2.8}$$

where $G_0(k, q; P) = \Delta_1(\eta_1 P + k)\Delta_1(\eta_2 P - k)$. The second term of equation (2.2), the integral of the kernel I and the Green's function G, in a similar way can be written in terms of the relative and global coordinates as to have $I(z_1, z_2; z_1', z_2') = I(z, z'; Z - Z')$ and $G(z_1', z_2'; y_1, y_2) = G(z', y; Z' - Y)$. Thus, through Fourier transformation presented

in equation (2.5), the term two (F_2) can expressed as:

$$F_2 = G_0(k,q;P)\int \frac{dq'}{(2\pi)^4} I(k,q';P)G(q',q;P)\,, \tag{2.9}$$

therein our four-point Green's function is written in the momentum space

$$G(k,q;P) = (2\pi)^4\delta^{(4)}(k-q)G_0(k,q;P)+G_0(k,q;P)\int \frac{dq'}{(2\pi)^4} I(k,q';P)G(q',q;P)\,. \tag{2.10}$$

The equation (2.10) can be visualized in the Fig. 2.1, in which the first term is representing the propagation of the free particles and the second one accounts for the interaction between them. Now that we have the four-point Green's function, we need to consider the pole term related to it, as it is connected to the bound state.

The bound state has all its information expressed by the Bethe-Salpeter (BS) amplitude, enabling the last to be used to evaluate the physical observables related to the first. Considering that $|P_B,\beta\rangle$ represents the bound state, with $P_B = (E_B, \mathbf{P})$, $E_B = \sqrt{\mathbf{P}^2 + M^2}$ where M is the bound state mass, and β is the set of the quantum numbers of it, it can be written the BS amplitude and its conjugate as

$$\begin{aligned}\Phi(x_1,x_2;P_B,\beta) &= \langle 0|T\{\phi_1(x_1)\phi_2(x_2)\}|P_B,\beta\rangle \\ \bar{\Phi}(x_1,x_2;P_B,\beta) &= \langle P_B,\beta|T\{\phi_1^\dagger(x_1)\phi_2^\dagger(x_2)\}|0\rangle\end{aligned} \tag{2.11}$$

Otherwise, applying a translational transformation in $\Phi(x_1,x_2;P_B,\beta)$ and considering the translation invariance of the vacuum, the Bethe-Salpeter amplitude can be written in a reduced form

$$\varphi(x;P_B,\beta) = (2\pi)^{3/2}\langle 0|T\{\phi_1(\eta x)\phi_2(-\eta x)\}|P_B,\beta\rangle\,, \tag{2.12}$$

where the relation between the BS amplitude and the reduced amplitude is

$$\Phi(x_1,x_2;P_B,\beta) = \frac{e^{-iP_B\cdot X}}{(2\pi)^{3/2}}\varphi(x;P_B,\beta)\,. \tag{2.13}$$

By considering that one bound state of two particles, when inserting a completeness relation $\sum_n |n><n| = 1$, with $|n>$ representing the Fock state with n particle, the

four-point Green's function turns to be

$$\begin{aligned} G(x_1,x_2;y_1,y_2) &= \theta[min(x_1^0,x_2^0)-max(y_1^0,y_2^0)]\int\frac{d^3P}{2E_B(2\pi)^3} \\ &\quad\times\langle 0|T\{\phi_1(x_1)\phi_2(x_2)\}|P_B,\beta><P_B,\beta|T\{\phi_1^\dagger(y_1)\phi_2^\dagger(y_2)\}|0\rangle \\ G(x_1,x_2;y_1,y_2) &= \theta[min(x_1^0,x_2^0)-max(y_1^0,y_2^0)] \\ &\quad\times\int\frac{d^3P}{2E_B(2\pi)^3}e^{-iP\cdot Z}\varphi(x;P_B,\beta)\bar{\varphi}(y;P_B,\beta)\,. \end{aligned} \tag{2.14}$$

The theta function, present in the equation above, can be rewritten in therms of relative coordinates present in equation (2.4), as its follow

$$\theta[min(x_1^0,x_2^0)-max(y_1^0,y_2^0)] = \theta[X^0-Y^0+f(x^0,y^0)] \tag{2.15}$$

$$f(x^0,y^0) = -\frac{x^0}{2}-\frac{y^0}{2}+\frac{(\eta_2-\eta_1)}{2}(x^0-y^0)\,, \tag{2.16}$$

and then by using the integral representation of the θ function can be expressed as

$$\theta[min(x_1^0,x_2^0)-max(y_1^0,y_2^0)] = \frac{1}{2\pi}\int\frac{e^{-it(X^0-Y^0+f(x^0,y^0))}}{t+i\epsilon}dt\,. \tag{2.17}$$

Our four-point Green's function is expressed, by using the identity present in equation (2.17), as

$$G(x_1,x_2;y_1,y_2) = \int\frac{d^4P}{(2\pi)^4}\frac{\varphi(x;P_B,\beta)\bar{\varphi}(y;P_B,\beta)}{2E_B[P_0-E_B+i\epsilon]}e^{-i((P_0-E_B)f(x^0,y^0)+(X-Y)\cdot P)}\,, \tag{2.18}$$

which shows that the mass of the bound state is the own pole of the Green's function. Then, we can think of it as having two contributions, the one that comes from the regular terms that has no pole at $P_0 = E_B$ and the one which has. With the Fourier transform of $G_B(x,y;X-Y)$

$$\begin{aligned} G_B(k,q;P) &= \int d^4x\,d^4y\,d^4Z\,e^{-ik\cdot x}e^{-iq\cdot y}e^{iP\cdot Z}G_B(x,y;Z) &(2.19)\\ &= i\frac{\varphi(k;P_B,\beta)\bar{\varphi}(q;P_B,\beta)}{2\omega_B(P_0-E_B+i\epsilon)}\,, &(2.20)\end{aligned}$$

we can rewrite the equation (2.10) as

$$\varphi(k;P_B,\beta)\bar{\varphi}(q;P_B,\beta) = G_0(k,P_B)\int\frac{d^4q'}{(2\pi)^4}I(k,q';P_B)\varphi(q';P_B,\alpha)\bar{\varphi}(q;P_B,\alpha)\,. \tag{2.21}$$

Finally we obtain

$$\varphi(k;P_B,\beta) = \Delta_1(\eta_1 P + k)\Delta_1(\eta_2 P - k)\int \frac{d^4q'}{(2\pi)^4} I(k,q';P_B)\varphi(q';P_B,\alpha)\,, \tag{2.22}$$

which is the integral equation in terms of the BS amplitude that is known as the homogeneous Bethe-Salpeter Equation. Note that the kernel of the BS equation $I(k,q';P_B)$ is the same of the integral equation for the four-point Green's function, equation (2.2).

2.3 Quantum Chromodynamics

The physics of strong interactions is related to phenomena pertaining to hadrons, their structure and interactions. The theory that describes such physics is known as Quantum Chromodynamics (QCD). It has as main objective to study the force ("color force") that binds quarks and gluons inside of the hadrons, such as protons and pions. Especially, it can be seen as the theory of strong interaction of quarks mediated by gluons, which are massless particles with integer spin and two polarization (left or right-handed).

Quarks are fermionic particles that have three basic color-charge configurations, labeled as red (r), green(g) and blue (b). Gluons also carry color charge. Each color has its own counterpart anticolor. Those color states of quarks are $SU(3)$ triplets.

The classical Lagrangian of the QCD can be expressed as (CHENG, 1984)

$$\mathcal{L} = \sum_{f=1}^{N_f}\sum_{c=r,g,b} \bar{\psi}_c^f \left(i\gamma^\mu D_\mu - m_0^f\right)\psi_c^f - \frac{1}{4}G^a_{\mu\nu}G_a^{a\mu\nu}\,, \tag{2.23}$$

with $\psi^f = \{\psi_r^f, \psi_g^f, \psi_b^f\}$ are the quark fields which are Dirac spinors and f and c refer to the flavor quantum number and to the color, respectively. The term $D_\mu = \partial_\mu - igA_\mu^a t^a$ is covariant gauge derivative, expressed in terms of coupling constant g, the Gell-Mann matrices [2] t^a, gauge field A_μ^a. And the tensor $G_{\mu\nu}^a$ is the color fields tensor given by

$$G^a_{\mu\nu} = \partial_\mu A^a_\nu - \partial_\nu A^a_\mu + g f^{abc} A^b_\mu A^c_\nu\,, \tag{2.24}$$

where f^{abc} is the structure constants of the SU(3) color group.

We have an invariant Lagrangian under global and local gauge transformations by writing the Lagrangian as expressed in equation (2.23). On other hand, if one explicitly writes every term of the Lagrangian, it will be clear the presence of quark-gluon

[2] Those matrices are known as the generators of $SU(3)$ group. They satisfy the following relations: $\left[\frac{\lambda_a}{2}, \frac{\lambda_b}{2}\right] = if^{abc}\frac{\lambda^c}{2}$; $tr(\lambda^a,\lambda^b) = 2\delta^{ab}$. The indices a runs between one and eight, representing each gauge boson or colored mediator boson.

interactions, 3-point gluon interaction and 4-point gluon interaction, as diagrammatically pictured in Fig.2.2. Therefore, because gluons carry color and anticolor charges, they can interact with each other.

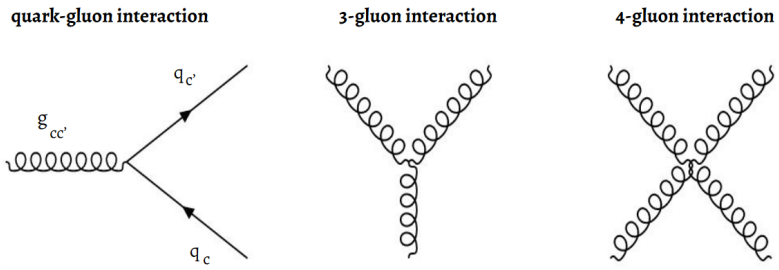

FIGURE 2.2 – The basic vertices of the Quantum Chromodynamics.

The quantized version of the classical QCD Lagrangian is derived by doing some considerations. In order to do the quantization of quantum field theory, in path integral formalism [3], it is necessary to take the path-integral over all the possible field configurations, which means having a generating functional

$$\mathcal{Z}[A,J] = \int \mathcal{D}A \left\{ exp\left[i \int d^4x \mathcal{L}(A) + J_\mu(x) A^\mu(x) \right] \right\}. \tag{2.25}$$

where $J_\mu(x)$ is the external source associated to the field $A^\mu(x)$.

The sum includes configurations that are connected by gauge transformations. It is necessary to identify the physical distinct field configurations, meaning that one needs "fix" the gauge. The usual method to do that is using the Faddev-Popov method, in which auxiliary fields[4] c and $\bar{c}$ (Faddeev-Popov ghosts) are introduced in the Lagrangian. By imposing that $\partial_\mu A^{a\mu} = 0$, we have as the gauge fixing term and the Faddev-Popov term of the Lagrangian

$$\mathcal{L}_{GF} = \frac{-1}{2\xi}(\partial_\mu A^{a\mu})^2 , \tag{2.26}$$

$$\mathcal{L}_{FP} = (\partial_\mu \bar{c}_a)(\delta^{ab}\partial^\mu - g f^{abc} A_c^\mu) c_b(x) , \tag{2.27}$$

then the quantization of the QCD results in a Lagrangian that is composed by three

[3] It was developed by Feynman in 1948, being a formulation of quantum mechanics equivalent to the formulations of Schrodinger's and Heisenberg (FEYNMAN, 1948; MACKENZIE, 2000).

[4] The ghosts fields c^a and $\bar{c}^a$ are two independent scalar Grassmann fields.

contributions

$$\begin{aligned}\mathcal{L}_{QCD} &= \mathcal{L}_{quark} + \mathcal{L}_{gauge} + \mathcal{L}_{FP\ ghosts} \\ \mathcal{L}_{QCD} &= \bar{\psi}\left(i\gamma^{\mu}D_{\mu} - m\right)\psi - \frac{1}{4}G^{a}_{\mu\nu}G^{a\mu\nu}_{a} - \frac{1}{2\xi}(\partial_{\mu}A^{a\mu})^{2} \\ &\quad +(\partial^{\mu}\bar{c}^{a})D^{ab}_{\mu}c_{b}\,. \end{aligned} \tag{2.28}$$

An important remark is that the Faddeev-Popov procedure is not enough to select a unique physical configuration. For an Abelian gauge theory, the gauge condition $\partial\cdot A = 0$ is sufficient to uniquely fix the gauge. While for a non-Abelian gauge theory, Gribov showed there are distinct transverse configurations, $A \neq A'$, that respect such gauge condition, related by a gauge transformation. These are known as Gribov copies (GRIBOV, 1978). Thus a non-Abelian gauge theory needs an additional constraint such as that the Gribov copies are identified physically. The solution to this problem is still a line of research (VANDERSICKEL; ZWANZIGER, 2012; DUDAL *et al.*, 2008; CAPRI *et al.*, 2021).

One final point is that by working with generating functional of the Lagrangian in equation (2.28) one can obtain the expression to quark, gluon and ghost field's propagator. It is also possible to derive the Feynman rules to quark-gluon interactions and gluon-gluon interactions. By doing so, we will have Green's functions of two, three, and four points. Along with each possible Green's function, it will be a Dyson-Schwinger equation, which is the result of doing a functional integral over a total derivative of the generating functional, which vanishes. In the next section, we will derive the expression for the quark propagator and the Dyson-Schwinger for a fermion propagator.

2.4 Mass Generation

The dynamics of a quantum field is determined by its Lagrangian. The classical field theory has the dynamics given by equations of motion, derived from the action of the Lagrangian using the action principle. The quantization of a classical field can be achieved by using the path-integral formalism, constructed by Feynman (FEYNMAN, 1948). The n-points Green functions, that describe the physical systems which quantum field theory has as object of study, can be calculated in this formalism by using integral equations, devised by Dyson and Schwinger independently (DYSON, 1949a; SCHWINGER, 1951). The Dyson-Schwinger (DS) equations give us an understanding that is a dynamic mass generation in the framework of the QCD. Besides, QCD theory points out that the fermions have their mass coming from the Higgs mechanism, and the hadronic matter gain mass by the dynamical chiral symmetry breaking (DCSB) mechanism. In this section, we will discuss about the DS equations and the breaking of the chiral symmetry as means of

mass generation.

2.4.1 Fermion Propagator

Fermions are described in quantum field as Dirac spinors fields $\psi(x)$. The Lagrangian for a free fermion field is written as

$$\mathcal{L}(\psi,\bar{\psi}) = \bar{\psi}_a(x)\left(i\gamma^\mu_{ab}\partial_\mu - m\delta_{ab}\right)\psi_b(x)\,, \tag{2.29}$$

where the indices a and b are spinors indices running from one to four. The adjoint spinor $\bar{\psi}_b(x)$ is defined by $\bar{\psi}_b(x) = \psi^\dagger_a(x)\gamma^0_{ab}$. The equation of motion derived from this Lagrangian is the Dirac equation. One consideration when one quantizes the fermion field is that they are anti-commuting operators, thus the path-integral has to be made over a function that has the same characteristic. One method of doing that is adopting Grassmann variables, as they are anti-commuting values (GRASSBERGER, 1978).

First, the vacuum-to-vacuum transition amplitude with external sources is expressed by

$$\mathcal{Z}[\eta,\bar{\eta}] = \int \mathcal{D}\psi\mathcal{D}\bar{\psi}\left\{\exp\left[i\int d^4x\mathcal{L}(\psi,\bar{\psi}) + \bar{\eta}_a\psi_a + \bar{\psi}_a\eta_a\right]\right\}, \tag{2.30}$$

with η and $\bar{\eta}$ being anti-commuting spinors with four components. The $\mathcal{Z}[\eta,\bar{\eta}]$ term is known also as the generating functional, and it is normalized to one if one considers the sources being zero. The next step is to do a differentiation with respect to η and another with respect to $\bar{\eta}$. Considering that the n-point functions can be, in general, calculated using the generating functional in the presence of external sources, we can write

$$\begin{aligned}&\langle 0|T\{\psi_{a_1}(x_1)\cdots\phi_{a_l}(x_l)\bar{\psi}_{b_1}(y_1)\cdots\bar{\psi}_{b_l}(y_n)\}|0\rangle \\ &= \left.\frac{(-i)^{l+n}\delta^{l+n}\mathcal{Z}[\eta_{b_l},...,\bar{\eta}_{a_n}]}{\delta\eta_{b_l}(y_l)\cdots\delta\eta_{b_1}(y_1)\delta\bar{\eta}_{a_n}(x_n)\cdots\delta\bar{\eta}_{a_1}(x_1)}\right|_{\eta_{b_l}=\bar{\eta}_{a_n}=0}.\end{aligned} \tag{2.31}$$

Wherein one also express the generating functional in terms of the Feynman propagator of the fermion field $S_F(x,y) \equiv S^F_{ab}$, as follows

$$\mathcal{Z}[\eta,\bar{\eta}] = N\exp\left[-i\int d^4xd^4y\bar{\eta}_a(x)S_F(x,y)\eta_b(y)\right], \tag{2.32}$$

where propagator satisfies: $(i\partial\!\!\!/_x - m)_{ab}S^F_{bc}(x,y) = \delta^4(x-y)\delta_{ac}$. One thing though, this is possible only if $(i\partial\!\!\!/_x - m)$ has an inverse. Therefore a two-point function can be written

as follow

$$\langle 0|T\{\psi_1(x)\bar{\psi}_2(y)\}|0\rangle = \frac{(-i)^2\delta^2\mathcal{Z}[\eta,\bar{\eta}]}{\delta\eta_b(y)\delta\bar{\eta}_a(x)}\bigg|_{\eta=\bar{\eta}=0} = iS_F(x,y). \tag{2.33}$$

It is interesting to point out that the Fourier representation of the fermion propagator is

$$S_F(x) = \int \frac{d^4k}{(2\pi)^4}\frac{\not{k}_{ab} + m\delta_{ab}}{k^2 - m^2 + i\epsilon}e^{-ikx}\,, \tag{2.34}$$

with the poles present at $k^2 = m^2$. In the momentum space one has

$$S_F(p) = \frac{\not{p} + m}{p^2 - m^2 + i\epsilon}\,. \tag{2.35}$$

2.4.2 Dyson-Schwinger Equation

The Dyson-Schwinger equations (DSE) are obtained through the path-integral formalism [5]. By considering that a functional integral over a total derivative is null, field equations are obtained. We will consider, for illustration of DSE derivation, the action of the QED

$$\begin{aligned} S[A,\psi,\bar{\psi}] &= \int d^4x\Big(\bar{\psi}(i\not{D} - m)\psi - \frac{1}{4}F_{\mu\nu}F^{\mu\nu} - \frac{1}{2\xi}(\partial_\mu A^\mu)^2 \\ &\quad + J_\mu(x)A^\mu(x) + \bar{\eta}(x)\phi(x) + \bar{\phi}(x)\eta(x)\Big)\,, \end{aligned} \tag{2.36}$$

with $D_\mu = \partial_\mu - igA^a_\mu(x)t^a$, the gauge field $A^a_\mu(x)$ and t^a are the generators of the Lie algebra. Therefore doing the derivative in terms of $\bar{\psi}(x)$

$$\begin{aligned} \int \mathcal{D}A\mathcal{D}\psi\mathcal{D}\bar{\psi}\frac{\delta}{\delta\bar{\psi}(x)}e^{iS[A,\psi,\bar{\psi}]} &= 0 \\ \int \mathcal{D}A\mathcal{D}\psi\mathcal{D}\bar{\psi}\left[\frac{\delta S[A,\psi,\bar{\psi}]}{\delta\bar{\psi}} + \eta(x)\right]\mathcal{Z}[A,\eta,\bar{\eta}] &= 0\,. \end{aligned} \tag{2.37}$$

Before performing the derivative of the action, we should consider the connected Green's functions, $\mathcal{W}[J,\eta,\bar{\eta}]$, and its relation with the effective action $\Gamma[A,\psi,\bar{\psi}]$:

$$\mathcal{W}[J,\eta,\bar{\eta}] \equiv i\Gamma[A,\psi,\bar{\psi}] + i\int d^4x[A_\mu J^\mu + \bar{\psi}\eta + \bar{\eta}\psi]\,, \tag{2.38}$$

[5] The derivation of DSE presented in this section is based on the doctoral work of Richard Williams (WILLIAMS, 2007).

wherein one can define the classical fields as

$$\psi = \frac{\delta \mathcal{W}}{i\,\delta\bar{\eta}}\,, \bar{\psi} = \frac{\delta \mathcal{W}}{-i\,\delta\eta}\,, A^{\mu} = \frac{\delta \mathcal{W}}{i\,\delta J_{\mu}}\,, \tag{2.39}$$

in similar manner

$$\eta = i\frac{\delta\Gamma}{\delta\psi}\,, \bar{\eta} = -i\frac{\delta\Gamma}{\delta\psi}\,, J_{\mu} = i\frac{\delta\Gamma}{\delta A^{\mu}}\,. \tag{2.40}$$

Now we can do the derivative and use the relations above:

$$\begin{aligned} \left[\eta(x) + (i\partial\!\!\!/ - m + e\gamma^{\mu}A_{\mu}(x))\,\psi(x)\right]\mathcal{Z}[J,\eta,\bar{\eta}] &= 0 \\ \left[\eta(x) + \left(i\partial\!\!\!/ - m + e\gamma^{\mu}(-i)\frac{\delta}{\delta J^{\mu}(x)}\right)(-i)\frac{\delta}{\delta\bar{\eta}(x)}\right]\mathcal{Z}[J,\eta,\bar{\eta}] &= 0\,, \end{aligned} \tag{2.41}$$

hence, doing another functional derivative in terms of η(y), one has as follow

$$\delta(x-y)\mathcal{Z}[J,\eta,\bar{\eta}] - \left(i\partial\!\!\!/ - m + e\gamma^{\mu}(-i)\frac{\delta}{\delta J^{\mu}(x)}\right)\mathcal{Z}[J,\eta,\bar{\eta}]S_F(x-y) = 0\,, \tag{2.42}$$

with $S_F(x-y)$ given in terms of equation (2.33). The generating functional is related to connected Green's functions as $\mathcal{Z}[J,\eta,\bar{\eta}] = \exp(\mathcal{W})[J,\eta,\bar{\eta}]$, applying it we have

$$\begin{aligned} e^{\mathcal{W}}\left[\delta(x-y) - \left(i\partial\!\!\!/ - m + e\gamma^{\mu}(-i)\left(\frac{\delta\mathcal{W}}{\delta J^{\mu}(x)} + \frac{\delta}{\delta J^{\mu}(x)}\right)\right)S_F(x-y)\right] = 0\,, \\ \delta(x-y) - \left(i\partial\!\!\!/ - m + e\gamma^{\mu}\left(A_{\mu}(x) + (-i)\frac{\delta}{\delta J^{\mu}(x)}\right)\right)S_F(x-y) = 0\,. \end{aligned} \tag{2.43}$$

Then again using the relation between the generating functional and the propagator, presented in equation (2.33), and using the ones in equation (2.40), one can obtain the expression to the term $(-i)\frac{\delta}{\delta J^{\mu}(x)}S_F(x-y)$

$$(-i)\frac{\delta}{\delta J^{\mu}(x)}S_F(x-y) = -ie\int d^4z d^4u d^4w D_{\mu\nu}S_F(x-w)\Gamma_{\nu}(u,w;z)S_F(w,y)\,, \tag{2.44}$$

hence, if we put the external sources equal to zero in equation (2.43) and multiplying its equation by $S_F^{-1}(y,y')$, its turns to be that we have

$$\delta(x-y)S_F^{-1}(y,y') = \left((i\partial\!\!\!/ - m) + e\gamma^{\mu}(-i)\frac{\delta}{\delta J^{\mu}(x)}\right)S_F(x-y)S_F^{-1}(y,y')\,, \tag{2.45}$$

integrating with respect to y'

$$S_F^{-1}(x,y) = -(i\partial\!\!\!/ - m)\delta(x-y) - ie^2\int d^4z d^4u D^{\mu\nu}(x,z)\gamma_{\mu}S_F\Gamma_{\nu}(u,y;z)\,, \tag{2.46}$$

then obtaining the Dyson-Schwinger equation for the fermion propagator of a quantum field theory QED like in coordinate space. And by doing the Fourier transformation of it, it follow the DSE in momentum space, i.e.

$$S_F^{-1}(p) = \not{p} - m_0 - \frac{ie^2}{(2\pi)^4}\int d^4k\gamma^\mu S(k)\Gamma^\nu(k,p;k-p)D_{\nu\mu}(k-p)\,. \tag{2.47}$$

The interpretation of the Dyson-Schwinger equation is the understanding of the dynamical mass generation, by looking in the Fig. 2.3 we can see that fermions can get mass that came through the interactions, when the coupling is large enough.

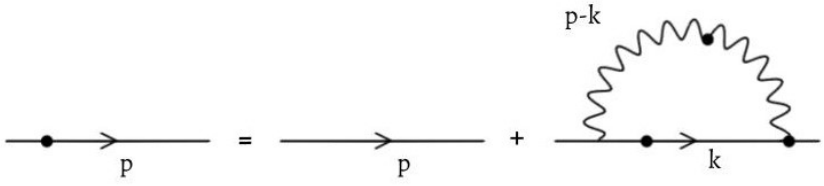

FIGURE 2.3 – The diagrammatic representation of the Dyson-Schwinger equation for a fermionic propagator.

The fermion propagator expression will be written differently, because now we understand that beyond "bare" mass we have also a mass that has a momentum dependency. The inverse of the propagator will be

$$S^{-1}(p) = \not{p} - m_0 - \Sigma(p)\,, \tag{2.48}$$

with m_0 being the bare mass and $\Sigma(p)$ being the self-energy of the fermion.

Another way of writing the quark propagator considering the dynamical mass generation is defining two functions $A(p^2)$ and $B(p^2)$, in such way that the fermion propagator can be written as

$$S(p) = \frac{A(p^2)\not{p} + B(p^2)}{A^2(p^2)p^2 - B^2(p^2)}\,, \tag{2.49}$$

where

$$\mathcal{M}(p^2) = \frac{B^2(p^2)}{A^2(p^2)}\,, \tag{2.50}$$

is the running mass function of the fermion.

2.4.3 Dynamical Chiral Symmetry Breaking & Pion

In 1935, Hideki Yukawa predicted the existence of particles that could be responsible for the short-range strong force between protons and neutrons (YUKAWA, 1935). Those particles, named pions, should be massive, around $\mu \sim 200\text{MeV}$, and were experimentally discovered in 1947 by Cecil Frank Powell, Giuseppe Occhialini and César Lattes (LATTES *et al.*, 1947). After that, in 1949, Yukawa was awarded with the Nobel Prize because of "his prediction of the existence of mesons on the basis of theoretical work on nuclear forces"(PRIZE, 2023).

Pions are mesons composed by a bound state of two quarks, making them the simplest hadrons. In nature, we observe three types of pions: π^+, π^-, and π^0. Those particles can be considered both as a hadron, a bound state of two fermions, and as the approximate Nambu–Goldstone bosons originated from the breaking of chiral symmetry. Because of those particular characteristics, pions can be seen as probes to better understand the physics of strong interactions (AGUILAR *et al.*, 2019; DING *et al.*, 2020; PAULA *et al.*, 2021; CHAVEZ *et al.*, 2021).

To understand what it means by saying that the pion is a Goldstone's boson we need to discuss one of the symmetries of the QCD: the chiral symmetry, a continuous symmetry of this theory. The appearance of the Goldstone's bosons is related to the dynamical breaking of this symmetry. Besides, the current understanding of how matter gains its mass is found in basically two phenomena: the Higgs mechanism and Dynamical Chiral Symmetry Breaking (DCSB). The Higgs boson is the particle behind the mass of all fermions and the hadronic particles have their mass originated dynamically within the QCD.

The chiral property refers to the aspect of the orientation of the particle's spin in relation to the direction of its movement. If we consider a massless quark, its spin can be right-handed (in the direction of the movement) or left-handed (in the opposite direction). In terms of Dirac spinors we can define a projection operator $P_\pm = \frac{1}{2}(1 \pm \gamma_5)$ that can be used to express our massless free quark chirality. Considering ψ as the total quark field we have

$$\psi = \psi_L + \psi_R \tag{2.51}$$

with

$$\psi_L = P_- \psi \, ; \, \psi_R = P_+ \psi \tag{2.52}$$

The Lagrangian $\mathcal{L}_q$ of free massless quark is written as

$$\mathcal{L}_q = \bar{\psi}\,(i\gamma^\mu \partial\mu)\,\psi\,, \tag{2.53}$$

by applying the expression (2.51) in the equation (2.53), the quark Lagrangian splits in two terms each connected with a chiral configuration,

$$\mathcal{L}_q = \bar{\psi_L}\,(i\gamma^\mu \partial\mu)\,\psi_L + \bar{\psi_R}\,(i\gamma^\mu \partial\mu)\,\psi_R\,. \tag{2.54}$$

It is interesting take a look closely at the algebra concerning the step between equation (2.53) and (2.54), we have

$$\begin{aligned}
i\overline{\psi}_L\gamma^\mu\partial_\mu\psi_R &= \frac{i}{4}\overline{\psi}(1+\gamma^5)\gamma^\mu\partial_\mu(1+\gamma^5)\psi \\
&= \frac{i}{4}(\overline{\psi}\gamma^\mu\partial_\mu\psi + \overline{\psi}\gamma^\mu\gamma^5\partial_\mu\psi + \overline{\psi}\gamma^5\gamma^\mu\partial_\mu\psi + \overline{\psi}\gamma^5\gamma^\mu\gamma^5\partial_\mu\psi) \\
&= \frac{i}{4}(\overline{\psi}\gamma^\mu\partial_\mu\psi + \overline{\psi}\gamma^\mu\gamma^5\partial_\mu\psi - \overline{\psi}\gamma^\mu\gamma^5\partial_\mu\psi - \overline{\psi}\gamma^\mu\partial_\mu\psi) \\
&= 0\,, \qquad (2.55) \\
i\overline{\psi}_R\gamma^\mu\partial_\mu\psi_L &= \frac{i}{4}\overline{\psi}(1-\gamma^5)\gamma^\mu\partial_\mu(1-\gamma^5)\psi \\
&= \frac{i}{4}(\overline{\psi}\gamma^\mu\partial_\mu\psi - \overline{\psi}\gamma^\mu\gamma^5\partial_\mu\psi - \overline{\psi}\gamma^5\gamma^\mu\partial_\mu\psi + \overline{\psi}\gamma^5\gamma^\mu\gamma^5\partial_\mu\psi) \\
&= \frac{i}{4}(\overline{\psi}\gamma^\mu\partial_\mu\psi - \overline{\psi}\gamma^\mu\gamma^5\partial_\mu\psi + \overline{\psi}\gamma^\mu\gamma^5\partial_\mu\psi - \overline{\psi}\gamma^\mu\partial_\mu\psi) \\
&= 0\,. \qquad (2.56)
\end{aligned}$$

This means that our massless quark Lagrangian will not have terms with a mix of ψ_L and ψ_r. Then when we apply a global transformation like $\psi \to \psi' = e^{i\beta\gamma^5}\psi$ in the Lagrangian it has no change, thus one can call it invariant under such transformation, that is called chiral transformation.

Now if consider, for example, the light quarks, up and down, that are not massless but have small mass, the Lagrangian will change

$$\begin{aligned}
\mathcal{L}_q &= i(\overline{\psi}_L + \overline{\psi}_R)\gamma^\mu\partial_\mu(\psi_L + \psi_R) - m(\overline{\psi}_L + \overline{\psi}_R)(\psi_L + \psi_R) \\
&= i\overline{\psi}_L\gamma^\mu\partial_\mu\psi_L + i\overline{\psi}_L\gamma^\mu\partial_\mu\psi_R + i\overline{\psi}_R\gamma^\mu\partial_\mu\psi_L + i\overline{\psi}_R\gamma^\mu\partial_\mu\psi_R \\
&+ m(\overline{\psi}_L\psi_L + \overline{\psi}_L\psi_R + \overline{\psi}_R\psi_L + \overline{\psi}_R\psi_R) \\
\mathcal{L}_q &= i\overline{\psi}_L\gamma^\mu\partial_\mu\psi_L + i\overline{\psi}_R\gamma^\mu\partial_\mu\psi_R + m(\overline{\psi}_L\psi_R + \overline{\psi}_R\psi_L)\,, \qquad (2.57)
\end{aligned}$$

where $\overline{\psi}_L\psi_L = \overline{\psi}_R\psi_R = 0$, the relations $\{\gamma^5, \gamma^\mu\} = 0$ and $(\gamma^5)^2 = \mathbf{1}$ were used. Thus the ψ_L and ψ_R that were decoupled from each other when the quark had zero mass, turns coupled in the presence of the mass term, as we can see in the Lagrangian. Therefore

the chiral symmetry is broken when the quark is massive. In fact, in nature until now we only have observed massive quarks (six types of quarks) with mass ranging between ~ 1.8 MeV/c^2 and ~ 172 GeV/c^2 (WORKMAN *et al.*, 2022).

As the physical quarks are not massless we have chiral symmetry breaking. However, according to Goldstone's theorem, when a spontaneous symmetry breaking occurs there will be at least one massless mode or boson in the spectrum of the theory (see (GOLDSTONE *et al.*, 1962)). Therefore, physically there should be a boson that comes from the dynamical breaking of the chiral symmetry (DCSB). In fact, the pion is the Goldstone's boson of QCD, with its mass coming from the fact that the light quarks are not massless. In nature we observe three pions: π^+,π^- and π^0, with their mass being between ~ 139.57 MeV/c^2, ($\pi\pm$), and ~ 134.97 MeV/c^2 (π^0)(WORKMAN *et al.*, 2022).

2.5 Integral Representation

In a free field theory, the two-point function is interpreted as the amplitude of a particle propagating between a point x and a point y. For an interacting field theory, the representation of the two-point function is called Källén-Lehmann (PESKIN; SCHROEDER, 1995). In turn, the generalization of that can be obtained by a perturbative method called Nakanishi Integral Representation (NIR), which can be applied as an ansatz to solve the Bethe-Salpeter equation (SALMÈ *et al.*, 2017; PAULA *et al.*, 2017; PAULA *et al.*, 2018; MOITA *et al.*, 2022).

2.5.1 Källén-Lehmann Representation

In this subsection, we review the derivation presented in Peskin (PESKIN; SCHROEDER, 1995). A first step to obtain the Källén-Lehmann representation is to consider a real scalar field theory valid to all kinds of interaction, without any perturbative theory dependency. This kind of consideration permits us to assume that the Hamiltonian $\hat{H}$ is a Lorentz invariant and the momentum operator $\hat{P}$ commutes with the operator $\hat{H}$. This is true because we are considering states that represent a set of particles that we treat as a single body, where the binding energy is already contained in the mass of the bound state, which in turn is free.

Let $|\lambda_{\vec{p}}\rangle$ be the eigenstate of $\hat{H}$ and $\hat{P}$, with λ carrying all quantum numbers of the possible quantum states. Each $|\lambda_{\vec{p}}\rangle$ is related through a Lorentz boost with the state corresponding to rest, called $|\lambda_0\rangle$. The eigenvalue equation is given by

$$\hat{H}|\lambda_{\vec{p}}\rangle = E_p|\lambda_{\vec{p}}\rangle; \hat{P}|\lambda_{\vec{p}}\rangle = \vec{p}|\lambda_{\vec{p}}\rangle. \tag{2.58}$$

The eigenstate $|\lambda_{\vec{p}}\rangle$ can represent one particle state $|1_{\vec{p}}\rangle$, with energy $E_p = \sqrt{\vec{p}^2 + m_\lambda^2}$ and rest mass m_λ. It can represent a bound state or a state of N-particles, with $N \geq 2$, composed of a 1-particle state and bound states. All states are created from the $|\Omega\rangle$ vacuum. The crucial difference between interacting scalar field theory and free field theory is that $\phi(x)$ cannot simply be a superposition of the operators $a(\vec{p})$ and $a^\dagger(\vec{p})$, as it does not obey the equations of free motion:

$$(\partial^2 + m^2)\phi \neq 0 \Longrightarrow (\partial^2 + m^2)\phi = j, \tag{2.59}$$

where j is the current. Thus, applying ϕ to Ω does not simply create a 1-particle state as in the free theory. Another important point is to note that in the completeness relation, in Hilbert space,

$$\hat{1} = |\Omega\rangle\langle\Omega| + \sum_\lambda \int \frac{d^3p}{(2\pi)^3} \frac{1}{E_p(\lambda)} |\lambda_{\vec{p}}\rangle\langle\lambda_{\vec{p}}|, \tag{2.60}$$

the sum in λ includes the 1-particle states, the bound states, and the multi-particle states, while the integral in p refers to the momentum of the center of mass $\vec{p}$ of states λ. In particular, specifying a multi-particle state requires specifying the relative momentum of each individual state plus the $\vec{p}$ momentum. Thus, the sum over λ is a sum over a continuum of states.

In free field theory the function of two points $\langle\Omega|T\phi(x)\phi(y)|\Omega\rangle$ is the amplitude for a particle to propagate from y to x. The question is if this interpretation follows in the interacting theory. The first objective is to obtain an expression for the interacting Feynman propagator:

$$\langle\Omega|\phi(x)\phi(y)|\Omega\rangle = \begin{cases} \langle\Omega|\phi(x)\phi(y)|\Omega\rangle & \textbf{if} \;\; x_0 > y_0 \\ \langle\Omega|T\phi(y)\phi(x)|\Omega\rangle & \textbf{if} \;\; y_0 > x_0. \end{cases}$$

By doing

$$\begin{aligned} \langle\Omega|\phi(x)\hat{1}\phi(y)|\Omega\rangle &= \langle\Omega|\phi(x)|\Omega\rangle\langle\Omega|\phi(y)|\Omega\rangle + \sum_\lambda \int \frac{d^3p}{(2\pi)^3} \frac{1}{E_p(\lambda)} \langle\Omega|\phi(x)|\lambda_{\vec{p}}\rangle\langle\lambda_{\vec{p}}|\phi(y)|\Omega\rangle, \\ &= \sum_\lambda \int \frac{d^3p}{(2\pi)^3} \frac{1}{E_p(\lambda)} \langle\Omega|\phi(x)|\lambda_{\vec{p}}\rangle\langle\lambda_{\vec{p}}|\phi(y)|\Omega\rangle, \end{aligned} \tag{2.61}$$

considering that $\langle\Omega|\phi(0)|\Omega\rangle = 0$. If $c \equiv \langle\Omega|\phi(0)|\Omega\rangle \neq 0$ one can redefine ϕ as $\phi \to \phi - c$, thus obtaining the result above. On the other hand, $\langle\Omega|\phi(x)|\lambda_{\vec{p}}\rangle$ can be written as

$$\langle\Omega|\phi(x)|\lambda_{\vec{p}}\rangle = \langle\Omega|e^{iP\cdot x}\phi_0 e^{-iP\cdot x}|\Omega\rangle = \langle\Omega|\phi_0|\Omega\rangle e^{-ip\cdot x}, \tag{2.62}$$

with $e^{-iP\cdot x}|\Omega\rangle = |\Omega\rangle e^{-ip\cdot x}$ and $\langle\Omega|e^{iP\cdot x} = \langle\Omega|$. The next step is to relate $|\lambda_{\vec{p}}\rangle$ to $|\lambda_0\rangle$ using

a boost. Considering that the classical scalar field transforms as $\phi(x) = U^{-1}(\Lambda)\phi(x')U(\Lambda)$, one have

$$\begin{aligned} \langle\alpha'|\phi(x')|\beta'\rangle &= \langle\alpha|U^{-1}(\Lambda)\phi(x')U(\Lambda)|\beta\rangle = \langle\alpha|\phi(x)|\beta\rangle. \quad (2.63) \\ \langle\Omega|\phi(x)|\lambda_{\vec{p}}\rangle &= \langle\Omega|U^{-1}U\phi(0)U^{-1}U|\lambda_{\vec{p}}\rangle e^{-ip\cdot x} = \langle\Omega|\phi(0)|\lambda_0\rangle e^{-ip\cdot x}. \quad (2.64) \end{aligned}$$

With that, the propagator can be expressed, without the time orderer, as

$$\langle\Omega|\phi(x)\phi(y)|\Omega\rangle = \sum_\lambda \int \frac{d^3p}{(2\pi)^3}\frac{1}{E_p(\lambda)}|\langle\Omega|\phi(0)|\lambda_0\rangle|^2 e^{-ip\cdot(x-y)}, \quad (2.65)$$

while the scalar field result of the free theory is written as

$$D(x-y) = \langle 0|\phi(x)\phi(y)|0\rangle = \int \frac{d^3p}{(2\pi)^3}\frac{1}{E_p(\lambda)}e^{-ip\cdot(x-y)}. \quad (2.66)$$

Rewriting the integral present in the equation (2.65) as

$$\int \frac{d^3p}{(2\pi)^3}\frac{1}{E_p(\lambda)}e^{-ip\cdot(x-y)} = \int \frac{d^4p}{(2\pi)^4}\frac{i}{p^2 - m_\lambda^2 + i\epsilon}e^{-ip\cdot(x-y)}, \quad (2.67)$$

one obtain the expression that relates the Feynman propagator $\mathcal{D}_F$ with the function of two points

$$\langle\Omega|T\phi(x)\phi(y)|\Omega\rangle = \sum_\lambda |\langle\Omega|\phi(0)|\lambda_0\rangle|^2 \mathcal{D}_F\big((x-y), m_\lambda^2\big), \quad (2.68)$$

For each state λ there will be a contribution to the two-point function and to the amplitude of creation from vacuum. Another way to write the sum in λ is

$$\begin{aligned} \langle\Omega|T\phi(x)\phi(y)|\Omega\rangle &= \int_0^\infty \frac{dM^2}{2\pi}\sum_\lambda 2\pi\delta(M^2 - m_\lambda^2)|\langle\Omega|\phi(0)|\lambda_0\rangle|^2 D_F\big((x-y), m^2\big), \\ &= \int_0^\infty \frac{dM^2}{2\pi}\rho(M^2)D_F((x-y), m_\lambda^2), \quad (2.69) \end{aligned}$$

with the spectral density $\rho(M^2) = \sum_\lambda 2\pi\delta(M^2 - m_\lambda^2)|\langle\Omega|\phi(0)|\lambda_0\rangle|^2$. This expression above corresponds to the spectral representation of Källén-Lehmann.

For an intermediate state of a particle, we will have $m_\lambda = m$, being m the energy eigenvalue of the interacting hamiltonian in the particle's rest frame. The mass m is the observable mass of the interacting particle and may differ from the bare mass m_0. In this case the spectral density will be (PESKIN; SCHROEDER, 1995)

$$\rho(M^2) = 2\pi\delta(M^2 - m^2)Z + \sigma(M^2), \quad (2.70)$$

with $Z = |\langle\Omega|\phi(0)|1_0\rangle|^2$, where 1_0 is the 1-particle state with zero momentum, and $\sigma(M^2)$ represents the contributions of N-particle states. Depending on the energy there can be production of two or more "free" real particles or bound states of two or more particles. In momentum space we have

$$\begin{aligned}\int d^4x e^{ipx}\langle\Omega|T\phi(x)\phi(y)|\Omega\rangle &= \int_0^\infty \frac{dM^2}{2\pi}\rho(M^2)\frac{i}{p^2-m^2+i\epsilon} \\ &= \frac{iZ}{p^2-m^2+i\epsilon}+\int_{m_e^2}^\infty \frac{dM^2}{2\pi}\frac{i\sigma(M^2)}{p^2-m^2+i\epsilon}, \end{aligned} \quad (2.71)$$

with m_e^2 being the mass of the bound state (PESKIN; SCHROEDER, 1995). For the free field case, we have

$$\int d^4x e^{ipx}\langle 0|T\phi(x)\phi(0)|0\rangle = \frac{i}{p^2-m_0^2+i\epsilon}. \quad (2.72)$$

The Källén-Lehmann representation is a one-variable integral representation for a two-point function. Next we will discuss about the Nakanishi integral representation, which is a generalized two-variable integral representation.

2.5.2 Nakanishi Integral Representation

The Nakanishi Integral Representation (NIR) formalism of a transition amplitude of a generic N-particle scattering is based on a perturbative treatment. However, despite being formulated in the perturbative regime, it can be used as an ansatz in the non-perturbative regime. This representation has been used in studies of bound state problems, with results in agreement with other methods in the literature (KUSAKA; WILLIAMS, 1995; FREDERICO *et al.*, 2012).

The probability amplitude of a certain process can be written in terms of a power series of the coupling constant, where each term can be interpreted as a sum of Feynman integrals generated by a particular Lagrangian and corresponding to a set of graphs of Feynman. Using Feynman's parametric integral, performing a change of integration variables that leads to a new set of variables that is equal to the number of independent variables, one can obtain the Nakanishi integral representation (NAKANISHI, 1971).

The perturbation theory integral representation (PTIR) permits to have a parametric representation of any Feynman diagram in the Minkowski space. Through the NIR, the amplitude is given in terms of an integral with a kernel function of real variables (Nakanishi weight function). Despite the perturbative framework where the Nakanishi Integral Representation has been originally devised, it can be extended or applied to the nonperturbative regime. This is the case when we use the NIR to obtain the solution of the bound state Bethe-Salpeter equation (NAKANISHI, 1971; FREDERICO *et al.*, 2013).

In this section, we will derive the expression of the NIR to the Bethe-Salpeter amplitude. As notation, we have the external 4-moment designated by p_i, such that, $\sum_i^N p_i = 0$, the 4-moment k_j and the mass m_j are associated with particles that propagate inside the loops, and q_l is the 4-moment at which the integration is performed in the l-th loop.

Considering sets of Feynman graphs G having N outer lines, with n inner propagations, V outer vertices and s loops, we have

$$k_j = \sum_{l=1}^{s} b_{jl} q_l + \sum_{i=1}^{N} c_{ji} p_i, \tag{2.73}$$

where b_{jl} and c_{ji} can assume the values $(-1, 0, 1)$ due to the conservation of moments at the vertices. The Feynman integral associated with G is represented (GóMEZ, 2016) as

$$f_G = \delta^{(4)}\Big(\sum_{i=1}^{N}(p_i)\Big) \int \Big(\prod_{s=1}^{n'} d^4 q_s\Big) \frac{1}{\prod_{j=1}^{n}(k_j^2 - m_j^2 + i\epsilon)}, \tag{2.74}$$

where $n' = n - (V - 1)$. To combine the n-denominators, Feynman's parametric formula is used

$$\frac{1}{[A_1 A_2 \dots A_n]} = (n-1)! \prod_{i=1}^{n} \int_0^1 d\alpha_i \frac{\delta(1 - \sum_{j=1}^{n} \alpha_j)}{[A_1\alpha_1 + A_2\alpha_2 + \dots + A_n\alpha_n]^n}, \tag{2.75}$$

as soon as,

$$f_G = (n-1)!\delta^{(4)}\Big(\sum_{i=1}^{N}(p_i)\Big) \int \Big(\prod_{s=1}^{n'} d^4 q_s\Big) \int_0^1 \prod_{j=1}^{n} d\alpha_n \frac{\delta(1 - \sum_{j=1}^{n} \alpha_j)}{\Big[\sum_{j=1}^{n}(k_j^2 - m_j^2 + i\epsilon)\alpha_j\Big]^n}. \tag{2.76}$$

In the equation (2.73) we have the relation between k_j and q_l, when substituting this relation in the equation (2.76) there will be quadratic and linear terms of q_j in the denominator. So that one can write

$$\begin{aligned}\left[\sum_{j=1}^{n}(k_j^2 - m_j^2 + i\epsilon)\alpha_j\right]^n \quad = \quad & \left[\sum_{s=1}^{n'} d_s q_s^2 + 2\sum_{s=1}^{n'}\sum_{i=1}^{N} B_{si}(q_s \cdot p_i)\right. \\ & \left. + \sum_{i=1}^{N}\sum_{i'=1}^{N} C_{ii'}(p_i \cdot p_i') - \sum_{j=1}^{n} m_j^2 \alpha_j + i\epsilon\right]^n,\end{aligned} \tag{2.77}$$

making the following change of variable,

$$q_s' = q_s + \frac{1}{d_s}\sum_{i=1}^{N} B_{si} p_i, \tag{2.78}$$

there is

$$\left[\sum_{j=1}^{n}(k_j^2 - m_j^2 + i\epsilon)\alpha_j\right]^n = \left[\sum_{s=1}^{n'} d_s q_s'^2 + \sum_{i=1}^{N}\sum_{i'=1}^{N}(p_i \cdot p_i')(C_{ii'} - \sum_{s=1}^{n'}\frac{1}{d_s}B_{si}B_{si'}) - \sum_{j=1}^{n} m_j^2\alpha_j + i\epsilon\right]^n, \tag{2.79}$$

where d_s is the set of eigenvalues corresponding to the matrix $D_{ss'}$, $D_{ss'} = \sum_j \alpha_j b_{js} b_{js'}$, and with $B_{ss'} = \sum_j \alpha_j b_{js} c_{ji}$ and $C_{ss'} = \sum_j \alpha_j c_{ji} b c_{ji'}$. The next step is to perform the integration on q_s', assuming that the integrate is convergent we can invert the order of integration:

$$\int \prod_{s=1}^{n'} d^4 q_s' \frac{1}{\left[\sum_{s=1}^{n'} d_s q_s'^2 + H(n, N, \alpha_j, p_i) + i\epsilon\right]^n} = \frac{(n-2n'-1)!(i\pi^2)^{n'}}{(n-1)!\left[\prod_{n'} d_{n'}\right]^2 \left[H(n, N, \alpha_j, p_i) + i\epsilon\right]^{n-2n'}}, \tag{2.80}$$

with

$$H(n, N, \alpha_j, p_i) = \sum_{i=1}^{N}\sum_{i'=1}^{N}(p_i \cdot p_i')(C_{ii'} - \sum_{s=1}^{n'}\frac{1}{d_s}B_{si}B_{si'}) - \sum_{j=1}^{n} m_j^2\alpha_j. \tag{2.81}$$

Substituting this result in the Feynman integral of the equation (2.76), we obtain

$$f_G = \delta^{(4)}\Big(\sum_{i=1}^{N}(p_i)\Big)\frac{(n-2n'-1)!(i\pi^2)^{n'}}{\left[\prod_{n'} d_{n'}\right]^2}\int_0^1 \prod_{j=1}^{n} d\alpha_n \frac{\delta(1 - \sum_{j=1}^{n}\alpha_j)}{\left[H(n, N, \alpha_j, p_i) + i\epsilon\right]^{n-2n'}}. \tag{2.82}$$

Note that in the Feynman integral, the denominator depends on the masses m_j and the number of loops. Nakanishi's idea is to move this dependency to the numerator. To move the dependency from the denominator to the numerator, it will be necessary to write the function f_G in terms of the weight function ϕ_G. Thus, we rewrite the equation (2.82) using a delta function, such that we have

$$f_G = \prod_h \int_0^1 dz_h \delta(1 - z_h)\int_0^\infty d\xi \frac{\phi_G(z, \xi)}{\left[\xi - \sum_h z_h a_h - i\epsilon\right]^{n-2n'}}, \tag{2.83}$$

with

$$\phi_G(z,\xi)\delta(1-\sum_h z_h) = const\prod_{j=1}^{n}\int d\alpha_j \frac{\delta(1-\sum_{j=1}^{n}\alpha_j)}{[\prod_{n'} d_{n'}]^2(-\beta)^{n-2n'}} \times \delta\left(z_h-\frac{\eta_h}{\beta}\right)\delta\left(\xi-\sum_l \frac{m_l^2\alpha_l}{\beta}\right)\delta\left(1-\sum_h z_h\right). \quad (2.84)$$

The variables η_h and β are given by the following relations:

$$\sum_h \eta_h\cdot s_h = \sum_i\sum_{i'} E_{ii'}(p_1\cdot p_i') \quad , \quad \beta=\sum_h \eta_h, \quad (2.85)$$

where s_h is the set of all independent variables that can be constructed with N external moments. To remove the dependence on n and n', we just perform integration by parts, where the surface terms cancel out due to the dependence of ϕ_G on ξ. After performing $n-2n'-1$ integrations, the result will be

$$f_G = \prod_h \int_0^1 dz_h \delta(1-\sum_h z_h)\int_0^\infty d\xi \frac{\phi_G'(z,\xi)}{[\xi-\sum_h z_h a_h - i\epsilon]}, \quad (2.86)$$

with $\sum z_h \neq 1$ and $z\phi_G'(z,\xi)$ written as

$$\phi_G'(z,\xi) = \frac{1}{n-2n'-1}\frac{\partial^{n-2n'-1}\phi_G(z,\xi)}{\partial\xi^{n-2n'-1}}. \quad (2.87)$$

To obtain the representation of the amputated amplitude or vertex, let's calculate the case of a three-legs diagram. For $G=3$ we have

$$f_3 = \int_0^1 dz_1\int_0^1 dz_2\int_0^1 dz_3\delta(1-z_1-z_2-z_3)\int_0^\infty d\xi\frac{\phi_3(z_1,z_2,z_3,\xi)}{[\xi-z_1a_1-z_2a_2-z_3a_3-i\epsilon]}, \quad (2.88)$$

integrating in α_3

$$f_3 = \int_0^1 dz_1\int_0^1 dz_2\int_0^\infty \frac{d\xi}{z_1+z_2}\frac{\phi_3(z_1,z_2,\xi)\theta(z_1+z_2)\theta(1-z_1-z_2)}{\left[\frac{\xi-z_1a_1-z_2a_2-(1-z_1z_2)a_3}{z_1+z_2}-i\epsilon\right]}. \quad (2.89)$$

Performing the following change of variable

$$\gamma = \frac{\xi}{z_1+z_2} - \frac{(1-z_1-z_2)}{z_1+z_2}a_3, \quad (2.90)$$

the equation (2.89) becomes

$$f_3 = \int_0^1 dz_1\int_0^1 dz_2\int_{\gamma_0}^\infty d\gamma\frac{\phi_3(z_1,z_2,\xi)\theta(z_1+z_2)\theta(1-z_1-z_2)}{\left[\gamma-\frac{z_1a_1+z_2a_2}{z_1+z_2}-i\epsilon\right]}, \quad (2.91)$$

with $\gamma_0 = -a_3(1 - z_1 - z_2)/(z_1 + z_2)$. Introducing the following variables

$$y = z_1 + z_2 \quad , \quad y' = \frac{z_1}{z_1 + z_2}, \tag{2.92}$$

we can redefine the weight function as

$$g_\Gamma(y', \gamma) = \int_0^1 y dy \phi_3(z, y, \gamma)\theta(y)\theta(1 - y)\theta(\gamma + a_3\frac{(1 - y)}{y}), \tag{2.93}$$

with $\gamma_0 = -a_3\frac{(1-y)}{y}$.

So the equation (2.91) will be

$$f_3 = \int_0^1 dy' \int_{-\infty}^{+\infty} d\gamma \frac{g_\Gamma(y', \gamma)}{\gamma - y'a_1 - (1 - y')a_2 - i\epsilon}, \tag{2.94}$$

Considering the bound state with momentum p and the constituent particles with momentum p_1 and p_2, where

$$p = p_1 + p_2 \quad , \quad k = (p_1 - p_2)/2, \tag{2.95}$$

the expression for the vertex, for $z = 1 - 2y'$, becomes:

$$\Gamma(k, p) = \int_0^1 dz \int_{-\infty}^{+\infty} d\gamma \frac{g_\Gamma(z, \gamma)}{[\gamma - \frac{M^2}{4} - k^2 - zp \cdot k - i\epsilon]}\,, \tag{2.96}$$

which is the Nakanishi integral representation for a 3-point function (NAKANISHI, 1964). By considering that $\Phi(k, p) = S_F(k + p/2)\Gamma(k, p)S_F(k - p/2)$ and applying the expression of $\Gamma(k, p)$ present in equation (2.96), we can write the Bethe-Salpeter amplitude in terms of the Nakanishi Integral Representation as

$$\Phi(k, p) = \int_{-1}^1 dz \int_{-\infty}^0 d\gamma \frac{g(\gamma, z)}{[k^2 + p{\cdot}k\, z - \kappa^2 - \gamma + i\epsilon]^3}\,, \tag{2.97}$$

where k is the relative momentum, p is the total momentum, $\kappa^2 = m^2 - M^2/4$.

3 General formalism for the two-fermion homogeneous BSE with dressed quark propagators

In this chapter, we analyze the 0^- bound-state, formed by a fermion and antifermion that interacts through a massive vector boson. The Bethe-Salpeter (BS) equation is shown for dressed quark propagator, where the Källen-Lehman spectral representation is used for its scalar and vector parts. In order to analyze the BS equation in Minkowski space, we introduce the Nakanishi Integral representation for the components of the Bethe-Salpeter amplitude, which allows us to perform the four-dimensional momentum loop integral. The BS equation is projected onto the light front and, finally, it is obtained a system of integral coupled equations in terms of the Nakanishi weight functions, suitable for numerical implementations.

3.1 Bethe-Salpeter Equation

The Bethe-Salpeter Equation for a 0^- fermion-antifermion bound state, with total momentum p and bound state mass M, $p^2 = M^2$, exchanging a vector boson with mass μ is given by (CARBONELL; KARMANOV, 2010; PAULA *et al.*, 2016)

$$\Phi(k,p) = S(k+p/2) \int \frac{d^4k'}{(2\pi)^4}\; D^{\mu\nu}(q)\Gamma_\mu(q)\Phi(k',p)\; \hat{\Gamma}_\nu(q)\; S(k-p/2)\,, \tag{3.1}$$

where k is half of the relative quark momentum and $q = k - k'$ is the gluon momentum. The dressed quark propagator [1] has as its form the Källen-Lehman spectral representation (ITZYKSON; ZUBER, 1980)

$$S(k) = i\int_0^\infty \frac{\not{k}}{k^2 - s + i\epsilon}\rho_V(s)\,ds + i\int_0^\infty \frac{\rho_S(s)}{k^2 - s + i\epsilon}\,ds\,, \tag{3.2}$$

[1] It's possible from equation (3.2) to obtain the quark propagator with constant mass, in Appendix A the connection is explicitly written.

with $\rho_{S(V)}(s)$ are the scalar (vector) spectral densities. The massive gluon propagator is given by $D^{\mu\nu}(q)$, in the Feynman gauge, as follow

$$D^{\mu\nu}(q) = -i\frac{g^{\mu\nu}}{(q^2 - \mu^2 + i\epsilon)}\,, \tag{3.3}$$

where μ is the effective gluon mass.

In general, the quark-gluon vertex $\Gamma^{\mu}(q)$ has two contributions, longitudinal and transverse ones relative to the gluon momentum. The longitudinal component is given by (OLIVEIRA *et al.*, 2018):

$$\Gamma^{L}_{\mu}(p_1, p_2, p_3) = -i\left(\lambda_1\gamma_\mu + \lambda_2(\not{p}_1 - \not{p}_2)(p_1 - p_2)_\mu + \lambda_3(p1 - p_2)_\mu + \lambda_4\sigma_{\mu\nu}(p_1 - p_2)^\nu\right), \tag{3.4}$$

In particular, in Ref. Oliveira *et al.* (2019a) and Oliveira *et al.* (2020), using a combined analysis of Lattice QCD calculation, Dyson-Schwinger Equations and Slanov-Taylor identities, it is shown that λ_1 has a huge increase in the Infrared (IF) region. Inspired by this achievement, in this model we consider the quark-gluon vertex with the λ_1 component as

$$\Gamma^{\mu}(q) = i\,g\,\frac{\mu^2 - \Lambda^2}{q^2 - \Lambda^2 + i\epsilon}\,\gamma^{\mu}\,, \tag{3.5}$$

where Λ represents the color distribution dressing for the interaction vertex. We also have that $\hat{\Gamma}_{\mu} = C\,\Gamma^{T}_{\mu}\,C^{-1}$, where $C = i\,\gamma^2\,\gamma^0$ is the charge-conjugation operator.

For a 0^- bound state, the Bethe Salpeter amplitude can be decomposed as

$$\Phi(k, p) = \sum_{i=1}^{4} S_i(k, p)\phi_i(k, p) \tag{3.6}$$

where S_i is an orthogonal basis, given by

$$\begin{aligned} S_1(k,p) &= \gamma^5 \quad ; \quad S_2(k,p) = \frac{\not{p}}{M}\gamma^5 \\ S_3(k,p) &= \frac{k\cdot p}{M^3}\not{p}\gamma^5 - \frac{\not{k}}{M}\gamma_5 \quad ; \quad S_4(k,p) = \frac{i\sigma^{\mu\nu}p_\mu k_\nu}{M^2}\gamma^5 \end{aligned} \tag{3.7}$$

The amplitude $\Phi(k, p)$ is antisymmetric by exchanging the fermionic constituents, that means $k \to -k$. It implies that the scalar functions ϕ_i, given in terms of $(k^2, p^2, k\cdot p)$, are even for $i = 1, 2, 4$ and odd for $i = 3$, with respect to the transformation $k \to -k$ (CARBONELL; KARMANOV, 2010). Thus in decomposing the BS amplitude as present in

equation (3.6), the Bethe-Salpeter equation is written as

$$\sum_{i=1}^{4} S_i(k,p)\phi_i(k,p) = \int_0^\infty ds \left[\frac{(\not{k}+\not{p}/2)\rho_V(s)}{(k+p/2)^2 - s + i\epsilon} + \frac{\rho_S(s)}{(k+p/2)^2 - s + i\epsilon}\right] \times \int \frac{d^4k'}{(2\pi)^4} \frac{ig^2(\mu^2-\Lambda^2)^2}{(k-k')^2-\mu^2+i\epsilon}\Gamma_1 \sum_{i=1}^{4} S_i(k',p)\phi_i(k',p)\ \hat{\Gamma}_2 \times \int_0^\infty ds' \left[\frac{(\not{k}-\not{p}/2)\rho_V(s')}{(k-p/2)^2 - s' + i\epsilon} + \frac{\rho_S(s')}{(k-p/2)^2 - s' + i\epsilon}\right]. \quad (3.8)$$

Multiplying equation (3.8) by S_j, performing the trace and using the orthogonality of the basis, we have

$$\phi_i = \int_0^\infty ds\ \frac{1}{(k+p/2)^2 - s + i\epsilon} \int_0^\infty ds' \frac{1}{(k-p/2)^2 - s' + i\epsilon} \times \int \frac{d^4k'}{(2\pi)^4} \frac{ig^2(\mu^2-\Lambda^2)^2}{(k-k')^2-\mu^2+i\epsilon} \sum_j^4 \sum_l P_l(s,s')C_{ij,l}(k,k',p)\phi_j(k',p), \quad (3.9)$$

where $C_{ij,l}(k,k',p)$ is given in Appendix B and $P_l(s,s')$ is given by

$$\begin{aligned} P_1(s,s') &= \rho_V(s)\,\rho_V(s') \\ P_2(s,s') &= \rho_V(s)\,\rho_S(s') \\ P_3(s,s') &= \rho_S(s)\rho_V(s') \\ P_4(s,s') &= \rho_S(s)\,\rho_S(s') \end{aligned} \quad (3.10)$$

We use the Nakanishi Integral Representation to represent the scalar functions $\phi_i(k,p)$ (NAKANISHI, 1963)

$$\phi_i(k,p) = \int_{-1}^{1} dz' \int_0^\infty d\gamma' \frac{g_i(\gamma',z')}{\left(k^2 + z'\,p\cdot k - \gamma' - \kappa^2 + i\epsilon\right)^3} \quad (3.11)$$

where $\kappa^2 = m_1^2 - \frac{M^2}{4}$, with m_1 as the lowest mass pole in the quark propagator. The Bethe-Salpeter equation for a fermion-antifermion bound state in terms of the Nakanishi

weight functions is a system of coupled integral equations given by:

$$\begin{aligned}
&\int_{-1}^{1} dz' \int_{0}^{\infty} d\gamma' \frac{g_i(\gamma', z')}{\left(k^2 + z'\, p\cdot k - \gamma' - \kappa^2 + i\epsilon\right)^3} \\
&= ig^2(\mu^2 - \Lambda^2)^2 \int_0^\infty ds \int_0^\infty ds' \int_{-1}^{1} dz' \int_0^\infty d\gamma' \int \frac{d^4k''}{(2\pi)^4} \\
&\quad \times \left[\frac{\sum_j \sum_l \; P_l(s,s') \; C_{ij,l}(k, k'', p)}{\left((k+p/2)^2 - s + i\epsilon\right)\left((k-p/2)^2 - s' + i\epsilon\right)\left((k-k'')^2 - \mu^2 + i\epsilon\right)} \right. \\
&\quad \left. \times \frac{g_j(\gamma', z')}{\left((k-k'')^2 - \Lambda^2 + i\epsilon\right)^2 \left(k''^2 + z'\, p\cdot k'' - \gamma' - \kappa^2 + i\epsilon\right)^3} \right] . \qquad (3.12)
\end{aligned}$$

3.2 Feynman's Parametrization

An important tool to deal with the BS equation in Minkowski space is the Nakanishi Integral representation, which gives the analytical structure in terms of the external momenta. It makes possible to perform the four-dimensional integration analytically. In this section, we present the relevant steps to solve the loop integration.

The starting point is equation (3.12), where we use the Feynman parametrization (WEINBERG, 2005) upon the denominators with k'' dependence. In the case of 3 factors in the denominator, a general expression for the Feynman parametrization is given as follows

$$\begin{aligned}
\frac{1}{X^m Y^n Z^l} &= \frac{\Gamma(m+n+l)}{\Gamma(m)\Gamma(n)\Gamma(l)} \\
&\quad \times \int_0^1 d\lambda_1 \int_0^1 d\lambda_2 \frac{\lambda_1^{m-1}\lambda_2^{n-1}(1-\lambda_1-\lambda_2)^{l-1}\Theta(1-\lambda_1-\lambda_2)}{[X\lambda_1 + Y\lambda_2 + Z(1-\lambda_1-\lambda_2)]^{m+n+l}} . \qquad (3.13)
\end{aligned}$$

Our terms of interest ($X(k'')$, $Y(k'')$, $Z(k'')$) will be present in $I(k'')$ function

$$I(k'') = \frac{1}{X^3(k'')Y(k'')^2 Z(k'')} , \qquad (3.14)$$

with

$$\begin{aligned}
Z(k'') &= (k-k'')^2 - \mu^2 + i\epsilon \\
Y(k'') &= (k-k'')^2 - \Lambda^2 + i\epsilon \\
X(k'') &= k''^2 + z' p\cdot k'' - \gamma' - \kappa^2 + i\epsilon . \qquad (3.15)
\end{aligned}$$

Hence, if we apply the Feynman parametrization we obtain

$$\begin{aligned} I(k'') &= 60 \int_0^1 dv \int_0^1 d\xi \; v^2 \xi \theta(1-v-\xi) \\ &\times \frac{1}{\Big[k''^2 - 2\left((1-v)k + vz'\frac{p}{2}\right)\cdot k'' + f(k,\gamma') + i\epsilon\Big]^6}\,. \end{aligned} \tag{3.16}$$

where $f(k,\gamma') = (1-v)(k^2-\mu^2) - v(\kappa^2+\gamma') + \xi(\mu^2-\Lambda^2)$.

3.3 Momentum Loop Integration

Now that we made Feynman's Parametrization we have

$$\begin{aligned} \phi_i(k,p) &= 60(ig^2)(\mu^2-\Lambda^2)^2 \int_{-1}^1 dz' \int_0^\infty d\gamma' \int_0^\infty ds \int_0^\infty ds' \int_0^1 dv \int_0^1 d\xi \\ &\times \int \frac{d^4k''}{(2\pi)^4} \frac{v^2\xi \; \theta(1-v-\xi) \sum_j \sum_l \; P_l(s,s') \; C_{ij,l}(k,k'',p) \; g_j(\gamma',z')}{\Big[k''^2 - 2\left((1-v)k + vz'\frac{p}{2}\right)\cdot k'' + f(k,\gamma') + i\epsilon\Big]^6} \\ &\times \frac{1}{\Big[(k+p/2)^2 - s + i\epsilon\Big]\Big[(k-p/2)^2 - s' + i\epsilon\Big]}, \end{aligned} \tag{3.17}$$

where the coefficient $C_{ij,l}(k,k'',p)$ can be written as follows

$$\begin{aligned} C_{ij,l}(k,k'',p) &= a^0_{ij,l} + a^1_{ij,l}\;(p\cdot k) + a^2_{ij,l}\;(p\cdot k)^2 + a^3_{ij,l}\;k^2 \\ &+ \frac{1}{B}\Big[(p\cdot k)(p\cdot k'') - M^2(k\cdot k'')\Big]\;\Big[b^0_{ij,l} + b^1_{ij,l}\;(p\cdot k) + b^2_{ij,l}\;(p\cdot k)^2 + b^3_{ij,l}\;k^2\Big] \\ &+ \Big[(p\cdot k)(p\cdot k'') - M^2(k\cdot k'')\Big]\;\Big[d^0_{ij,l} + d^1_{i,j}\;(p\cdot k)\Big], \end{aligned} \tag{3.18}$$

with $B = (p\cdot k)^2 - M^2k^2$. The coefficients $a^n_{ij,l}$, $b^n_{ij,l}$ and $d^n_{ij,l}$, are given in Appendix B. The integration in d^4k'', after a change of variable such as $k'' \to q + (1-v)k - z'vp/2$, can be calculated as (YAN, 1973)

$$\int \frac{d^4q}{\big[q^2+b+i\epsilon\big]^n} = \frac{i\pi^2}{(n-1)(n-2)b^{n-2}}. \tag{3.19}$$

For the terms in $C_{ij,l}(k,k'',p)$ that do not contain k'', the following integral is relevant

$$\begin{aligned}\mathcal{I}_1 &= \int d^4k''\ \frac{1}{\Big[k''^2 - 2\left((1-v)k + vz'\frac{p}{2}\right)\cdot k'' + f(k,\gamma') + i\epsilon + i\epsilon\Big]^6} \\ &= \int d^4q\ \frac{1}{\Big[q^2 - \Big((1-v)k - z'v\frac{p}{2}\Big)^2 + f(k,\gamma') + i\epsilon\Big]^6} \\ &= i\frac{\pi^2}{20}\ \frac{1}{\Big[-\Big((1-v)k - z'v\frac{p}{2}\Big)^2 + f(k,\gamma') + i\,\epsilon\Big]^4}\,, \end{aligned} \tag{3.20}$$

where $q = k'' - (1-v)k + z'v\ p/2$. Then another integral we will use is $\mathcal{I}_2$, that is expressed as follows

$$\mathcal{I}_2 = 3i\pi^2\ \int_0^1 dv \int_0^{1-v} d\xi\ \frac{v^2\xi}{\Big[A(v,k,z,z',\gamma';\kappa^2,\mu^2) + \xi\Big(\mu^2 - \Lambda^2\Big) + i\epsilon\Big]^4}\,, \tag{3.21}$$

which by integrating it over ξ one gets

$$\begin{aligned}\mathcal{I}_2 &= \frac{i\pi^2}{2}\ \int_0^1 dv\ v^2\ (1-v)^2 \frac{3A(v,k,z,z',\gamma';\kappa^2,\mu^2) + (1-v)\Big(\mu^2 - \Lambda^2\Big)}{\Big[A(v,k,z,z',\gamma';\kappa^2,\mu^2) + (1-v)(\mu^2-\Lambda^2) + i\epsilon\Big]^3} \\ &\quad \times \frac{1}{\Big[A(v,k,z,z',\gamma';\kappa^2,\mu^2) + i\epsilon\Big]^2}. \end{aligned} \tag{3.22}$$

where $A(v,k,z,z',\gamma';\kappa^2,\mu^2) = k^-\ k_D^+ + \ell_D$, with

$$\begin{aligned} k_D^+ &= v(1-v)\frac{M}{2}\ (z'-z) \\ \ell_D &= -v(1-v)\Big(\gamma + zz'\frac{M^2}{4}\Big) - v^2z'^2\frac{M^2}{4} - v(\gamma'+\kappa^2) - (1-v)\mu^2\ . \end{aligned} \tag{3.23}$$

We also have to deal with the terms in $C_{ij,l}(k,k'',p)$ that are dependent on k''. In equation (3.18), we can see that one has $(p\cdot k)(p\cdot k'') - M^2(k\cdot k'')$ multiplying $b_{ij,l}$ and $d_{ij,l}$ coefficients. If we perform change of variable $k'' \to q + (1-v)k - z'vp/2$, we obtain

$$(p\cdot k)(p\cdot k'') - M^2(k\cdot k'') = (p\cdot k)(p\cdot q) - M^2(k\cdot q) + (1-v)\big[(p\cdot k) - M^2k^2\big]. \tag{3.24}$$

With that, we can integrate over k'' the integrand of equation (3.12) that contains k''

dependence as follows

$$\begin{aligned}
\mathcal{I}_3 &= \int d^4k'' \frac{V(k'')}{\left[k''^2 - 2\left((1-v)k + vz'\frac{p}{2}\right)\cdot k'' + f(k,\gamma') + i\epsilon\right]^6} \\
&= \int d^4q \, \frac{V(q)}{\left[q^2 - \left((1-v)k - z'v\frac{p}{2}\right)^2 + f(k,\gamma') + i\epsilon\right]^6} \\
&= i\frac{\pi^2}{20} \, \frac{(1-v)\left[b^0_{ij,l} + b^1_{ij,l}\,(p\cdot k) + b^2_{ij,l}\,(p\cdot k)^2 + b^3_{ij,l}\,k^2\right]}{\left[-\left((1-v)k - z'v\frac{p}{2}\right)^2 + f(k,\gamma') + i\epsilon\right]^4} \\
&\quad + i\frac{\pi^2}{20} \, \frac{(1-v)\left[(p\cdot k) - M^2k^2\right]\left[d^0_{ij,l} + d^1_{ij,l}\,(p\cdot k)\right]}{\left[-\left((1-v)k - z'v\frac{p}{2}\right)^2 + f(k,\gamma') + i\epsilon\right]^4},
\end{aligned} \tag{3.25}$$

where the contribution containing $p\cdot q, k\cdot q$ is vanishing and

$$\begin{aligned}
V(k'') &= \frac{1}{B}\Big[(p\cdot k)(p\cdot k'') - M^2(k\cdot k'')\Big]\,\left[b^0_{ij,l} + b^1_{ij,l}\,(p\cdot k) + b^2_{ij,l}\,(p\cdot k)^2 + b^3_{ij,l}\,k^2\right] \\
&\quad + \Big[(p\cdot k)(p\cdot k'') - M^2(k\cdot k'')\Big]\,\left[d^0_{ij,l} + d^1_{ij,l}\,(p\cdot k)\right],
\end{aligned} \tag{3.26}$$

and after change of variables turns to be

$$\begin{aligned}
V(q) &= \Big[(p\cdot k)(p\cdot q) - M^2(k\cdot q)\Big]\left[\frac{1}{B}\left[b^0_{ij,l} + b^1_{ij,l}\,(p\cdot k) + b^2_{ij,l}\,(p\cdot k)^2 + b^3_{ij,l}\,k^2\right]\right. \\
&\quad \left. + \left[d^0_{ij,l} + d^1_{ij,l}\,(p\cdot k)\right]\right] + \left[(1-v)\big[(p\cdot k)^2 - M^2k^2\big]\right] \times \\
&\quad \times \left[\frac{1}{B}\left[b^0_{ij,l} + b^1_{ij,l}\,(p\cdot k) + b^2_{ij,l}\,(p\cdot k)^2 + b^3_{ij,l}\,k^2\right] + \left[d^0_{ij,l} + d^1_{ij,l}\,(p\cdot k)\right]\right]
\end{aligned} \tag{3.27}$$

where the contribution containing $V\cdot q$ is vanishing.

Therefore, the BS equation now has the following form

$$\int_{-1}^{+1} dz' \int_0^\infty d\gamma' \frac{g_i(\gamma', z')}{\Big[k^2 + p\cdot k z' - \gamma' - \kappa^2 + i\epsilon\Big]^3} = (\mu^2-\Lambda^2)^2 \frac{i\pi^2 (ig^2)}{2(2\pi)^4} \int_{-1}^{1} dz' \int_0^\infty d\gamma'$$
$$\times \int_0^\infty ds' \int_0^\infty ds \int_0^1 dv\; v^2(1-v)^2 \Big[\sum_l \sum_j\; P_l(s,s')\; \mathcal{C}_{ij,l}(k,p)\; g_j(\gamma', z')\Big]$$
$$\times \frac{\Big[A(v,k,z,z',\gamma';\kappa^2,\mu^2) + (1-v)\Big(\mu^2-\Lambda^2\Big)\Big]}{\Big[(k+p/2)^2 - s + i\epsilon\Big]\Big[(k-p/2)^2 - s' + i\epsilon\Big]\Big[A(v,k,z,z',\gamma';\kappa^2,\mu^2) + i\epsilon\Big]^2}$$
$$\times \frac{1}{\Big[A(v,k,z,z',\gamma';\kappa^2,\mu^2) + (1-v)\Big(\mu^2-\Lambda^2\Big) + i\epsilon\Big]^3}\,. \tag{3.28}$$

which the coefficients are written as follows

$$\begin{aligned}
\mathcal{C}_{ij,l}(k,p) &= a^0_{ij,l} + a^1_{ij,l}\;(p\cdot k) + a^2_{ij,l}\;(p\cdot k)^2 + a^3_{ij,l}\;k^2 + \\
&+ (1-v)\;\Big[b^0_{ij,l} + b^1_{ij,l}\;(p\cdot k) + b^2_{ij,l}\;(p\cdot k)^2 + b^3_{ij,l}\;k^2\Big] \\
&+ (1-v)\Big[(p\cdot k)^2 - M^2k^2\Big]\;\Big[d^0_{ij,l} + d^1_{ij,l}\;(p\cdot k)\Big],
\end{aligned} \tag{3.29}$$

3.4 Light-Front Projection

A physical system can be described in the Minkowski space by choosing a suitable set of variables, known as Light-Front dynamics. This framework considers the hypersurface tangent to the light-cone, where $x^+ = x^0 + x^3$. The four-vector x^μ in this choice of dynamics is given by $x^\mu = (x^-, x^+, x^1, x^2)$, where $x^- = x^0 - x^3$. In this section some relations will be useful such as

$$k^2_\perp = \gamma \quad , \quad k^+ = \frac{-zM}{2}, \quad k^2 = k^-k^+ - k^2_\perp \quad , \quad p\cdot k = (k^- + k^+)\frac{M}{2}, \tag{3.30}$$

so that we will have

$$(k+p/2)^2 - s = \frac{M(1-z)}{2}\Big[k^- + \frac{M}{2} - \frac{2}{M}\frac{(\gamma+s)}{(1-z)}\Big], \tag{3.31}$$

$$(k-p/2)^2 - s' = -\frac{M(1+z)}{2}\Big[k^- - \frac{M}{2} + \frac{2}{M}\frac{(\gamma+s')}{(1+z)}\Big]\,, \tag{3.32}$$

$$(p\cdot k) = \tfrac{M}{2}\left(-z\tfrac{M}{2}+k^-\right) = -z\tfrac{M^2}{4}+\tfrac{M}{2}\ k^-\,, \tag{3.33}$$

$$k^2 = -z\tfrac{M}{2}k^- - \gamma = -\gamma - z\tfrac{M}{2}k^-\,, \tag{3.34}$$

$$(p\cdot k)\ k^2 = \tfrac{M^2}{4}z\gamma - \tfrac{M}{2}\left(\gamma - z^2\tfrac{M^2}{4}\right)k^- - z\tfrac{M^2}{4}(k^-)^2\,, \tag{3.35}$$

$$(p\cdot k)^2 = z^2\tfrac{M^4}{2^4} - 2z\tfrac{M^3}{2^3}k^- + \tfrac{M^2}{4}\ (k^-)^2\,, \tag{3.36}$$

$$(p\cdot k)^3 = -z^3\tfrac{M^6}{2^6} + 3z^2\tfrac{M^5}{2^5}\ k^- - 3z\tfrac{M^4}{2^4}(k^-)^2 + \tfrac{M^3}{8}\ (k^-)^3\,. \tag{3.37}$$

Integration on k^- of the left-hand side of Eq. (3.28)

The projection of the Bethe-Salpeter equation onto the Light-Front can be done by performing an integration over k^- in both sides of the BS equation(PAULA *et al.*, 2017). Therefore, the Light-Front projection of the LHS of equation (3.28) is given as follows

$$\begin{aligned}
&\int \frac{dk^-}{2\pi}\int_{-1}^{+1} dz'\int_0^\infty d\gamma' \frac{g_i(\gamma',z')}{\Big[k^2+p\cdot kz'-\gamma'-\kappa^2+i\epsilon\Big]^3} = \\
&= \int \frac{dk^-}{2\pi}\int_{-1}^{+1} dz'\int_0^\infty d\gamma' \frac{g_i(\gamma',z')}{\Big[k^-(z'-z)M/2-\gamma-z'zM^2/4-\gamma'-\kappa^2+i\epsilon\Big]^3} \\
&= \frac{-i}{M}\int_{-1}^{+1} dz\int_0^\infty d\gamma' \frac{g_i(\gamma',z')\delta(z'-z)}{\Big[\gamma+z'zM^2/4+\gamma'+\kappa^2-i\epsilon\Big]^2} \\
&= \frac{-i}{M}\int_0^\infty d\gamma' \frac{g_i(\gamma',z)}{\Big[\gamma+z^2M^2/4+\gamma'+\kappa^2-i\epsilon\Big]^2}\,,
\end{aligned} \tag{3.38}$$

where the four-dimensional integration on k^- can be performed by considering that (YAN, 1973)

$$\int \frac{dx}{2\pi}\frac{1}{[\beta\ x-y\mp\ i\epsilon]^n} = \pm\frac{i}{n-1}\frac{\delta(\beta)}{[-y\mp\ i\epsilon]^{n-1}}\,. \tag{3.39}$$

Integration on k^- of the right-hand side of Eq. (3.28)

In the right-hand side of equation (3.28) we have three kinds of integration terms $\mathcal{V}^n_{ij}$, that after performing the change of variable to the Light-Front variables it can be

expressed as

$$\mathcal{V}^1_{ij} = \frac{g^2}{2(4\pi)^2}(\mu^2-\Lambda^2)^2\ \frac{4}{M^2}\int_0^\infty ds'\int_0^\infty ds\int_0^1 dv\ v^2\ (1-v)^2$$
$$\times\sum_l\int\frac{dk^-}{2\pi}\ \frac{P_l(s,s')\ \Big[a^0_{ij,l}+a^1_{ij,l}\ (p\cdot k)+a^2_{ij,l}\ (p\cdot k)^2+a^3_{ij,l}\ k^2\Big]}{(1-z)(1+z)\Big[k^-+\frac{M}{2}-\frac{2}{M}\frac{(\gamma+s)}{(1-z)}+i\epsilon\Big]\ \Big[k^--\frac{M}{2}+\frac{2}{M}\frac{(\gamma+s')}{(1+z)}-i\epsilon\Big]}$$
$$\times\frac{3k^-k_D^+ + 3\ell_D + (1-v)\Big(\mu^2-\Lambda^2\Big)}{\Big[k_D^+k^-+\ell_D+(1-v)\Big(\mu^2-\Lambda^2\Big)+i\epsilon\Big]^3\ \Big[k_D^+k^-+\ell_D+i\epsilon\Big]^2}\,, \quad (3.40)$$

$$\mathcal{V}^2_{ij} = \frac{g^2}{2(4\pi)^2}(\mu^2-\Lambda^2)^2\frac{4}{M^2}\int_0^\infty ds'\int_0^\infty ds\int_0^1 dv\ v^2\ (1-v)^3$$
$$\times\ \sum_l\int\frac{dk^-}{2\pi}\ \frac{P_l(s,s')\ \Big[b^0_{ij,l}+b^1_{ij,l}\ (p\cdot k)+b^2_{ij,l}\ (p\cdot k)^2+b^3_{ij,l}\ k^2\Big]}{(1-z)(1+z)\Big[k^-+\frac{M}{2}-\frac{2}{M}\frac{(\gamma+s)}{(1-z)}+i\epsilon\Big]\ \Big[k^--\frac{M}{2}+\frac{2}{M}\frac{(\gamma+s')}{(1+z)}-i\epsilon\Big]}$$
$$\times\frac{3k^-k_D^+ + 3\ell_D + (1-v)\Big(\mu^2-\Lambda^2\Big)}{\Big[k_D^+k^-+\ell_D+(1-v)\Big(\mu^2-\Lambda^2\Big)+i\epsilon\Big]^3\ \Big[k_D^+k^-+\ell_D+i\epsilon\Big]^2}\,, \quad (3.41)$$

$$\mathcal{V}^3_{ij} = \frac{g^2}{2(4\pi)^2}(\mu^2-\Lambda^2)^2\frac{4}{M^2}\int_0^\infty ds'\int_0^\infty ds\int_0^1 dv\ v^2\ (1-v)^3\times$$
$$\times\sum_l\int\frac{dk^-}{2\pi}\frac{P_l(s,s')\ \Big[(p\cdot k)^2-M^2k^2\Big]\Big[d^0_{ij,l}+d^1_{ij,l}\ (p\cdot k)\Big]}{(1-z)(1+z)\Big[k^-+\frac{M}{2}-\frac{2}{M}\frac{(\gamma+s)}{(1-z)}+i\epsilon\Big]\ \Big[k^--\frac{M}{2}+\frac{2}{M}\frac{(\gamma+s')}{(1+z)}-i\epsilon\Big]}$$
$$\times\frac{3k^-k_D^+ + 3\ell_D + (1-v)\Big(\mu^2-\Lambda^2\Big)}{\Big[k_D^+k^-+\ell_D+(1-v)\Big(\mu^2-\Lambda^2\Big)+i\epsilon\Big]^3\ \Big[k_D^+k^-+\ell_D+i\epsilon\Big]^2}\,, \quad (3.42)$$

where those can be united as: $\mathcal{L}_{ij}(\gamma,z,s;\gamma',z',s') = iM\left(\mathcal{V}^1_{ij}+\mathcal{V}^2_{ij}+\mathcal{V}^3_{ij}\right)$. In a more explicitly way we have

$$\mathcal{L}_{ij}(\gamma,z,s;\gamma',z',s') = (\mu^2-\Lambda^2)^2\ \frac{i}{M}\ \int_0^1 dv\ v^2\ (1-v)^2\ \int_0^\infty ds\int_0^\infty ds'\ \int\frac{dk^-}{2\pi}$$
$$\times\ \frac{\sum_l\ P_l(s,s')\ \mathcal{F}_{ij,l}(v,\gamma,z,k^-,p)}{\Big[(1-z)k^- + (1-z)\frac{M}{2}-\frac{2}{M}(\gamma+s)+i\epsilon\Big]\ \Big[(1+z)k^- - (1+z)\frac{M}{2}+\frac{2}{M}(\gamma+s')-i\epsilon\Big]}$$
$$\times\ \frac{3k^-k_D^+ + 3\ell_D + (1-v)\Big(\mu^2-\Lambda^2\Big)}{\Big[k_D^+k^-+\ell_D+(1-v)\Big(\mu^2-\Lambda^2\Big)+i\epsilon\Big]^3\ \Big[k_D^+k^-+\ell_D+i\epsilon\Big]^2}\,, \quad (3.43)$$

with

$$\mathcal{F}_{ij,l}(v,\gamma,z,k^-,p) = F_{0;ij,l} + k^-\ F_{1;ij,l} + (k^-)^2\ F_{2;ij,l} + (k^-)^3\ F_{3;ij,l}. \tag{3.44}$$

with $F_{n;ij,l}$ are explicitly written in Appendix C. Therefore, after a light-front projection, we rewrite the equation (3.28), thus having the Bethe-Salpeter equation written as

$$\int_0^\infty d\gamma' \frac{g_i(\gamma',z)}{\Big[\gamma + z^2M^2/4 + \gamma' + \kappa^2 - i\epsilon\Big]^2} = \frac{\alpha}{2\pi}\sum_j \int_{-1}^1 dz' \int_0^\infty d\gamma' \mathcal{L}_{ij}(\gamma,z,s;\gamma',z',s')\, g_j(\gamma',z')\,, \tag{3.45}$$

where $\alpha = \frac{g^2}{4\pi}$.

Another way of writing the $\mathcal{L}_{ij}(\gamma,z,s;\gamma',z',s')$ terms is

$$\begin{aligned}\mathcal{L}_{ij}(\gamma,z,s;\gamma',z',s') &= \frac{i(\mu^2-\Lambda^2)^2}{M}\int_0^1 dv\ v^2(1-v)^2 \sum_l P_l(s,s') \\ &\quad \times \sum_{n=0}^{3} F_{n;ij,l}(v,\gamma,z,p)\mathcal{C}_n\,,\end{aligned} \tag{3.46}$$

which the $\mathcal{C}_n$ terms carries the dk^- integral terms. We have non-singular and singular terms. It is necessary to take into account the poles in the denominators to classify those. From now on, we omit the dependence $(\gamma,z,s;\gamma',z',s')$ to simplify the notation, i.e. $\mathcal{L}_{ij} \equiv \mathcal{L}_{ij}(\gamma,z,s;\gamma',z',s')$.

Non-singular contributions to $\mathcal{L}_{ij}$

Now we will solve the integration through Cauchy's integral theorem. Therefore we need to determine the position of the poles, paying attention to k_D^+ in particular. Looking at $\mathcal{C}_n$, that is explicitly written as

$$\begin{aligned}\mathcal{C}_n &= \int \frac{dk^-}{2\pi} \frac{(k^-)^n\ \Big[3k^-k_D^+ + 3\ell_D + (1-v)\Big(\mu^2-\Lambda^2\Big)\Big]}{\Big[(1-z)k^- - (1-z)k_d^- + i\epsilon\Big]\ \Big[(1+z)k^- - (1+z)k_u^- - i\epsilon\Big]} \\ &\quad \times \frac{1}{\Big[k_D^+k^- + \ell_D + (1-v)\Big(\mu^2-\Lambda^2\Big) + i\epsilon\Big]^3\ \Big[k_D^+k^- + \ell_D + i\epsilon\Big]^2}\,,\end{aligned} \tag{3.47}$$

where

$$
\begin{aligned}
k_u^- &= \frac{M}{2} - \frac{2}{M(1+z)}(\gamma + s') = \frac{2}{M(1+z)}\ \left[\frac{M^2}{4}(1+z) - (\gamma + s')\right] \\
k_d^- &= -\frac{M}{2} + \frac{2}{M(1-z)}(\gamma + s) = -\frac{2}{M(1-z)}\ \left[\frac{M^2}{4}(1-z) - (\gamma + s)\right] \\
k_D^+ &= v(1-v)\Big(k^+ + z'\frac{M}{2}\Big) = v(1-v)\frac{M}{2}(z'-z)\,, \\
\ell_D &= -v(1-v)\Big(\gamma + zz'\frac{M^2}{4}\Big) - v^2 z'^2\frac{M^2}{4} - v(\gamma' + \kappa^2) - (1-v)\mu^2\,, \qquad (3.48)
\end{aligned}
$$

if we consider that $k_D^+ \neq 0$ and $k_D^+ > 0$, we can perform a closed curve in the upper semi-plane and get the residue at the pole k_u^-. Thus we obtain

$$
\begin{aligned}
\mathcal{C}_n^+(\eta) &= \frac{i}{(1-z^2)}\ \theta(k_D^+ - \eta)\ \frac{(k_u^-)^n\ \Big[3k_u^- k_D^+ + 3\ell_D + (1-v)\Big(\mu^2 - \Lambda^2\Big)\Big]}{\Big[k_u^- - k_d^- + i\epsilon\Big]} \\
&\quad \times \frac{1}{\Big[k_D^+ k_u^- + \ell_D + (1-v)\Big(\mu^2 - \Lambda^2\Big) + i\epsilon\Big]^3\ \Big[k_D^+ k_u^- + \ell_D + i\epsilon\Big]^2}\,, \\
&= i\,\theta(k_D^+ - \eta)\ (1+z)^4\ \frac{M}{4}\ \frac{(k_u^-)^n}{\Big[\gamma + s'/2 + s/2 + z(s-s')/2 - (1-z^2)M^2/4 - i\epsilon\Big]} \\
&\quad \times \frac{\Big[-3D(\gamma, -z, \gamma', -z', v) + (1-v)(1+z)\Big(\mu^2 - \Lambda^2\Big)\Big]}{\Big[D(\gamma, -z, \gamma', -z', v) - (1-v)(1+z)\Big(\mu^2 - \Lambda^2\Big) - i\epsilon(1+z)\Big]^3} \\
&\quad \times \frac{1}{\Big[D(\gamma, -z, \gamma', -z', v) - i\epsilon(1+z)\Big]^2}, \qquad (3.49)
\end{aligned}
$$

where in the denominator we used the following relations

$$
\begin{aligned}
k_D^+ k_u^- + \ell_D &= \frac{-1}{1+z} D(\gamma, -z, \gamma', -z', v)\,, \qquad (3.50) \\
(1-z^2)\ (k_u^- - k_d^-) &= -\frac{4}{M}\ \Big[\gamma + s'/2 + s/2 + z(s-s')/2 - (1-z^2)M^2/4\Big], \qquad (3.51)
\end{aligned}
$$

which $D(\gamma, -z, \gamma', -z', v) = v^2\,A + v\,B + C$ and

$$
\begin{aligned}
A &= (z'-z)\big[(1+z)M^2/4 - (\gamma + s')\big] - (1+z)(\gamma + (zz' - z'^2)M^2/4), \\
B &= (z-z')\big[(1+z)M^2/4 - (\gamma + s')\big] + (1+z)(\gamma + zz'M^2/4 + \gamma' + \kappa^2 - \mu^2), \\
C &= (1+z)\mu^2. \qquad (3.52)
\end{aligned}
$$

Analogously, for $k_D^+ < 0$ we can close in lower semi-plane, taking the residue at k_d^-,

obtaining the following result

$$\begin{aligned}
\mathcal{C}_n^-(\eta) &= -\frac{i}{(1-z^2)}\,\theta(-\eta-k_D^+)\,\frac{(k_d^-)^n\,\Big[3k_d^-k_D^+ + 3\ell_D + (1-v)\Big(\mu^2-\Lambda^2\Big)\Big]}{\Big[k_d^- - k_u^- - i\epsilon\Big]} \\
&\quad\times\frac{1}{\Big[k_D^+k_d^- + \ell_D + (1-v)\Big(\mu^2-\Lambda^2\Big) + i\epsilon\Big]^3\,\Big[k_D^+k_d^- + \ell_D + i\epsilon\Big]^2}\,, \\
&= -i\,\theta(-k_D^+-\eta)\,(1-z)^4\,\frac{M}{4}\,\frac{(k_d^-)^n}{\Big[\gamma + s'/2 + s/2 + z(s-s')/2 - (1-z^2)M^2/4 + i\epsilon\Big]} \\
&\quad\times\frac{[3D(\gamma,z,\gamma',z',v,s) + (1-v)(1-z)(\Lambda^2-\mu^2)]}{\Big[D(\gamma,z,\gamma',z',v,s) - (1-v)(1-z)(\mu^2-\Lambda^2) - i\epsilon(1-z)\Big]^3} \\
&\quad\times\frac{1}{\Big[D(\gamma,z,\gamma',z',v,s) - i\epsilon(1-z)\Big]^2}\,. \qquad (3.53)
\end{aligned}$$

with

$$k_D^+k_d^- + \ell_D = -\frac{1}{1-z}D(\gamma,z,\gamma',z',v)\,, \qquad (3.54)$$

with $D(\gamma,z,\gamma',z',v) = D(\gamma,-z,\gamma',-z',v)\big|_{z\to-z}$. Now with the those resulting C_n we will build the non-singular $\mathcal{L}_{ij}^{NS}$ contributions. Those are written as

$$\begin{aligned}
\mathcal{L}_{ij}^{NS} &= -\frac{i}{M}\,(\mu^2-\Lambda^2)^2\;\frac{(1-z)^4}{4}\;\int_0^1 dv\;v^2\;(1-v)^2\;\theta(-k_D^+) \\
&\quad\times\int_0^\infty ds'\int_0^\infty ds\sum_l P_l(s,s')\;\mathcal{F}_{ij,l}^{NS}(v,\gamma,z,k_d^-,p) \\
&\quad\times\frac{1}{\Big[\gamma + s'/2 + s/2 + z(s-s')/2 - (1-z^2)M^2/4 + i\epsilon\Big]} \\
&\quad\times\frac{\Big[3D(\gamma,z,\gamma',z',v,s) + (1-v)(1-z)\Big(\Lambda^2-\mu^2\Big)\Big]}{\Big[D(\gamma,z,\gamma',z',v,s) - (1-v)(1-z)\Big(\mu^2-\Lambda^2\Big) - i\epsilon(1-z)\Big]^3} \\
&\quad\times\frac{1}{\Big[D(\gamma,z,\gamma',z',v,s) - i\epsilon(1-z)\Big]^2} + \Big[z\to(-z)\text{ and }z'\to(-z')\Big], \qquad (3.55)
\end{aligned}$$

which under the transformation $(z \to -z, z' \to -z', s \to s')$ obey the relations

$$k_D^+ \to -k_D^+, \tag{3.56a}$$
$$\ell_D \to \ell_D, \tag{3.56b}$$
$$k_d^- \to -k_u^- \tag{3.56c}$$
$$D(\gamma, z, \gamma', z', v) \to D(\gamma, -z, \gamma', -z', v) \tag{3.56d}$$

As well we have

$$\begin{aligned}
k_D^+ &= v(1-v)M(z'-z)/2\,, \\
k_d^- &= -\frac{2}{M(1-z)}\left[\frac{M^2}{4}(1-z) - \gamma - s\right], \\
\mathcal{F}^{NS}_{ij,l}(v,\gamma,z,k_d^-,p) &= F_{0;ij,l} + k_d^-\ F_{1;ij,l} + (k_d^-)^2\ F_{2;ij,l} + (k_d^-)^3\ F_{3;ij,l}\,, \\
D(\gamma,z,\gamma',z',v) &= v^2(z-z')\big[(1-z)M^2/4 - (\gamma+s)\big] - v^2(1-z)(\gamma + (zz' - z'^2)M^2/4) \\
&\quad + v(z'-z)\big[(1-z)M^2/4 - (\gamma+s)\big] + v(1-z)(\gamma + zz'M^2/4) \\
&\quad + v(1-z)(\gamma' + \kappa^2 - \mu^2) + (1-z)\mu^2\,.
\end{aligned} \tag{3.57}$$

Singular Contributions to $\mathcal{L}_{ij}$

Now we should carefully consider the value of C_n in the case of $k_D^+ = 0$, which means to consider when $z' = z$. The C_n can be written as

$$\mathcal{C}_n = 3\ \mathcal{B}(n) - (1-v)\Big(\mu^2 - \Lambda^2\Big)\ \frac{\partial}{\partial E}\mathcal{B}(n)\ , \tag{3.58}$$

where

$$\begin{aligned}
\mathcal{B}(n) &= \int \frac{dk^-}{2\pi} \frac{(k^-)^n}{\Big[(1-z)k^- - (1-z)k_d^- + i\epsilon\Big]\ \Big[(1+z)k^- - (1+z)k_u^- - i\epsilon\Big]} \\
&\times \quad \frac{1}{\Big[k_D^+ k^- + C + i\epsilon\Big]^3\ \Big[k_D^+ k^- + E + i\epsilon\Big]}\ ,
\end{aligned} \tag{3.59}$$

with $C = \ell_D + (1-v)\Big(\mu^2 - \Lambda^2\Big)$ and $E = \ell_D$, with ℓ_D given in equation (3.48). At this point, we should remember that n varies between zero and three. Thus we need to consider C_n for each value of n. For $n = 0$, we have

$$\begin{aligned}
\mathcal{B}(0) &= \int \frac{dk^-}{2\pi} \frac{(k^-)^0}{\Big[(1-z)k^- - (1-z)k_d^- + i\epsilon\Big]\ \Big[(1+z)k^- - (1+z)k_u^- - i\epsilon\Big]} \\
&\times \quad \frac{1}{\Big[k_D^+ k^- + C + i\epsilon\Big]^3\ \Big[k_D^+ k^- + E + i\epsilon\Big]}\ ,
\end{aligned} \tag{3.60}$$

if we consider the integral $I_M^{(0)}$ as follow in equation (3.61), we can rewrite $\mathcal{B}(0)$ in terms of it.

$$\begin{aligned} I_M^{(0)} &= \int \frac{dk^-}{2\pi} \frac{1}{\Big[(1-z)k^- - (1-z)k_d^- + i\epsilon\Big]\ \Big[(1+z)k^- - (1+z)k_u^- - i\epsilon\Big]} \\ &\times \frac{1}{\Big[k_D^+ k^- + C + i\epsilon\Big]\ \Big[k_D^+ k^- + E + i\epsilon\Big]} \ . \end{aligned} \tag{3.61}$$

Looking at equation (3.61), we apply the residue theorem to evaluate $I_M^{(0)}$ taking the following considerations: i. one pole at $k_u^- + i\epsilon/(1+z) \in$ the upper plane; ii. one pole at $k_d^- - i\epsilon/(1-z) \in$ the lower plane; iii. one pole at $-C/k_D^+ - i\epsilon/k_D^+$; iv. one pole at $-E/k_D^+ - i\epsilon/k_D^+$. The result after the application of the Cauchy's integration in $I_M^{(0)}$ is

$$\begin{aligned} I_M^{(0)} = \frac{i}{(1-z^2)} \Big\{ &\frac{\theta(k_D^+)}{\Big[k_u^- - k_d^-\Big]\ \Big[k_D^+ k_u^- + C + i\epsilon\Big]\ \Big[k_D^+ k_u^- + E + i\epsilon\Big]} \\ &- \frac{\theta(-k_D^+)}{\Big[k_d^- - k_u^-\Big]\ \Big[k_D^+ k_d^- + C + i\epsilon\Big]\ \Big[k_D^+ k_d^- + E + i\epsilon\Big]} \Big\} \ . \end{aligned} \tag{3.62}$$

Therefore $\mathcal{B}(0)$ will be expressed as

$$\begin{aligned} \mathcal{B}(0) &= \frac{1}{2}\frac{\partial^2}{\partial C^2}\ I_M^{(0)} \\ &= i\frac{1}{(1-z^2)}\ \frac{1}{\Big[k_u^- - k_d^-\Big]} \Big\{ \frac{\theta(k_D^+)}{\Big[k_D^+ k_u^- + C + i\epsilon\Big]^3\ \Big[k_D^+ k_u^- + E + i\epsilon\Big]} \\ &+ \frac{\theta(-k_D^+)}{\Big[k_D^+ k_d^- + C + i\epsilon\Big]^3\ \Big[k_D^+ k_d^- + E + i\epsilon\Big]} \Big\} \ . \end{aligned} \tag{3.63}$$

It does not contain any singular contribution, leading to the expression of C_0 as follow

$$\mathcal{C}_0 = \lim_{\eta\to 0}\Big[\mathcal{C}_0^+(\eta) + \mathcal{C}_0^-(\eta)\Big] = 3\ \mathcal{B}(0) - (1-v)\Big(\mu^2 - \Lambda^2\Big)\ \frac{\partial}{\partial E}\mathcal{B}(0) \ . \tag{3.64}$$

To $n = 1, 2, 3$, we will perform the same ideas where the next calculations are more explicitly done in Appendix E. The term $\mathcal{B}(1)$ has the first power of k^-, and it is given by

$$\mathcal{B}(1) = \frac{1}{(1+z)}\frac{1}{2}\frac{\partial^2}{\partial C^2}\ I_M^{(1)} + k_u^-\ \mathcal{B}(0) \ , \tag{3.65}$$

where

$$I_M^{(1)} = \int \frac{dk^-}{2\pi} \frac{1}{\Big[(1-z)k^- - (1-z)k_d^- + i\epsilon\Big]} \; \frac{1}{\Big[k_D^+ k^- + C + i\epsilon\Big] \; \Big[k_D^+ k^- + E + i\epsilon\Big]} \, . \tag{3.66}$$

Solving the integration in k^- we obtain

$$I_M^{(1)} = -i \; \frac{1}{(1-z)} \; \frac{\theta(-k_D^+)}{[k_d^- k_D^+ + E] \; [k_d^- k_D^+ + C]} \, , \tag{3.67}$$

which means we have

$$\begin{aligned} \mathcal{B}(1) \;\; &= \;\; i \; \frac{1}{(1-z^2)} \; \frac{1}{(k_u^- - k_d^-)} \; \Bigg[\frac{k_u^- \; \theta(k_D^+)}{\Big[k_D^+ k_u^- + C + i\epsilon\Big]^3 \; \Big[k_D^+ k_u^- + E + i\epsilon\Big]} \\ &+ \frac{k_d^- \; \theta(-k_D^+)}{[k_d^- k_D^+ + C]^3 \; [k_d^- k_D^+ + E]} \Bigg] \, . \end{aligned} \tag{3.68}$$

In conclusion, there is no singular correction for $\mathcal{B}(1)$. Therefore one can verify that

$$\mathcal{C}_1 = \lim_{\eta \to 0} \Big[\mathcal{C}_1^+(\eta) + \mathcal{C}_1^-(\eta) \Big] = 3 \; \mathcal{B}(1) - (1-v) \Big(\mu^2 - \Lambda^2 \Big) \; \frac{\partial}{\partial E} \mathcal{B}(1) \, . \tag{3.69}$$

The next term is $\mathcal{B}(2)$, that can be written as

$$\mathcal{B}(2) \;\; = \;\; \frac{1}{2} \; \frac{1}{(1-z^2)} \; \frac{\partial^2}{\partial C^2} I_M^{(2)} + (k_u^- + k_d^-) \; \mathcal{B}(1) - k_u^- \; k_d^- \; \mathcal{B}(0) \, . \tag{3.70}$$

where

$$I_M^{(2)} = \int \frac{dk^-}{2\pi} \; \frac{1}{\Big[k_D^+ k^- + C + i\epsilon\Big] \; \Big[k_D^+ k^- + E + i\epsilon\Big]} \, . \tag{3.71}$$

In this case we need consider the following relation

$$\int_{-\infty}^{\infty} dx \; \frac{1}{\Big[\beta \; x - y \mp i\epsilon\Big]^2} = \; \pm (2\pi) i \; \frac{\delta(\beta)}{\Big[-y \mp i\epsilon\Big]} \, , \tag{3.72}$$

Thus we have

$$I_M^{(2)} \;\; = \;\; -i \frac{\delta(k_D^+)}{(E-C)} \; \ln\left(\frac{E}{C}\right) \, , \tag{3.73}$$

$$\frac{1}{2} \; \frac{\partial^2}{\partial C^2} I_M^{(2)} \;\; = \;\; -i \; \delta(k_D^+) \frac{1}{(E-C)^2} \; \left[\frac{1}{(E-C)} \; \ln\left(\frac{E}{C}\right) + \frac{(E-3C)}{2C^2} \right] \tag{3.74}$$

Then one gets $\mathcal{B}(2)$ composed of two terms, one that is the singular part while and the second term yields the standard contribution, as we can see in the following equation:

$$\mathcal{B}(2) = -\frac{i}{(1-z^2)}\ \delta(k_D^+)\ \mathcal{S}_2(C,E) + \mathcal{B}^{NS}(2)\ , \tag{3.75}$$

with

$$\begin{aligned}
\mathcal{B}^{NS}(2) &= \frac{i}{(1-z^2)}\ \frac{1}{(k_u^- - k_d^-)}\ \frac{(k_u^-)^2\ \theta(k_D^+)}{\Big[k_D^+ k_u^- + C + i\epsilon\Big]^3\ \Big[k_D^+ k_u^- + E + i\epsilon\Big]} \\
&\quad + \frac{i}{(1-z^2)}\ \frac{1}{(k_u^- - k_d^-)}\ \frac{(k_d^-)^2\ \theta(-k_D^+)}{[k_d^- k_D^+ + C]^3\ [k_d^- k_D^+ + E]}\Bigg] \qquad (3.76) \\
\mathcal{S}_2(C,E) &= \frac{1}{(E-C)^2}\ \left[\frac{1}{(E-C)}\ \ln\left(\frac{E}{C}\right) + \frac{(E-3C)}{2C^2}\right]\ . \qquad (3.77)
\end{aligned}$$

Then singular contribution of $\mathcal{B}(2)$ will give us the expression $\mathcal{C}_2$ as one can see in the following expression

$$\begin{aligned}
\mathcal{C}_2 &= 3\ \mathcal{B}(2) - (1-v)\Big(\mu^2 - \Lambda^2\Big)\ \frac{\partial}{\partial E}\mathcal{B}(2) \\
&= -\frac{i}{(1-z^2)}\ \delta(k_D^+)\ \Big[3\ \mathcal{S}_2(C,E) + (E-C)\ \frac{\partial}{\partial E}\mathcal{S}_2(C,E)\Big] \\
&\quad + \lim_{\eta\to 0}\Big[\mathcal{C}_2^+(\eta) + \mathcal{C}_2^-(\eta)\Big]\ , \qquad (3.78)
\end{aligned}$$

with $E - C = -(1-v)\ (\mu^2 - \Lambda^2)$. Also, we have to pay attention to the singular behavior for $v = 1$. Now considering that

$$3\ \mathcal{S}_2(C,E) + (E-C)\ \frac{\partial}{\partial E}\mathcal{S}_2(C,E) = \frac{1}{EC^2}\ . \tag{3.79}$$

The singular contribution to $\mathcal{C}_2$ will be

$$\mathcal{C}_2^S = -\frac{i}{(1-z^2)}\ \delta(k_D^+)\ \frac{1}{EC^2}. \tag{3.80}$$

The last integral is $\mathcal{B}(3)$ that can be expressed as

$$\mathcal{B}(3) = \frac{1}{(1-z^2)} I_M^{(3)} - \frac{1}{2}\ \frac{E}{k_D^+(1-z^2)}\ \frac{\partial^2}{\partial C^2} I_M^{(2)} + (k_u^- + k_d^-)\ \mathcal{B}(2) - k_u^-\ k_d^- \mathcal{B}(1)\ . \tag{3.81}$$

with

$$I_M^{(3)} = \frac{1}{k_D^+}\int \frac{dk^-}{2\pi}\frac{1}{\Big[k_D^+ k^- + C + i\epsilon\Big]^3} = \frac{i}{2}\ \frac{\delta'(k_D^+)}{[C+i\epsilon]^2}\,. \tag{3.82}$$

We observe that it was used that $\frac{\delta(x)}{x} = -\delta'(x)$ and

$$\int_{-\infty}^{\infty} dx \; \frac{1}{\Big[\beta\; x - y \mp i\epsilon\Big]^3} = \pm\pi i \; \frac{\delta'(\beta)}{\Big[-y \mp i\epsilon\Big]^2} \; . \tag{3.83}$$

Then $\mathcal{B}(3)$ is explicitly written as

$$\begin{aligned}
\mathcal{B}(3) \;\; = \;\; & \frac{i}{2(1-z^2)}\; \delta'(k_D^+) \left[\frac{1}{C^2} - 2E\; \mathcal{S}_2(C,E)\right] - \frac{i}{(1-z^2)}(k_u^- + k_d^-)\; \delta(k_D^+)\; \mathcal{S}_2(C,E) \\
& + \frac{i}{(1-z^2)} \frac{1}{(k_u^- - k_d^-)} \Bigg[\frac{(k_u^-)^3 \theta(k_D^+)}{\Big[k_D^+ k_u^- + C + i\epsilon\Big]^3 \Big[k_D^+ k_u^- + E + i\epsilon\Big]} \\
& + \frac{(k_d^-)^3 \theta(-k_D^+)}{[k_d^- k_D^+ + C]^3 [k_d^- k_D^+ + E]} \Bigg] .
\end{aligned} \tag{3.84}$$

Thus having $\mathcal{C}_3 = \big(3\; \mathcal{B}(3) - (1-v)\big(\mu^2 - \Lambda^2\big)\; \frac{\partial}{\partial E}\mathcal{B}(3)\big)$ and $\mathcal{B}(3)$ as given in equation (3.84), the singular part of it will be

$$\begin{aligned}
\mathcal{C}_3^S \;\; = \;\; & \frac{i}{2(1-z^2)}\; \delta'(k_D^+)\; \left[\frac{3}{C^2} - \frac{2}{C^2} - 2(E-C)\mathcal{S}_2(C,E)\right] + (k_u^- + k_d^-)\; \mathcal{C}_2^S \\
= \;\; & \frac{i}{(1-z^2)} \delta'(k_D^+) \frac{1}{(E-C)} \left[\frac{1}{C} - \frac{1}{(E-C)} \ln\left(\frac{E}{C}\right)\right] \\
& + \frac{2}{M} \frac{2z\gamma - s' + s + z(s'+s)}{(1-z^2)} \mathcal{C}_2^S
\end{aligned} \tag{3.85}$$

The singular functions $\mathcal{C}_2^S$ and $\mathcal{C}_3^S$ are proportional to distributions such as $\delta(z'-z)$ or $\delta'(z'-z)$ as we can see in equation (3.80) and (3.85), respectively. It is suitable to write the delta function of k_D^+ as $\delta(z'-z)$ and do the same to the derivative of the delta. As one can see in equation (3.57), we have k_D^+ with dependence in z' and z. Thus we can write

$$\delta(k_D^+) = \frac{2\; \delta(z'-z)}{M\; v(1-v)} \; ; \; \frac{\partial}{\partial k_D^+}\delta(k_D^+) = \frac{4}{[M\; v(1-v)]^2} \; \Big[\frac{\partial}{\partial z'}\delta(z'-z)\Big] . \tag{3.86}$$

In particular, it should be pointed out that C, $E = \ell_D$, $\delta(k_D^+)$ and $\delta'(k_D^+)$ are even for the exchanges $z \to -z$ and $z' \to -z'$, as easily seen bellow

$$\begin{aligned}
C \;\; & = \;\; \ell_D + (1-v)\Big(\mu^2 - \Lambda^2\Big) \; , \\
E \;\; & = \;\; \ell_D = -v(1-v)\Big(\gamma + zz'\frac{M^2}{4}\Big) - v^2 z'^2 M^2/2 - v(\gamma' + \kappa^2) - (1-v)\mu^2 \; .
\end{aligned} \tag{3.87}$$

Therefore, by taking those considerations and defining

$$D_\ell = \Big[\tilde{\ell}_D + (1-v)\Big(\mu^2 - \Lambda^2\Big)\Big]^2 \; \tilde{\ell}_D \; ; \; \tilde{\ell}_D = \ell_D\Big|_{z'=z} \, , \tag{3.88}$$

one has for $\mathcal{C}_2^S$

$$\mathcal{C}_2^S = -\frac{i}{1-z^2} \; \delta(k_D^+) \; \frac{1}{C^2 E} = -\frac{i}{M} \; \frac{\delta(z'-z)}{v(1-v)(1-z^2)} \; \frac{2}{D_\ell} \, , \tag{3.89}$$

and for $\mathcal{C}_3^S$

$$\begin{aligned} \mathcal{C}_3^S &= \frac{i}{(1-z^2)} \; \delta'(k_D^+) \; \frac{1}{(E-C)} \left\{ \frac{1}{C} - \frac{1}{(E-C)} \; \ln\left(\frac{E}{C}\right) \right\} \\ &\quad + \frac{2}{M} \; \frac{2z\gamma - s' + s + z(s'+s)}{(1-z^2)} \mathcal{C}_2^S \\ &= -\frac{i}{M} \; \frac{4}{M \; v(1-v)(1-z^2)} \; \Big[\frac{\mathcal{D}_3^S}{v(1-v)} \\ &\quad + \frac{\delta(z'-z)(2z\gamma - s' + s + z(s'+s))}{(1-z^2) \; D_\ell} \Big], \end{aligned} \tag{3.90}$$

with

$$\begin{aligned} \mathcal{D}_3^S &= \frac{1}{\Big[(1-v)\Big(\mu^2 - \Lambda^2\Big)\Big]^2} \; \Big[\frac{\partial}{\partial z'} \delta(z'-z) \Big] \\ &\times \left[\frac{(1-v)\Big(\mu^2 - \Lambda^2\Big)}{\Big[\ell_D + (1-v)\Big(\mu^2 - \Lambda^2\Big)\Big]} + \ln\left\{ \frac{\ell_D}{\Big[\ell_D + (1-v)\Big(\mu^2 - \Lambda^2\Big)\Big]} \right\} \right] \, . \end{aligned} \tag{3.91}$$

Finally, from equation (3.46), one can write $\mathcal{L}_{ij}^S$ as

$$\begin{aligned} \mathcal{L}_{ij}^S &= \frac{i(\mu^2 - \Lambda^2)^2}{M} \int_0^1 dv v^2 (1-v)^2 \int_0^\infty ds \int_0^\infty ds' \sum_l P_l \\ &\quad \times \Big[F_{2;ij,l}(v,\gamma,z) \mathcal{C}_2^S + F_{3;ij,l}(v,\gamma,z) \mathcal{C}_3^S \Big] \\ &= \frac{2}{M^2} \frac{(\mu^2 - \Lambda^2)^2}{(1-z^2)} \; \int_0^1 dv \; v \; (1-v) \sum_l \; P_l \\ &\quad \times \; \Big\{ \delta(z'-z) \; \frac{1}{D_\ell} \Big[F_{2;ij,l}(v,\gamma,z) + 2 \frac{(2z\gamma - s' + s + z(s'+s))}{M \; (1-z^2)} F_{3;ij,l}(v,\gamma,z) \Big] \\ &\quad + \frac{2}{v(1-v)M} \; F_{3;ij,l}(v,\gamma,z) \; \mathcal{D}_3^S \Big\} \, , \end{aligned} \tag{3.92}$$

with $F_{n;ij,l}$ derived in Appendix C. In particular:

$$\begin{aligned} F_{2;ij,l} &= \frac{M^2}{4}\left\{a^2_{ij} + (1-v)b^2_{ij,l} + (1-v)d^0_{ij,l} + (1-v)\frac{M^2}{4}z\ d^1_{ij,l}\right\}, \\ F_{3;ij,l} &= (1-v)\ \frac{M^3}{8}\ d^1_{ij,l}\ . \end{aligned} \tag{3.93}$$

If one consider the only non-zero $F_{n;ij,l}$ terms present in Appendix C, the surviving singular contributions will be

$$\begin{aligned} \mathcal{L}^S_{13} &= \frac{2}{M^2}\frac{(\mu^2-\Lambda^2)^2}{(1-z^2)}\ \int_0^1 dv\ v\ (1-v)^2\Big\{\frac{\delta(z'-z)}{4M\ D_\ell} \\ &\quad\times\int_0^\infty ds\int_0^\infty ds'\Big[\rho_V(s,)\rho_S(s') - \rho_S(s,)\rho_V(s')\Big]\Big\}\ , \end{aligned} \tag{3.94}$$

$$\mathcal{L}^S_{14} = -\frac{2}{M^2}\frac{(\mu^2-\Lambda^2)^2}{(1-z^2)}\int_0^1 v(1-v)^2dv\frac{\delta(z'-z)}{4D_\ell}\int_0^\infty ds\int_0^\infty ds'\rho_V(s,)\rho_V(s')\,, \tag{3.95}$$

$$\mathcal{L}^S_{22} = -\frac{1}{M^2}\frac{(\mu^2-\Lambda^2)^2}{(1-z^2)}\int_0^1 v(1-v)dv\frac{\delta(z'-z)}{D_\ell}\int_0^\infty ds\int_0^\infty ds'\rho_V(s,)\rho_V(s')\,, \tag{3.96}$$

$$\begin{aligned} \mathcal{L}^S_{23} &= -\frac{2}{M^2}\frac{(\mu^2-\Lambda^2)^2}{2(1-z^2)}\int_0^1 dv\ v(1-v)\int_0^\infty ds\int_0^\infty ds'\rho_V(s,)\rho_V(s') \\ &\times\Bigg[(1-v)\delta(z'-z)\frac{1}{4D_\ell}\Big[z+4\frac{(2z\gamma - s'+s+z(s'+s))}{M^2(1-z^2)}\Big] + \frac{1}{vM^2}\frac{1}{\Big[(1-v)(\mu^2-\Lambda^2)\Big]^2} \\ &\times\left[\frac{\partial}{\partial z'}\delta(z'-z)\right]\left[\frac{(1-v)(\mu^2-\Lambda^2)}{\big(\ell_D+(1-v)(\mu^2-\Lambda^2)\big)} + \ln\left[\frac{\ell_D}{\big(\ell_D+(1-v)(\mu^2-\Lambda^2)\big)}\right]\right]\Bigg], \end{aligned} \tag{3.97}$$

$$\begin{aligned} \mathcal{L}^S_{24} &= -\frac{2}{M^2}\frac{(\mu^2-\Lambda^2)^2}{(1-z^2)}\int_0^1 dv\ v\ (1-v)^2\Big\{\delta(z'-z)\ \frac{1}{4M\ D_\ell} \\ &\quad\times\int_0^\infty ds\int_0^\infty ds'\Big[\rho_V(s,)\rho_S(s') + \rho_S(s,)\rho_V(s')\Big]\Big\}\,, \end{aligned} \tag{3.98}$$

$$\mathcal{L}^S_{33} = \frac{1}{M^2}\frac{(\mu^2-\Lambda^2)^2}{(1-z^2)}\int_0^1 v(1-v)^2dv\frac{\delta(z'-z)}{D_\ell}\int_0^\infty ds\int_0^\infty ds'\rho_V(s,)\rho_V(s')\,. \tag{3.99}$$

Furthermore, with the results present in equations (3.55) and (3.95)-(3.99), the com-

plete BS equation is now expressed as follow

$$\int_0^\infty d\gamma' \frac{g_i(\gamma', z)}{\Big[\gamma + z^2 M^2/4 + \gamma' + \kappa^2 - i\epsilon\Big]^2} = \frac{\alpha}{2\pi} \sum_j \int_{-1}^{1} dz' \int_0^\infty d\gamma' \times \left[\mathcal{L}_{ij}^{NS}(\gamma, z, s, s'; \gamma', z') + \mathcal{L}_{ij}^{S}(\gamma, z, s, s'; \gamma', z')\right] g_j(\gamma', z') \quad (3.100)$$

with $\alpha = \frac{g^2}{4\pi}$. This equation is almost ready for using a numerical method to obtain the relation between the coupling constant and the binding energy. It is still necessary to deal with the delta functions present in the singular terms and with the theta functions present in the non-singular terms. The numerical method chosen for this work is the discretization of the Nakanishi weight function $g_i(\gamma, z)$ onto a bi-orthogonal basis of Laguerre (to γ variable) and Gegenbauer polynomials (to z variable). Thus, in doing that we reduce the BS equation into a generalized eigenvalue problem, where the coupling constant α is the eigenvalue.

3.5 Explicit Removal of the Theta and Delta Functions

To perform the numerical calculations it is important to explicitly remove the theta functions in equation (3.55), and the delta functions in equations (3.95)-(3.99). This can be done by carefully considering the integrations over z' in equation (3.56). We first consider the non-singular contribution. One can rewrite $\mathcal{L}_{ij}^{(ns)}$ as

$$\mathcal{L}_{ij}^{(ns)}(\gamma, z, s, s'; \gamma', z') = \theta(z - z')\mathcal{L}_{ij}^{(ns,1)}(\gamma, z, s, s'; \gamma', z') + \theta(z' - z)\mathcal{L}_{ij}^{(ns,2)}(\gamma, z, s, s'; \gamma', z'), \quad (3.101)$$

where

$$\begin{aligned}\mathcal{L}_{ij}^{(ns,1)}(\gamma, z, s, s'; \gamma', z') &= \frac{1}{4}(\mu^2 - \Lambda^2)^2 \\ &\times \int_0^\infty ds' \int_0^\infty ds \frac{\sum_l P_l \, \mathcal{F}_{ij,l}^{NS}(v, \gamma, z, k_d^-, p)}{\Big[\gamma + s'/2 + s/2 + z(s - s')/2 - (1 - z^2)M^2/4 + i\epsilon\Big]} \\ &\times \int_0^1 dv \frac{v^2(1 - v)^2\big[3k_d^- k_D^+ + 3\ell_D + (1 - v)(\mu^2 - \Lambda^2)\big]}{\big[k_D^+ k_d^- + \ell_D + (1 - v)(\mu^2 - \Lambda^2) + i\epsilon\big]^3 \big[k_D^+ k_d^- + \ell_D + i\epsilon\big]^2}, \end{aligned} \quad (3.102)$$

$$\mathcal{L}_{ij}^{(ns,2)}(\gamma,z,s,s';\gamma',z') = \frac{1}{4}(\mu^2-\Lambda^2)^2 \times \int_0^\infty ds' \int_0^\infty ds \frac{\sum_l P_l\ \mathcal{F}_{ij,l}^{NS}(v,\gamma,z,k_u^-,p)}{\Big[\gamma + s'/2 + s/2 + z(s-s')/2 - (1-z^2)M^2/4 + i\epsilon\Big]} \times \int_0^1 dv \frac{v^2(1-v)^2\big[3k_u^-k_D^+ + 3\ell_D + (1-v)(\mu^2-\Lambda^2)\big]}{\big[k_D^+k_u^- + \ell_D + (1-v)(\mu^2-\Lambda^2) + i\epsilon\big]^3\big[k_D^+k_u^- + \ell_D + i\epsilon\big]^2}. \quad (3.103)$$

If we define $\mathcal{H}_{ij}^{(ns)}(\gamma,z)$ as being

$$\mathcal{H}_{ij}^{(ns)}(\gamma,z) = \frac{1}{2\pi}\int_{-1}^1 dz' \int_0^\infty d\gamma' \mathcal{L}_{ij}^{(ns)}(\gamma,z,s,s';\gamma',z') g_j(\gamma',z')\,, \quad (3.104)$$

one can write

$$\mathcal{H}_{ij}^{(ns)}(\gamma,z) = \frac{1}{2\pi}\int_0^\infty d\gamma' \Bigg[\int_{-1}^z dz' \mathcal{L}_{ij}^{(ns,1)}(\gamma,z,s,s';\gamma',z') g_j(\gamma',z') + \int_z^1 dz' \mathcal{L}_{ij}^{(ns,2)}(\gamma,z,s,s';\gamma',z') g_j(\gamma',z')\Bigg], \quad (3.105)$$

It is seen from Eqs. (3.94) - (3.99) that one has a singular contribution for $(i,j) = (1,3)$,$(1,4)$, $(2,2)$, $(2,4)$, $(3,3)$, $(2,3)$ when $z = z'$. In the same way, if we define $\mathcal{H}_{ij}^{(s)}(\gamma,z)$ as

$$\mathcal{H}_{ij}^{(s)}(\gamma,z) = \frac{1}{2\pi}\int_{-1}^1 dz' \int_0^\infty d\gamma' \mathcal{L}_{ij}^{(s)}(\gamma,z,s,s';\gamma',z') g_j(\gamma',z')\,, \quad (3.106)$$

and taking in consideration the equations (3.95)-(3.99), after the z' integration, the sin-

gular terms will be written as follow

$$\mathcal{H}_{13}^{(s)}(\gamma,z) = \frac{(\mu^2-\Lambda^2)^2}{2\pi M^2}\frac{2}{(1-z^2)}\int_0^\infty ds'\int_0^\infty ds\int_0^\infty d\gamma'\int_0^1 dv \times\frac{v(1-v)^2}{4MD_\ell}\Big[\rho_V(s,)\rho_S(s')-\rho_S(s,)\rho_V(s')\Big]g_3(\gamma',z)\,, \tag{3.107}$$

$$\mathcal{H}_{14}^{(s)}(\gamma,z) = -\frac{(\mu^2-\Lambda^2)^2}{2\pi M^2}\frac{1}{2(1-z^2)}\int_0^\infty ds'\int_0^\infty ds\int_0^\infty d\gamma'\int_0^1 dv \times\frac{v(1-v)^2}{D_\ell}\rho_V(s,)\rho_V(s')g_4(\gamma',z)\,, \tag{3.108}$$

$$\mathcal{H}_{22}^{(s)}(\gamma,z) = -\frac{(\mu^2-\Lambda^2)^2}{2\pi M^2}\frac{1}{(1-z^2)}\int_0^\infty ds'\int_0^\infty ds\int_0^\infty d\gamma'\int_0^1 dv \times\frac{v(1-v)}{D_\ell}\Big[\rho_V(s,)\rho_V(s')\Big]g_2(\gamma',z)\,, \tag{3.109}$$

$$\mathcal{H}_{24}^{(s)}(\gamma,z) = -\frac{(\mu^2-\Lambda^2)^2}{2\pi M^2}\frac{2}{(1-z^2)}\int_0^\infty ds'\int_0^\infty ds\int_0^\infty d\gamma'\int_0^1 dv\frac{v(1-v)^2}{4MD_\ell} \times\Big[\rho_V(s,)\rho_S(s')+\rho_S(s,)\rho_V(s')\Big]\Big\}g_4(\gamma',z)\,, \tag{3.110}$$

$$\mathcal{H}_{33}^{(s)}(\gamma,z) = \frac{(\mu^2-\Lambda^2)^2}{2\pi M^2}\frac{1}{(1-z^2)}\int_0^\infty ds'\int_0^\infty ds\int_0^\infty d\gamma'\int_0^1 dv \times\frac{v(1-v)^2}{D_\ell}\Big[\rho_V(s,)\rho_V(s')\Big]g_3(\gamma',z)\,. \tag{3.111}$$

We have to consider more carefully the last term $\mathcal{H}_{23}^{(s)}$, which has two parts:

$$\mathcal{L}_{23}^{(s,a)} = -\frac{2}{M^2}\frac{(\mu^2-\Lambda^2)^2}{2(1-z^2)}\int_0^1 dv\; v\;(1-v)\int_0^\infty ds\int_0^\infty ds'\rho_V(s,)\rho_V(s') \times\Big\{(1-v)\delta(z'-z)\;\frac{1}{4D_\ell}\Big[z+4\frac{(2z\gamma-s'+s+z(s'+s))}{M^2(1-z^2)}\Big] \tag{3.112}$$

$$\mathcal{L}_{23}^{(s,b)} = -\frac{2}{M^2}\frac{(\mu^2-\Lambda^2)^2}{2(1-z^2)}\int_0^1 dv\; v\;(1-v)\int_0^\infty ds\int_0^\infty ds'\rho_V(s,)\rho_V(s')\,, \times\frac{1}{vM^2}\frac{1}{\Big[(1-v)\Big(\mu^2-\Lambda^2\Big)\Big]^2}\left[\frac{\partial}{\partial z'}\delta(z'-z)\right] \times\left[\frac{(1-v)\Big(\mu^2-\Lambda^2\Big)}{\Big[\ell_D+(1-v)\Big(\mu^2-\Lambda^2\Big)\Big]}+\ln\left\{\frac{\ell_D}{\Big[\ell_D+(1-v)\Big(\mu^2-\Lambda^2\Big)\Big]}\right\}\right]\Big\}\,, \tag{3.113}$$

that yields to us

$$\begin{aligned}\mathcal{H}_{23}^{(s,a)}(\gamma,z) &= \frac{1}{2\pi}\int_{-1}^{1}dz'\int_{0}^{\infty}d\gamma'\mathcal{L}_{23}^{(s,a)}(\gamma,z,s,s';\gamma',z')g_3(\gamma',z') \\ &= -\frac{(\mu^2-\Lambda^2)^2}{2\pi M^2}\frac{1}{(1-z^2)}\int_0^\infty ds'\int_0^\infty ds\int_0^\infty d\gamma'\int_0^1 dv\frac{v(1-v)^2}{4D_\ell} \\ &\times\Big[z+4\frac{(2z\gamma-s'+s+z(s'+s)}{M^2\ (1-z^2)}\Big]\rho_V(s,)\rho_V(s')g_3(\gamma',z).\end{aligned} \tag{3.114}$$

$$\begin{aligned}\mathcal{H}_{23}^{(s,b)}(\gamma,z) &= \frac{1}{2\pi}\int_{-1}^{1}dz'\int_{0}^{\infty}d\gamma'\mathcal{L}_{23}^{(s,b)}(\gamma,z,s,s';\gamma',z')g_3(\gamma',z') \\ &= \frac{1}{2\pi M^4(1-z^2)}\int_0^\infty ds'\int_0^\infty ds\ \rho_V(s,)\ \rho_V(s')\ \int_0^\infty d\gamma'\Bigg\{\frac{\partial g_3(\gamma',z)}{\partial z} \\ &\times \int_0^1\frac{dv}{(1-v)}\Bigg[\frac{(1-v)(\mu^2-\Lambda^2)}{\tilde{\ell}_D+(1-v)(\mu^2-\Lambda^2)}+\log\Big(\frac{\tilde{\ell}_D}{\tilde{\ell}_D+(1-v)(\mu^2-\Lambda^2)}\Big)\Bigg] \\ &- \frac{zM^2}{4}(\mu^2-\Lambda^2)^2g_3(\gamma',z)\int_0^1 dv\frac{v(1-v^2)}{D_l}\Bigg\}.\end{aligned} \tag{3.115}$$

On the contrary, the contribution coming from $\mathcal{L}_{23}^{(s,b)}$ is proportional to $\frac{\partial}{\partial z'}\delta(z'-z)$, that is handled by doing a partial integration where the surface term vanishes and the derivative in (3.113) is written as

$$\begin{aligned}&\frac{\partial}{\partial z'}\Bigg[\frac{(1-v)(\mu^2-\Lambda^2)}{\ell_D+(1-v)(\mu^2-\Lambda^2)}+\log\Big(\frac{\ell_D}{\ell_D+(1-v)(\mu^2-\Lambda^2)}\Big)\Bigg]= \\ =\ &\frac{\partial\ell_D}{\partial z'}\Bigg[\frac{-(1-v)(\mu^2-\Lambda^2}{[\ell_D+(1-v)(\mu^2-\Lambda^2]^2}+\frac{(1-v)(\mu^2-\Lambda^2)}{\ell_D[\ell_D+(1-v)(\mu^2-\Lambda^2)]}\Bigg] \\ =\ &\frac{-v(1-v)^2(\mu^2-\Lambda^2)^2[z(1-v)+2z'v]M^2}{4\ell_D[\ell_D+(1-v)(\mu^2-\Lambda^2]^2}.\end{aligned} \tag{3.116}$$

3.6 Generalized eigenvalue equation for the Nakanishi weight functions

Now we write the equation (3.100) in matrix form by using the Laguerre and Gengenbauer basis (PAULA *et al.*, 2016). So, the Nakanishi weight function of each component i is given as expansion of the form

$$g_i(\gamma,z)=\sum_{k=1}^{N_z}\sum_{n=1}^{N_\gamma}A_{kn}^{i}G_{2(k-1)+r_i}^{\lambda_i}(z)\mathcal{L}_{n-1}(\gamma), \tag{3.117}$$

where A^i_{kn} are the coefficients to be determined.

The functions $G^{\lambda_i}_{2m+r_i}$, and $\mathcal{L}_n$ are defined by

$$\begin{aligned} G^{\lambda}_{n}(z) &= (1-z^2)^{(2\lambda-1)/4}\Gamma(\lambda)\sqrt{\frac{n!(n+\lambda)}{2^{1-2\lambda}\pi\Gamma(n+2\lambda)}}C^{\lambda}_{n}(z), \\ \mathcal{L}_n(\gamma) &= \sqrt{a}L_n(a\gamma)e^{-a\gamma/2}, \end{aligned} \tag{3.118}$$

where C^{λ}_{n} denotes Gegenbauer polynomial and L_n is a Laguerre polynomial. Thus, in regards to obtain the Bethe-Salpeter equation as eigenvalue problem we define

$$\mathcal{A}^{(i)}_{kn}(\gamma,z) = G^{(l_i+1/2)}_{2(k-1)+r_i}(z)\int_0^\infty d\gamma' \frac{\mathcal{L}_{n-1}(\gamma')}{[\gamma+\gamma+M^2z^2/4+\kappa^2]^2}, \tag{3.119}$$

$$\mathcal{B}^{(ij)}_{kn}(\gamma,z) = \mathcal{B}^{(ij,ns)}_{kn}(\gamma,z)+\mathcal{B}^{(ij,s)}_{kn}(\gamma,z), \tag{3.120}$$

where

$$\begin{aligned} \mathcal{B}^{(ij,ns)}_{kn}(\gamma,z) = \frac{1}{2\pi}\int_0^\infty d\gamma'\mathcal{L}_{n-1}(\gamma')\int_{-1}^{z} dz'\mathcal{L}^{(ns,1)}_{ij}(\gamma,z,s,s';\gamma',z')G^{(l_j+1/2)}_{2(k-1)+r_j}(z') \\ +\frac{1}{2\pi}\int_0^\infty d\gamma'\mathcal{L}_{n-1}(\gamma')\int_{z}^{1} dz'\mathcal{L}^{(ns,2)}_{ij}(\gamma,z,s,s';\gamma',z')G^{(l_j+1/2)}_{2(k-1)+r_j}(z'), \end{aligned} \tag{3.121}$$

which the $\mathcal{L}^{(ns,1)}_{ij}$ and $\mathcal{L}^{(ns,2)}_{ij}$ terms are defined by equation (3.102). By defining the following terms

$$\begin{aligned} I_1(\gamma,z,\gamma') &= \int_0^1 dv \frac{v(1-v)^2}{D_\ell(\gamma,z,\gamma')}, \\ I_2(\gamma,z,\gamma') &= \int_0^1 dv \frac{v(1-v)}{D_\ell(\gamma,z,\gamma')}, \\ I_3(\gamma,z,\gamma') &= \int_0^1 \frac{dv}{(1-v)}\left[\frac{(1-v)(\mu^2-\Lambda^2)}{\tilde{\ell}_D+(1-v)(\mu^2-\Lambda^2)}+\log\Big(\frac{\tilde{\ell}_D}{\tilde{\ell}_D+(1-v)(\mu^2-\Lambda^2)}\Big)\right], \\ I_4(\gamma,z,\gamma') &= \int_0^1 dv \frac{v(1-v^2)}{D_\ell(\gamma,z,\gamma')}, \end{aligned} \tag{3.122}$$

the singular contributions are written as

$$
\begin{aligned}
\mathcal{B}^{(13,s)}_{kn}(\gamma,z) &= \frac{(\mu^2-\Lambda^2)^2}{2\pi M^2}\frac{1}{2M(1-z^2)}G^{(l_3+1/2)}_{2(k-1)}(z)\int_0^\infty d\gamma'\mathcal{L}_{n-1}(\gamma')I_1(\gamma,z,\gamma')\\
&\times \int_0^\infty ds'\int_0^\infty ds\,\Big[\rho_V(s,)\rho_S(s')-\rho_S(s,)\rho_V(s')\Big],\\
\mathcal{B}^{(14,s)}_{kn}(\gamma,z) &= -\frac{(\mu^2-\Lambda^2)^2}{2\pi M^2}\frac{1}{2(1-z^2)}G^{(l_4+1/2)}_{2(k-1)}(z)\int_0^\infty d\gamma'\mathcal{L}_{n-1}(\gamma')\;I_1(\gamma,z,\gamma')\\
&\times \int_0^\infty ds'\int_0^\infty ds\Big[\rho_V(s,)\rho_V(s')\Big],\\
\mathcal{B}^{(22,s)}_{kn}(\gamma,z) &= -\frac{(\mu^2-\Lambda^2)^2}{2\pi M^2}\frac{1}{(1-z^2)}G^{(l_2+1/2)}_{2(k-1)}(z)\\
&\times \int_0^\infty d\gamma'\mathcal{L}_{n-1}(\gamma')I_2(\gamma,z,\gamma')\int_0^\infty ds'\int_0^\infty ds\Big[\rho_V(s,)\rho_V(s')\Big],\\
\mathcal{B}^{(24,s)}_{kn}(\gamma,z) &= -\frac{(\mu^2-\Lambda^2)^2}{2\pi M^2}\frac{1}{2M(1-z^2)}G^{(l_4+1/2)}_{2(k-1)}(z)\int_0^\infty d\gamma'\mathcal{L}_{n-1}(\gamma')\;I_1(\gamma,z,\gamma')\\
&\times \int_0^\infty ds'\int_0^\infty ds\Big[\rho_V(s,)\rho_S(s')+\rho_S(s,)\rho_V(s')\Big],\\
\mathcal{B}^{(33,s)}_{kn}(\gamma,z) &= \frac{(\mu^2-\Lambda^2)^2}{2\pi M^2}\frac{1}{(1-z^2)}G^{(l_3+1/2)}_{2(k-1)+1}(z)\int_0^\infty d\gamma'\mathcal{L}_{n-1}(\gamma')I_1(\gamma,z,\gamma')\\
&\times \int_0^\infty ds'\int_0^\infty ds\Big[\rho_V(s,)\rho_V(s')\Big],\\
\mathcal{B}^{(23,s)}_{kn}(\gamma,z) &= -\frac{(\mu^2-\Lambda^2)^2}{2\pi M^2}\frac{1}{4(1-z^2)}G^{(l_3+1/2)}_{2(k-1)+1}(z)\int_0^\infty d\gamma'\mathcal{L}_{n-1}(\gamma')I_1(\gamma,z,\gamma')\\
&\times \int_0^\infty ds'\int_0^\infty ds\Big[z+4\frac{2z\gamma-s'+s+z(s'+s)}{M^2\;(1-z^2)}\Big]\Big[\rho_V(s,)\rho_V(s')\Big]\\
&+ \frac{1}{2\pi M^4(1-z^2)}\frac{\partial G^{(l_3+1/2)}_{2(k-1)+1}(z)}{\partial z}\int_0^\infty d\gamma'\mathcal{L}_{n-1}(\gamma')\;I_3(\gamma,z,\gamma')\\
&\times \int_0^\infty ds'\int_0^\infty ds\Big[\rho_V(s,)\rho_V(s')\Big]\\
&- \frac{z(\mu^2-\Lambda^2)^2}{8\pi M^2(1-z^2)}G^{(l_3+1/2)}_{2(k-1)+1}(z)\int_0^\infty d\gamma'\mathcal{L}_{n-1}(\gamma')I_4(\gamma,z,\gamma')\\
&\times \int_0^\infty ds'\int_0^\infty ds\Big[\rho_V(s,)\rho_V(s')\Big]. \qquad (3.123)
\end{aligned}
$$

Hence the Equation (3.100) is given now by

$$\sum_{kn}\mathcal{A}^{(i)}_{kn}(\gamma,z)A^i_{kn}=\alpha\sum_j\sum_{kn}\mathcal{B}^{(ij)}_{kn}(\gamma,z)A^j_{kn},\quad i=1,2,3,4\,. \qquad (3.124)$$

We then act on each side of equation (3.124) the operator

$$\int_0^\infty d\gamma\int_{-1}^1 dz\,G^{(l_i+1/2)}_{2(k'-1)+r_i}(z)\mathcal{L}_{n'-1}(\gamma)$$

we obtain

$$\sum_j \sum_{kn} \tilde{\mathcal{A}}^{ij}_{k'n',kn} A^j_{kn} = \alpha \sum_j \sum_{kn} \tilde{\mathcal{B}}^{ij}_{k'n',kn} A^j_{kn}, \tag{3.125}$$

with $\alpha = \frac{g^2}{4\pi^2}$ and

$$\tilde{\mathcal{A}}^{ij}_{k'n',kn} = \delta_{ij} \int_0^\infty d\gamma \mathcal{L}_{n'-1}(\gamma) \int_{-1}^1 dz G^{(l_i+1/2)}_{2(k'-1)+r_i}(z) \mathcal{A}^{(i)}_{kn}(\gamma, z), \tag{3.126}$$

$$\tilde{\mathcal{B}}^{ij}_{k'n',kn} = \int_0^\infty d\gamma \mathcal{L}_{n'-1}(\gamma) \int_{-1}^1 dz G^{(l_i+1/2)}_{2(k'-1)+r_i}(z) \mathcal{B}^{(ij)}_{kn}(\gamma, z)\,. \tag{3.127}$$

The coefficients for the Nakanishi weight functions and the coupling constant α are thus obtained by solving a generalized eigenvalue problem of the form

$$\hat{\mathcal{A}} a = \alpha \hat{\mathcal{B}} a, \tag{3.128}$$

where $\hat{\mathcal{A}}$ and $\hat{\mathcal{B}}$ are square matrices. The one-dimensional eigenvector α enable us to reconstruct Nakanishi weight functions $g_i(\gamma, z)$, thus we can obtain the Bethe-Salpeter amplitude of the bound-state.

4 Phenomenological Mass Function

In this chapter, we solve the Bethe-Salpeter equation for a phenomenological dressed quark propagator, where the correspondent running mass is consistent with Euclidean Lattice QCD simulations (OLIVEIRA *et al.*, 2019; PARAPPILLY *et al.*, 2006). The functional form used for the propagator was proposed in Mello *et al.* (2017) [1]. Within this choice, we solve the BS equation and we intend to calculate hadronic observables. As a first step, we obtain the relevant coefficients for the numerical implementation. In addition, we present the analytical expressions of the valence probability and the light-front momentum distributions.

4.1 The Dressed Quark Propagator

As discussed in section 2.4.2, an interesting property of QCD is the appearance of mass due to the non-perturbative effects of the strong interaction in the deep IR. Even if one considers a zero bare quark mass, by solving the Dyson-Schwinger equation one obtains a non-zero running mass $M(k^2)$ (chiral symmetry breaking). In general, the dressed quark propagator is given by (PESKIN; SCHROEDER, 1995)

$$S_F(k) = i\frac{Z(k^2)}{\not{k} - \mathcal{M}(k^2) + i\epsilon} \tag{4.1}$$

where, $Z(k^2)$ is the wave function renormalization factor. In this thesis, it is considered a model where $Z(k^2) = 1$ and the dynamical mass function $M(k^2)$ is renormalization-point-independent (FISCHER; ALKOFER, 2003) and has a phenomenological form given by Mello *et al.* (2017)

$$\mathcal{M}(k^2) = m_0 - m^3[k^2 - \lambda^2 + i\epsilon]^{-1}\,, \tag{4.2}$$

where m_0, m and λ are free parameters. We fix the parametrizations in order to adjust the mass function to recent Lattice QCD calculations (OLIVEIRA *et al.*, 2019; PARAPPILLY *et al.*, 2006). In particular, given a set of m_0, m and λ, we can obtain the masses m_1, m_2

[1] See also the works of Moita *et al.* (2022a) and Moita *et al.* (2022b).

and m_3 (they are the poles positions) by solving the following equation

$$m_i(m_i - \lambda^2) = \pm[m_0(k^2 - \lambda^2) - m^3]\,, \tag{4.3}$$

that arises from analyzing the poles of the propagator (4.1), when considering the mass function given by (4.2).

Spectral decomposition of the quark propagator

The quark propagator also can be written as

$$S_F(k) = i\left(S_V(k^2)\not{k} + S_S(k^2)\right) \tag{4.4}$$

where the spectral decomposition of that propagator is given by (ITZYKSON; ZUBER, 1980)

$$S_{S(V)}(k^2) = \int_0^\infty ds \frac{\rho_{S(V)}(s)}{k^2 - s^2 + i\epsilon} \tag{4.5}$$

where the correspondent scalar and vector spectral densities, $\rho_S(s)$ and $\rho_V(s)$, for such model, is given by a sum of delta functions, as follow

$$\rho_S(s) = \sum_a R_a^S \delta(s - m_a^2)\ ;\ \rho_V(s) = \sum_a R_a^V \delta(s - m_a^2) \tag{4.6}$$

where the $R_a^{S(V)}$ are residues, expressed as

$$\begin{aligned} R_a^{(V)} &= \frac{(\lambda^2 - m_a^2)^2}{(m_a^2 - m_b^2)(m_a^2 - m_c^2)}\,, \\ R_a^{(S)} &= \frac{m^3(\lambda^2 - m_a^2)}{(m_a^2 - m_b^2)(m_a^2 - m_c^2)} + m_0\, R_a^{(V)}\,, \end{aligned} \tag{4.7}$$

with the indices $\{a, b, c\}$ following the cyclic permutation $\{1, 2, 3\}$.

The functions $R_a^{S(V)}$ fulfill some interesting properties:

$$\sum_{a=1}^{3} R_a^V = 1\,; \sum_{a=1}^{3} R_a^S = m_0\ ; \sum_{a=1}^{3} m_a^2 R_a^V = -2\lambda^2 + \sum_{a=1}^{3} m_a^2\,. \tag{4.8}$$

4.2 The Kernel for a Phenomenological Mass Function

In this section we obtain the relevant coefficients necessary to numerically solve the BS equation given the phenomenological mass function expressed by (4.2).

The BS equation (3.100) obtained in the previous chapter is given by

$$\int_0^\infty d\gamma' \frac{g_i(\gamma', z)}{\left[\gamma + z^2 M^2/4 + \gamma' + \kappa^2 - i\epsilon\right]^2} = \alpha \sum_j \int_{-1}^{1} dz' \int_0^\infty d\gamma' \times \left[\mathcal{L}_{ij}^{ns}(\gamma, z; \gamma', z') + \mathcal{L}_{ij}^{s}(\gamma, z; \gamma', z')\right] g_j(\gamma', z')\,, \quad (4.9)$$

where $\alpha = \frac{g^2}{4\pi}$, $\kappa^2 = m_1 - \frac{M^2}{4}$, with m_1 being the lightest pole and the functions $\mathcal{L}_{ij}^{ns(s)}(\gamma, z; \gamma', z')$ are given in equations (3.55) and (3.92). To solve the BS equation numerically, we chose to expand the Nakanishi weight function on a basis of Gegenbauer and Laguerre functions, as we have discussed in Chapter 3. The equation to be solved is

$$\sum_j \sum_{kn} \tilde{\mathcal{A}}^{ij}_{k'n',kn} A^j_{kn} = \alpha \sum_j \sum_{kn} \tilde{\mathcal{B}}^{ij}_{k'n',kn} A^j_{kn}, \quad (4.10)$$

with

$$\mathcal{A}^{(i)}_{kn}(\gamma, z) = G^{(l_i+1/2)}_{2(k-1)+r_i}(z) \int_0^\infty d\gamma' \frac{\mathcal{L}_{n-1}(\gamma')}{[\gamma + \gamma' + M^2 z^2/4 + \kappa^2]^2}\,, \quad (4.11)$$

$$\tilde{\mathcal{A}}^{ij}_{k'n',kn} = \delta_{ij} \int_0^\infty d\gamma \mathcal{L}_{n'-1}(\gamma) \int_{-1}^{1} dz G^{(l_i+1/2)}_{2(k'-1)+r_i}(z) \mathcal{A}^{(i)}_{kn}(\gamma, z), \quad (4.12)$$

$$\tilde{\mathcal{B}}^{ij}_{k'n',kn} = \int_0^\infty d\gamma \mathcal{L}_{n'-1}(\gamma) \int_{-1}^{1} dz G^{(l_i+1/2)}_{2(k'-1)+r_i}(z) \mathcal{B}^{(ij)}_{kn}(\gamma, z)\,, \quad (4.13)$$

$$\mathcal{B}^{(ij)}_{kn}(\gamma, z) = \mathcal{B}^{(ij,ns)}_{kn}(\gamma, z) + \mathcal{B}^{(ij,s)}_{kn}(\gamma, z)\,. \quad (4.14)$$

Regarding to $\mathcal{B}^{(ij,ns)}_{kn}$ and $\mathcal{B}^{(ij,s)}_{kn}$, we apply to the equations (3.121) and (3.123) our expression of the spectral densities defined in (4.6). By doing that the non-singular contribution of the $\mathcal{B}^{(ij)}_{kn}(\gamma, z)$ tensor is given by the following expression

$$\mathcal{B}^{(ij,ns)}_{kn}(\gamma, z) = \int_0^\infty d\gamma' \mathcal{L}_{n-1}(\gamma') \int_{-1}^{z} dz' \mathcal{L}^{(ns,1)}_{ij}(\gamma, z, \gamma', z') G^{(l_j+1/2)}_{2(k-1)+r_j}(z') + \sigma_{ij} \int_0^\infty d\gamma' \int_z^1 dz' \left[z \to -z; z' \to -z'; m_a \to m_{a'}; m_{a'} \to m_a\right]\,, \quad (4.15)$$

with

$$\begin{aligned}
&\mathcal{L}_{ij}^{(ns,1)}(\gamma,z,\gamma',z') = \frac{1}{2\pi}\frac{(\mu^2-\Lambda^2)^2}{4}\int_0^1 dv v^2(1-v)^2 \\
\times\ &\sum_{a,a'}\Big[R_a^{(v)}R_{a'}^{(v)}\mathcal{F}_{ij,1}^{ns}(v,\gamma,z,m_{a/a'}^2) + R_a^{(v)}R_{a'}^{(s)}\mathcal{F}_{ij,2}^{ns}(v,\gamma,z,m_{a/a'}^2) \\
+\ &R_a^{(s)}R_{a'}^{(v)}\mathcal{F}_{ij,3}^{ns}(v,\gamma,z,m_{a/a'}^2) + R_a^{(s)}R_{a'}^{(s)}\mathcal{F}_{ij,4}^{ns}(v,\gamma,z,m_{a/a'}^2)\Big] \\
\times\ &\frac{1}{\Big(\gamma+(m_{a'}^2+m_a^2)/2+z(m_a^2-m_{a'}^2)/2-(1-z^2)M^2/4+i\epsilon\Big)} \\
\times\ &\frac{3D(\gamma,z,\gamma',z',v)+(1-v)(1-z)(\Lambda^2-\mu^2)}{\big(D(\gamma,z,\gamma',z',v)+(1-v)(1-z)(\Lambda^2-\mu^2)-i\epsilon\big)^3\big(D(\gamma,z,\gamma',z',v)-i\epsilon\big)^2}\ ,
\end{aligned} \tag{4.16}$$

where the coefficients $\mathcal{F}_{ij,l}^{ns}$ are given in Appendix E and $D(\gamma,z,\gamma',z',v)$ is expressed as

$$\begin{aligned}
D(\gamma,z,\gamma',z',v) \ =\ & v^2(z-z')\big[(1-z)M^2/4-(\gamma+m_a^2)\big]-v^2(1-z)(\gamma+(zz'-z'^2)M^2/4) \\
&+v(z'-z)\big[(1-z)M^2/4-(\gamma+m_a^2)\big]+v(1-z)(\gamma+zz'M^2/4) \\
&+v(1-z)(\gamma'+\kappa^2-\mu^2)+(1-z)\mu^2.
\end{aligned} \tag{4.17}$$

We can write $\mathcal{L}_{ij}^{ns}$ in a more easier way to implement by using the decomposition $\mathcal{F}_{ijl}^{ns} = \tilde{\mathcal{F}}_{ijl}^{(1)} + (1-v)\tilde{\mathcal{F}}_{ijl}^{(2)}$. We define

$$\begin{aligned}
\chi^{(1)}(m_a^2,\gamma,z,\gamma',z') &= \int_0^1 \frac{dv v^2(1-v)^2[3D(\gamma,z,\gamma',z',v)-(1-v)(1-z)(\mu^2-\Lambda^2)]}{\big(D(\gamma,z,\gamma',z',v)-(1-v)(1-z)(\mu^2-\Lambda^2)\big)^3\big(D(\gamma,z,\gamma',z',v)\big)^2}, \\
\chi^{(2)}(m_a^2,\gamma,z,\gamma',z') &= \int_0^1 \frac{dv v^2(1-v)^3[3D(\gamma,z,\gamma',z',v)-(1-v)(1-z)(\mu^2-\Lambda^2)]}{\big(D(\gamma,z,\gamma',z',v)-(1-v)(1-z)(\mu^2-\Lambda^2)\big)^3\big(D(\gamma,z,\gamma',z',v)\big)^2}.
\end{aligned} \tag{4.18}$$

Thus having

$$\begin{aligned}
&\mathcal{L}_{ij}^{(ns,1)}(\gamma,z,\gamma',z') = \frac{1}{2\pi}\frac{(\mu^2-\Lambda^2)^2}{4}\sum_a\Big\{\chi^{(1)}(m_a^2,\gamma,z,\gamma',z') \\
\times\ &\Big[R_a^{(v)}\tilde{R}_a^{(v)}(m_a^2,\gamma,z)\tilde{\mathcal{F}}_{ij,1}^{(1)}(\gamma,z,m_a^2) + R_a^{(v)}\tilde{R}_a^{(s)}(m_a^2,\gamma,z)\tilde{\mathcal{F}}_{ij,2}^{(1)}(\gamma,z,m_a^2) \\
+\ &R_a^{(s)}\tilde{R}_a^{(v)}(m_a^2,\gamma,z)\tilde{\mathcal{F}}_{ij,3}^{(1)}(\gamma,z,m_a^2) + R_a^{(s)}\tilde{R}_a^{(s)}(m_a^2,\gamma,z)\tilde{\mathcal{F}}_{ij,4}^{(1)}(\gamma,z,m_a^2)\Big] \\
+\ &\chi^{(2)}(m_a^2,\gamma,z,\gamma',z')\Big[R_a^{(v)}\tilde{R}_a^{(v)}(m_a^2,\gamma,z)\tilde{\mathcal{F}}_{ij,1}^{(2)}(\gamma,z,m_a^2) + R_a^{(v)}\tilde{R}_a^{(s)}(m_a^2,\gamma,z)\tilde{\mathcal{F}}_{ij,2}^{(2)}(\gamma,z,m_a^2) \\
+\ &R_a^{(s)}\tilde{R}_a^{(v)}(m_a^2,\gamma,z)\tilde{\mathcal{F}}_{ij,3}^{(2)}(\gamma,z,m_a^2) + R_a^{(s)}\tilde{R}_a^{(s)}(m_a^2,\gamma,z)\tilde{\mathcal{F}}_{ij,4}^{(2)}(\gamma,z,m_a^2)\Big]\Big\},
\end{aligned} \tag{4.19}$$

where the $\mathcal{L}_{ij}^{ns}$ coefficients are given in appendix D.

The singular contribution of the $\mathcal{B}^{(ij)}_{kn}(\gamma,z)$ tensor is given by

$$
\begin{aligned}
\mathcal{B}^{(14,s)}_{kn}(\gamma,z) &= -\frac{1}{2}G^{(l_4+1/2)}_{2(k-1)}(z)\int_0^\infty d\gamma'\mathcal{L}_{n-1}(\gamma')\tilde{I}_2(\gamma,z,\gamma'),\\
\mathcal{B}^{(22,s)}_{kn}(\gamma,z) &= -G^{(l_2+1/2)}_{2(k-1)}(z)\int_0^\infty d\gamma'\mathcal{L}_{n-1}(\gamma')\tilde{I}_3(\gamma,z,\gamma'),\\
\mathcal{B}^{(24,s)}_{kn}(\gamma,z) &= -\frac{1}{2M}G^{(l_4+1/2)}_{2(k-1)}(z)\int_0^\infty d\gamma'\mathcal{L}_{n-1}(\gamma')\tilde{I}_1(\gamma,z,\gamma'),\\
\mathcal{B}^{(33,s)}_{kn}(\gamma,z) &= G^{(l_3+1/2)}_{2(k-1)+1}(z)\int_0^\infty d\gamma'\mathcal{L}_{n-1}(\gamma')\tilde{I}_2(\gamma,z,\gamma'),\\
\mathcal{B}^{(23,s)}_{kn}(\gamma,z) &= -G^{(l_3+1/2)}_{2(k-1)+1}(z)\int_0^\infty d\gamma'\mathcal{L}_{n-1}(\gamma')\tilde{I}_6(\gamma,z,\gamma')\\
&\quad+\frac{\partial G^{(l_3+1/2)}_{2(k-1)+1}(z)}{\partial z}\int_0^\infty d\gamma'\mathcal{L}_{n-1}(\gamma')\tilde{I}_4(\gamma,z,\gamma')\\
&\quad-G^{(l_3+1/2)}_{2(k-1)+1}(z)\int_0^\infty d\gamma'\mathcal{L}_{n-1}(\gamma')\tilde{I}_5(\gamma,z,\gamma'),
\end{aligned}
\tag{4.20}
$$

with $\tilde{I}_1,\tilde{I}_2,\tilde{I}_3,\tilde{I}_4,\tilde{I}_5,\tilde{I}_6$ are expressed as

$$
\tilde{I}_1(\gamma,z,\gamma') = \frac{(\mu^2-\Lambda^2)^2}{2\pi M^2(1-z^2)}\sum_{a,a'}\Big[R^{(v)}_aR^{(s)}_{a'}+R^{(s)}_aR^{(v)}_{a'}\Big]\int_0^1 dv\frac{v(1-v)^2}{D_\ell(\gamma,z,\gamma')}\ , \tag{4.21}
$$

$$
\tilde{I}_2(\gamma,z,\gamma') = \frac{(\mu^2-\Lambda^2)^2}{2\pi M^2(1-z^2)}\sum_{a,a'}\Big[R^{(v)}_aR^{(v)}_{a'}\Big]\int_0^1 dv\frac{v(1-v)^2}{D_\ell(\gamma,z,\gamma')}, \tag{4.22}
$$

$$
\tilde{I}_3(\gamma,z,\gamma') = \frac{(\mu^2-\Lambda^2)^2}{2\pi M^2(1-z^2)}\sum_{a,a'}\Big[R^{(v)}_aR^{(v)}_{a'}\Big]\int_0^1 dv\frac{v(1-v)}{D_\ell(\gamma,z,\gamma')}, \tag{4.23}
$$

$$
\begin{aligned}
\tilde{I}_4(\gamma,z,\gamma') &= \frac{1}{2\pi M^4(1-z^2)}\sum_{a,a'}\Big[R^{(v)}_aR^{(v)}_{a'}\Big]\int_0^1\frac{dv}{(1-v)}\\
&\quad\times\Big[\frac{(1-v)(\mu^2-\Lambda^2)}{\tilde{\ell}_D+(1-v)(\mu^2-\Lambda^2)}+\log\Big(\frac{\tilde{\ell}_D}{\tilde{\ell}_D+(1-v)(\mu^2-\Lambda^2)}\Big)\Big],
\end{aligned}
\tag{4.24}
$$

$$
\tilde{I}_5(\gamma,z,\gamma') = \frac{z(\mu^2-\Lambda^2)^2}{8\pi M^2(1-z^2)}\sum_{a,a'}\Big[R^{(v)}_aR^{(v)}_{a'}\Big]\int_0^1 dv\frac{v(1-v^2)}{D_\ell(\gamma,z,\gamma')}., \tag{4.25}
$$

$$
\begin{aligned}
\tilde{I}_6(\gamma,z,\gamma') &= \frac{z(\mu^2-\Lambda^2)^2}{8\pi M^4(1-z^2)^2}\int_0^1 dv\frac{v(1-v)^2}{D_\ell(\gamma,z,\gamma')}\Big\{\big((1-z^2)M^2+8\gamma\big)\sum_{a,a'}R^{(v)}_aR^{(v)}_{a'}\\
&\quad+8\sum_{a,a'}R^{(v)}_aR^{(v)}_{a'}m_a^2\Big\}.
\end{aligned}
\tag{4.26}
$$

Using the set of coefficients given in (4.19) and (4.20), one can numerically solve the BS equation to obtain the Nakanishi weight functions, which allow us to reconstruct the BS amplitude and then calculate hadronic observables.

4.3 Valence Probability and Light-Front Momentum Distributions

In this section we follow the derivation of the valence probabilities expressions, as shown in Paula *et al.* (2021). In particular, we demonstrate that the valence component can be decomposed into two spin contributions, where one configuration corresponds to a total spin of the quark-antiquark pair $S = 0$, while the other one corresponds to a spin state $S = 1$.

A fermionic field on the null plane component is described as follow:

$$\psi^{(+)}(\tilde{x}, x^+ = 0^+) = \int \frac{d\tilde{q}}{(2\pi)^{3/2}} \frac{\theta(q^+)}{\sqrt{2q^+}} \sum_\sigma [U^{(+)}(\tilde{q},\sigma) b(\tilde{q},\sigma) e^{i\tilde{q}\cdot\tilde{x}} + V^{(+)} d^\dagger(\tilde{q},\sigma) e^{-i\tilde{q}\cdot\tilde{x}}] \quad (4.27)$$

with $U^{(+)}(\tilde{q},\sigma) = \Lambda^{(+)} u(\tilde{q},\sigma)$, $V^{(+)}(\tilde{q},\sigma) = \Lambda^{(+)} v(\tilde{q},\sigma)$ and the normalization given by $\bar{u}u = 2m$ and $\bar{v}(\tilde{q},\sigma')v(\tilde{q},\sigma) = -2m$. The creation and annihilation operators enable the construction of the Fock space. We define the valence component as the state with the lowest number of constituents. Therefore we can now introduce the Light Front (LF) valence amplitude φ_2:

$$\begin{aligned} \varphi_2(\xi, \mathbf{k}_\perp, \sigma_i; M, J^\pi, J_z) &= (2\pi)^3 \sqrt{N_c}\, 2p^+ \sqrt{\xi(1-\xi)} \langle 0 | b(\tilde{q}_2,\sigma_2) d(\tilde{q}_1,\sigma_1) | \tilde{p}, M, J^\pi, J_z \rangle \\ &= \frac{\sqrt{N_c}}{4p^+} \bar{u}_\alpha(\tilde{q}_2,\sigma_2) \int \frac{dk^-}{2\pi} \left[\gamma^+ \Phi(k,p) \gamma^+\right]_{\alpha\beta} v_\beta(\tilde{q}_1,\sigma_1), \end{aligned} \quad (4.28)$$

with $\tilde{q}_1 \equiv \{M(1-\xi), -\mathbf{k}_\perp\}$, $\tilde{q}_2 \equiv \{M\xi, \mathbf{k}_\perp\}$ and $\xi = \frac{1}{2} + \frac{k^+}{p^+}$. The steps between the two lines above come from writing the Bethe Salpeter (BS) amplitude, in coordinate space, as follow

$$\Psi(x_1, x_2, p) = e^{-ip\cdot X} \langle 0 | T \left\{ U\left(\frac{x}{2}\right) \bar{D}\left(\frac{-x}{2}\right) \right\} | \pi^+ \rangle \quad (4.29)$$

$$\bar{\Psi}(x_1, x_2, p) = e^{ip\cdot X} \langle \pi^+ | T \left\{ D\left(\frac{-x}{2}\right) \bar{U}\left(\frac{x}{2}\right) \right\} | 0 \rangle \quad (4.30)$$

in which U and D are fields with quantum numbers corresponding to u and d quarks.

In order to obtain a more explicit expression of φ_2 one need expand the BS amplitude in terms of orthogonal basis (equation (4.31)) that enable to have the BS equation as a system of four coupled integral equations (one to each ϕ_i). As well, the scalar functions

can be conveniently written in terms of the Nakanishi Integral Representation (NIR).

$$\begin{aligned}\Phi(k,p) &= \sum_{i=1}^{4} S_i\phi_i = \gamma_5\phi_1(k,p) + \frac{\not{p}}{M}\gamma_5\phi_2(k,p) \\ &+ \left(\frac{k\cdot p}{M}\not{p} - \frac{\not{k}}{M}\right)\gamma_5\phi_3(k,p) + \frac{i}{M^2}\sigma^{\mu\nu}p_\mu k_\nu\gamma_5\phi_4(k,p)\ . \end{aligned} \tag{4.31}$$

Consequently one has

$$\begin{aligned}\varphi_2\left(\xi,\mathbf{k}_\perp,\sigma_i;M,J^\pi,J_z\right) &= \frac{\sqrt{N_c}}{4p^+}\,\bar{u}_\alpha(\tilde{q}_2,\sigma_2)\int\frac{dk^-}{2\pi}\gamma^+ \\ &\times\left\{\frac{p}{M}\phi_2 + \left(\frac{k\cdot p}{M}\not{p} - \frac{\not{k}}{M}\right)\phi_3 - \frac{1}{M^2}\not{p}\not{k}\phi_4\right\}\gamma_5\gamma^+ v(\tilde{q}_1,\sigma_1) \\ &= -\frac{\sqrt{N_c}}{p^+}\int\frac{dk^-}{2\pi}\Bigg[\left\{\phi_2 + \left(\frac{k^-}{2M}+\frac{z}{4}\right)\phi_3\right\}\mathcal{D}_1^{\sigma_1\sigma_2}(\tilde{q}_1,\tilde{q}_2) \\ &-\frac{1}{M}\mathcal{D}_2^{\sigma_1\sigma_2}(\tilde{q}_1,\tilde{q}_2)\phi_4\Bigg]\ , \end{aligned} \tag{4.32}$$

with $\mathcal{D}_1^{\sigma_1\sigma_2}$, $\mathcal{D}_2^{\sigma_1\sigma_2}$ and the u and v spinors (in LF variables) written as follow

$$\begin{aligned}\mathcal{D}_1^{\sigma_1\sigma_2}(\tilde{q}_1,\tilde{q}_2) &= Tr\left\{v(\tilde{q}_1,\sigma_1)u^\dagger(\tilde{q}_2,\sigma_2)\gamma_5\,\Lambda^+\right\}\ , \\ \mathcal{D}_2^{\sigma_1\sigma_2}(\tilde{q}_1,\tilde{q}_2) &= Tr\left\{v(\tilde{q}_1,\sigma_1)u^\dagger(\tilde{q}_2,\sigma_2)(\mathbf{k}_\perp\cdot\gamma_\perp)\gamma_5\,\Lambda^+\right\}\ , \\ u(\tilde{q},\sigma) &= \frac{1}{\sqrt{2q^+}}(q^+ + \gamma^0 m_1 + \gamma^0 q_\perp\cdot\gamma_\perp)\begin{pmatrix}\chi^\sigma\\ \sigma\chi^\sigma\end{pmatrix}\ , \\ v(\tilde{q},-\sigma) &= \frac{1}{\sqrt{2q^+}}(q^+ - \gamma^0 m_1 + \gamma^0 q_\perp\cdot\gamma_\perp)\begin{pmatrix}\chi^\sigma\\ \sigma\chi^\sigma\end{pmatrix}\ . \end{aligned} \tag{4.33}$$

After doing the necessary products and traces operations present in equation (4.32) one will obtain that $\mathcal{D}_1^{\sigma\sigma} = \mathcal{D}_2^{-\sigma\sigma} = 0$ and

$$\begin{aligned}\mathcal{D}_1^{-\sigma\sigma}(\tilde{q}_1,\tilde{q}_2) &= \sigma M\sqrt{\xi(1-\xi)} = \frac{\sigma M}{2}\sqrt{1-z^2} \\ \mathcal{D}_2^{\sigma\sigma}(\tilde{q}_1,\tilde{q}_2) &= \sigma\, k_{L(R)}\, M\sqrt{\frac{1-z^2}{2}}\ , \end{aligned} \tag{4.34}$$

where $k_{R(L)} = \mp\frac{1}{\sqrt{2}}(k_x \pm ik_y)$. Hence, the LF valence amplitude φ_2 can be expressed as

$$\begin{aligned}\varphi_2\left(\xi,\mathbf{k}_\perp,\sigma_i;M,J^\pi,J_z\right) &= -\frac{\sigma_2}{2}\sqrt{N_c}\sqrt{1-z^2}\int\frac{dk^-}{2\pi}\Bigg\{\delta_{\sigma_2,-\sigma_1}\Bigg(\phi_2(k,p) \\ &+ \left(\frac{k^-}{2M}+\frac{z}{4}\right)\phi_3(k,p)\Bigg) - \frac{\sqrt{2}}{M}k_{L(R)}\delta_{\sigma_2,\sigma_1}\phi_4(k,p)\Bigg\}. \end{aligned} \tag{4.35}$$

The integration over k^- can be performed if we use the NIR of the scalar functions ϕ_i as given in equation (3.11), allowing us to define

$$\psi_i(\gamma,z) = \int \frac{dk^-}{2\pi}\phi_i(k,p) = -\frac{i}{M}\int_0^\infty d\gamma' \frac{g_i(\gamma',z)}{\left(\gamma'+\gamma+m_1^2z^2+(1-z^2)\kappa^2\right)^2}, \quad (4.36)$$

where $\gamma = |\mathbf{k}_\perp|^2$ and $\xi = \frac{1}{2}+\frac{k^+}{p^+}$. Therefore we can write valence component of light-front wave function

$$\begin{aligned}\varphi_2\left(\xi,\mathbf{k}_\perp,\sigma_i;M,J^\pi,J_z\right) &= -\frac{\sigma_2}{2}\sqrt{N_c}\sqrt{1-z^2} \\ &\times\Bigg\{\delta_{\sigma_2,-\sigma_1}\Bigg[\psi_2(\gamma,z)+\frac{z}{2}\psi_3(\gamma,z) \\ &+\frac{i}{M^3}\int_0^\infty \gamma'\frac{\partial g_3(\gamma',z';\kappa^2)/\partial z}{\gamma+\gamma'+m_1^2z^2+(1-z^2)\kappa^2-i\epsilon}\Bigg] \\ &-\frac{k_{L(R)}\sqrt{2}}{M}\delta_{\sigma_2,\sigma_1}\psi_4(\gamma,z)\Bigg\}, \end{aligned} \quad (4.37)$$

where $k_{L(R)} = \pm\frac{1}{\sqrt{2}}(k_x \mp ik_y)$. By looking at $\delta_{\sigma_2,-\sigma_1}$ and $\delta_{\sigma_2,\sigma_1}$, we can see that, depending on the spin configuration, the first or the second term of the valence amplitude φ_2 will survive. Thus, we can define two contributions, aligned and anti-aligned, as follow

$$\begin{aligned}\psi_{\uparrow\uparrow} &= \psi_{\downarrow\downarrow} = \frac{\sqrt{\gamma}}{M}\psi_4(\gamma,z)\ , \\ \psi_{\uparrow\downarrow} &= \psi_{\downarrow\uparrow} = \psi_2(\gamma,z)+\frac{z}{2}\psi_3(\gamma,z) \\ &\quad +\frac{i}{M^3}\int_0^\infty d\gamma'\frac{\partial g_3(\gamma',z';\kappa^2)/\partial z}{\gamma+\gamma'+m_1^2z^2+(1-z^2)\kappa^2-i\epsilon}\ . \end{aligned} \quad (4.38)$$

Now we can account for the valence probability, which is the probability to measure the valence state of the pion, in terms of the valence momentum distributions density:

$$\begin{aligned}P_{val} &= \frac{1}{(2\pi)^3}\sum_{\sigma 1\sigma_2}\int_{-1}^1\frac{dz}{(1-z^2)}\int d\mathbf{k}_\perp|\varphi_{n=2}(\xi,\mathbf{k}_\perp,\sigma_i;M,J^\pi,J_z)|^2 \\ &= \int_{-1}^1 dz\int_0^\infty d\gamma\mathcal{P}_{val}(\gamma,z)\ , \end{aligned} \quad (4.39)$$

where $z = 1-2\xi$ and the $\mathcal{P}_{val}(\gamma,z)$ is given in terms of the antialigned and the aligned

probability densities as follow

$$\mathcal{P}_{val}(\gamma, z) = \mathcal{P}_{\uparrow\downarrow}(\gamma, z) + \mathcal{P}_{\uparrow\uparrow}(\gamma, z) \tag{4.40}$$

$$\mathcal{P}_{\uparrow\downarrow}(\gamma, z) = \frac{N_c}{16\pi^2}|\psi_{\uparrow\downarrow}(\gamma, z)|^2 \tag{4.41}$$

$$\mathcal{P}_{\uparrow\uparrow}(\gamma, z) = \frac{N_c}{16\pi^2}|\psi_{\uparrow\uparrow}(\gamma, z)|^2 \ . \tag{4.42}$$

The valence longitudinal $\phi(\xi)$ and transverse $P(\gamma)$ light-front momentum distributions densities are give as follow

$$\phi(\xi) = \int_0^\infty d\gamma \left(\mathcal{P}_{\uparrow\downarrow}(\gamma, z) + \mathcal{P}_{\uparrow\uparrow}(\gamma, z)\right) , \tag{4.43}$$

$$P(\gamma) = \int_1^{-1} dz \left(\mathcal{P}_{\uparrow\downarrow}(\gamma, z) + \mathcal{P}_{\uparrow\uparrow}(\gamma, z)\right) . \tag{4.44}$$

The two spin configurations, anti-aligned and aligned, correspond to a total spin $S = 0$ and $S = 1$, respectively. To a model considering a bound state where the quark propagator has a fixed mass, the anti-aligned configuration yields the largest contribution and is related to the eigenstate of the operator L_z with eigenvalue $l_z = 0$. Besides, the aligned configuration is connected to $l_z = \pm 1$, whose contribution reveals a signature of the relativistic dynamical regime inside of the pion (PAULA *et al.*, 2021). In the next chapter, we will discuss those contributions to a bound state of quark and antiquark considering a phenomenological dressed quark propagator. Thus we will be able to evaluate the contribution of those configurations and understand better the relativistic features inside light hadrons.

5 Numerical Results

In this chapter, we discuss the static and dynamical quantities obtained from the solution of the BSE for a pseudoscalar bound-system, with a ladder kernel with massive gluons, a dynamically-dressed quark mass function and an extended quark-gluon vertex. We call the attention to the reader that there is a competition between three gluonic phenomena: the dressing of the quark propagator, the extension of the quark-gluon vertex and the ladder exchange of massive gluons.

In the dressed quark propagator, it is used a phenomenological mass function (CASTRO *et al.*, 2023). The solutions of the pion BSE have been obtained by using two sets of parameters, $\{m_0,m,\lambda\}$, in equations (4.1) and (4.2). They have been extracted after fitting LQCD calculations with very different bare quark mass, m_0^{LQCD}, in order to explore the sensitivity of the present approach. In particular, we got two sets of fitting parameters: i) Model I, which corresponds to LQCD calculations with $m_0^{LQCD} = 155$ MeV (BOWMAN *et al.*, 2005), and ii) Model II, which corresponds to the ones with $m^{LQCD} = 8\,\text{MeV}$ (OLIVEIRA *et al.*, 2019). The two sets of fitting parameters of the mass function are shown in Table 5.1.

In special, we study the behavior of the coupling constant of our model in comparison with the results of a model with a bare quark propagator. We also study two cases from Lattice QCD, in which we adjust our parameters aiming to be able to compare our results with the fixed mass case. The first one is from LQCD calculations of Ref. Bowman *et al.* (2005), where we fit the parameters of the mass function (4.2) accordingly. The second case we want to compare is the one of Ref. Oliveira *et al.* (2019) The parameters that correspond to each case are described in the Table 5.1.

TABLE 5.1 – Fitting parameters of the mass function and the poles defining the weight functions in equation (4.6). Those parameters correspond to the LQCD calculations of Ref. Bowman *et al.* (2005), with $m_0^{LQCD} = 155$ MeV, and to the ones of Ref. Oliveira *et al.* (2019), with $m_0^{LQCD} = 8$ MeV.

Model	m_0 GeV	m GeV	λ GeV	$\mathcal{M}(0)$ GeV	m_1 GeV	m_2 GeV	m_3 GeV
I	0.175	0.770	1.170	0.508	0.674	0.796	1.29
II	0.008	0.648	0.900	0.344	0.469	0.573	1.035

5.1 Heavy Quark Bare Mass

In this subsection we solve the BS equation considering a constituent gluon mass of 637 MeV, $\Lambda = 306$ MeV and the bound state mass M equal to the pion mass of 140 MeV for different parametrizations of the quark-mass function $\mathcal{M}(p^2)$. In particular, we obtain a set of parameters compatible with LQCD calculations with bare quark mass m^{LQCD} of 155 MeV (BOWMAN *et al.*, 2005), which we call Model I, as shown in Fig. 5.1.

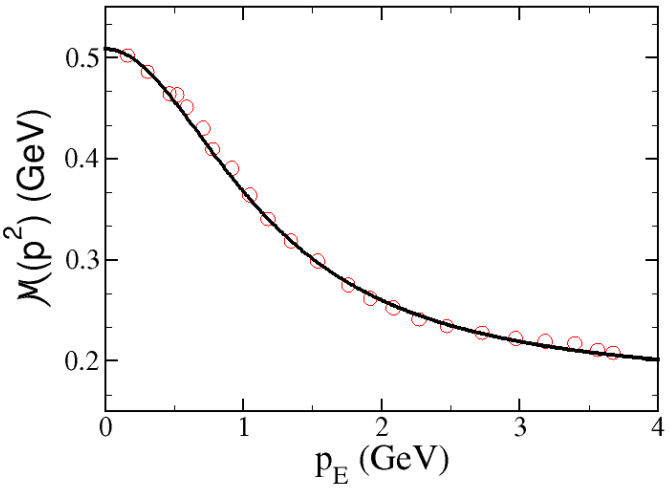

FIGURE 5.1 – The running quark-mass, $\mathcal{M}(p^2)$, as a function of the Euclidean momentum $p_E = \sqrt{-p^2}$. Solid line: Model I, with $m_0 = 175$MeV, $m = 770$MeV and $\lambda = 1.17$GeV in the fitting expression (4.2). Circles: LQCD calculations from Ref. Bowman *et al.* (2005).

TABLE 5.2 – The mass pole positions for each value of m. In all cases, $\lambda = 1.17\,\text{GeV}$ and bare mass $m_0 = 0.175\,\text{GeV}$. The mass values are in GeV.

m	m_1	m_2	m_3	$\mathcal{M}(0)$
0.05	0.1750	1.16994	1.17004	0.1751
0.10	0.1757	1.16957	1.17031	0.1757
0.20	0.1809	1.16654	1.17253	0.1808
0.40	0.2235	1.14134	1.18987	0.2218
0.50	0.2715	1.11149	1.20800	0.2663
0.60	0.3481	1.06066	1.23378	0.3328
0.70	0.4750	0.96752	1.26754	0.4256
0.77	0.6745	0.79630	1.29587	0.5085

In order to understand the impact of considering a dynamical mass function over the solutions of the BS equations, we vary the parameter m from 0 to 0.77 GeV, keeping fixed $m_0 = 0.175$ GeV and $\lambda = 1.17$ GeV. In this way, we interpolate between the constituent

quark mass and Model I. The pole positions and the Infrared (IR) mass $\mathcal{M}(0)$ are shown in Table 5.2. In Fig. 5.2 it is shown that the coupling constant increases quadratically with the value of the parameter m, which tune the effect of the running quark mass.

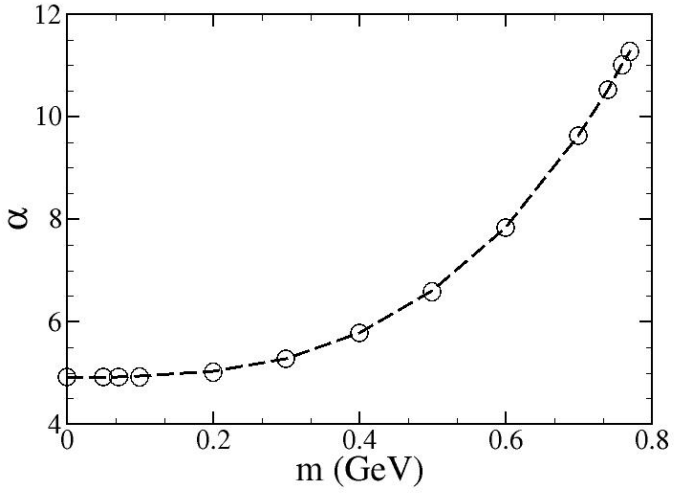

FIGURE 5.2 – The coupling constant α as a function of m. The parameters are: $\mu = 637\,\text{MeV}$, $\Lambda = 306\,\text{MeV}$, $m_0 = 175\,\text{MeV}$, $\lambda = 1.17\,\text{GeV}$ and pion mass of 140 MeV. The point $m = 0$ corresponds to a constituent quark mass of 175MeV, that gives a coupling constant of $\alpha = 4.918$. The point $m = 770\text{MeV}$ corresponds to Model I.

In Chapter 4, we have seen that the phenomenological dressed quark propagator has three poles, which combined effects is able to reproduce the expected quark mass function from lattice QCD computations (BOWMAN *et al.*, 2005). In contrast, the constituent quark mass model has a single pole. So, in order to better capture the dressing effect, in Fig. 5.3 the coupling constant α is shown as a function of the respective lightest pole m_1 for a given value of m. In the same figure, it is also presented the solution of the BSE considering a constituent quark mass of m_1.

In Table 5.2 is presented the mass pole positions for each value of m. For small values of m, the poles m_2 and m_3 are almost the same. This fact leads to a cancellation of their effect in the quark propagator. Indeed, in Fig. 5.3, it is observed an agreement between the constituent mass computation and the one considering dressing quark propagator for $m \leq 0.06$ GeV. For higher values of m (> 0.06 GeV), the difference of m_2 and m_3 becomes large and a detachment is seen between the curves.

The QCD IR dynamics have a pivotal role in the hadronic structure. The quark-gluon vertex has a huge enhancement in the deep IR, as discussed in Refs. Oliveira *et al.* (2019) and Oliveira *et al.* (2020) This outcome was used in the actual model to set the parameter Λ. In this way, it is expected that IR quantities could be responsible for determining the general features of the particles. With this in mind, in Fig. 5.4 is shown the coupling

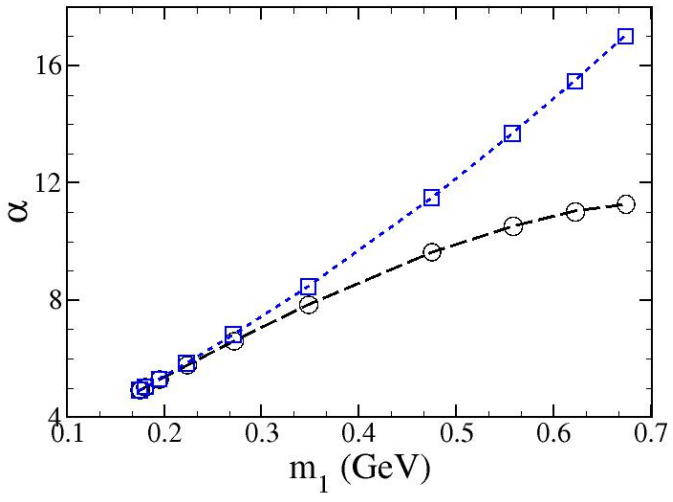

FIGURE 5.3 – The coupling constant vs the lightest quark propagator mass pole m_1. Circles: coupling constant obtained by using the running mass function with $m_0 = 175\,\text{MeV}$ and $\lambda = 1.17\,\text{GeV}$. Square: coupling constant for a constituent quark mass of m_1. The parameters are: $\mu = 637$ MeV, $\Lambda = 306$ MeV and pion mass of 140 MeV.

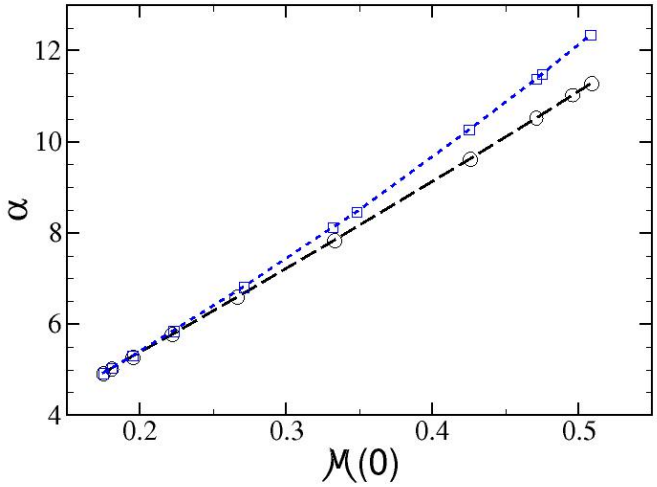

FIGURE 5.4 – The coupling constant vs the IR mass $\mathcal{M}(0)$. Circles: dressed quark propagator model with $m_0 = 175$ MeV and $\lambda = 1.17$ GeV. Square: constituent quark mass of $\mathcal{M}(0)$. The parameters are $\mu = 637$ MeV, $\Lambda = 306$ MeV, and pion mass of 140 MeV.

constant vs the deep IR mass $\mathcal{M}(p^2 = 0)$, where it was fixed $m_0 = 175$ MeV and $\lambda = 1.17$ GeV. It is observed an almost linear behavior and a small deviation from the constituent quark mass calculation, which illustrates the importance of the IR mass in the bound state formation.

5.2 Light Quark Bare Mass

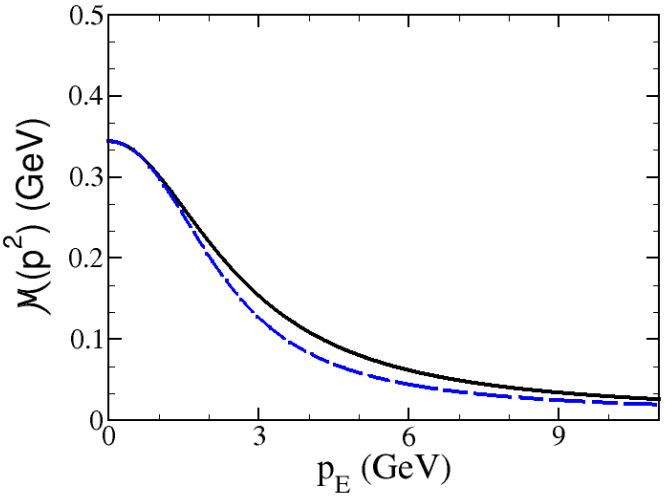

FIGURE 5.5 – The quark running-mass, $\mathcal{M}(p^2)$, as a function of the Euclidean momentum $p_E = \sqrt{-p^2}$. Solid line: equation (4.2) with $m_0 = 0.008\,\text{GeV}$, $m = 0.648\,\text{GeV}$ and $\lambda = 0.9\,\text{GeV}$. Dashed line: parameterization proposed in Ref. Oliveira *et al.* (2020) of the LQCD calculations in Ref. Oliveira *et al.* (2019).

In this subsection, the BS equation is solved for $\mu = 637$ MeV, $\Lambda = 306$ MeV, and pion mass of 140 MeV. It is also considered a dynamical mass function with different sets of parameters. In particular, we present a particular parametrization able to fit the running mass function LQCD calculation with a quark bare mass of 8 MeV (OLIVEIRA *et al.*, 2019), which we call Model II. In Fig. 5.5, it is shown Model II and the parametrization of LQCD calculations proposed in Ref. Oliveira *et al.* (2020), which is described by a dynamical mass function $M_l(k^2)$ given in the following

$$M_l(k^2) = \frac{m_q(k^2)}{\left[A + log(k^2 + \lambda m_q^2(k^2))\right]^{\gamma_m}}, \tag{5.1}$$

$$m_q(k^2) = M_q \frac{k^2 + m_1}{k^4 + m_2^2 k^2 + m_3^4} + m_0 \tag{5.2}$$

where the parameters used are $\gamma_m = \frac{12}{29}$, the quark anomalous dimension for $N_f = 2$, the gluon anomalous dimension equal to γ_A=$-13/22$, Z=1.36486 $\pm$ 0.00097, M_1^2=2.510 $\pm$ 0.030 GeV^2, M_2^2=0.471 $\pm$ 0.0014 GeV^2, M_3^4=0.3621 $\pm$ 0.0038 GeV^4, M_0^2=0.216 $\pm$ 0.026 GeV^2, $\omega = 33\,\alpha_s(k^2)/12\pi$ and $\Lambda_{QCD} = 0.425$ GeV with the running coupling constant $\alpha_s(9\text{ GeV}^2) = 0.3837$.

In order to illustrate the difference between the constituent and the dressed quark propagator, we present in Fig. 5.6 two quantities: $S^V(p^2)\,[p^2 - \mathcal{M}^2(0)]$ and $S^S(p^2)\,[p^2 - \mathcal{M}^2(0)]/\mathcal{M}(0)$ (cf. equation (4.4)), obtained by means of equation (4.6), with poles and

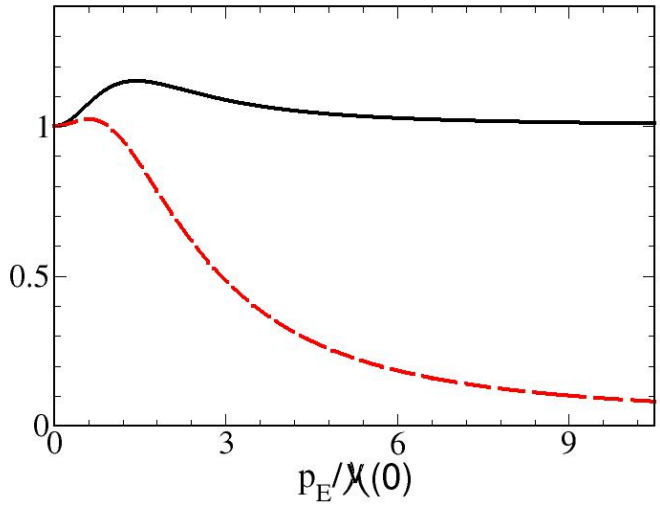

FIGURE 5.6 – The two quantities $S^V(p^2)\,[p^2-\mathcal{M}^2(0)]$ (solid line) and $S^S(p^2)\,[p^2-\mathcal{M}^2(0)]/\mathcal{M}(0)$ (dashed line) vs. $p_E/\mathcal{M}(0)$.

residues given in Table 5.3. It is worth noting that, for both functions, the tails are the expected ones in the limit $p_E \gg \mathcal{M}(0)$, i.e. the ones pertaining to a massless quark propagator, $\not{p}/p^2$.

TABLE 5.3 – Poles, m_i, and residues, R_i,(cf equations (4.6) and (4.7)) for the fit to the LQCD mass function in Ref. Oliveira *et al.* (2019). The IR mass $\mathcal{M}(0) = m_0 + m^3/\lambda^2$ is 0.344 GeV, and the parameters of the running mass are also given in the Table 5.1.

i	$m_i/\mathcal{M}(0)$	R_i^V	$R_i^S/\mathcal{M}(0)$
1	1.365	3.7784	5.1578
2	1.667	-2.8863	-4.8099
3	3.008	0.1079	-0.3244

In Fig. 5.7, the parameter m is used to interpolate between a current-mass quark scenario and a fully-dressed one (Model II). For each case, we kept fixed the IR mass $\mathcal{M}(0) = 344$ MeV and $\lambda = 900$ MeV. As expected from the discussion regarding Fig. 5.4, the coupling constant has a small variation between the constituent quark mass and Model II. The reason is that the relevant parameter in the bound state formation dynamics is the IR mass.

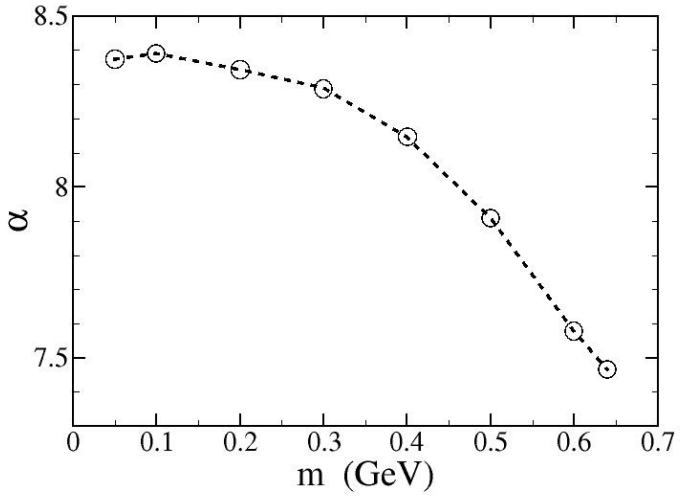

FIGURE 5.7 – The coupling constant vs m for a fixed IR mass of 344 MeV. The parameters are: $\lambda = 900$ MeV, $\mu = 637$ MeV, $\Lambda = 306$ MeV and pion mass of 140 MeV.

5.3 Light-front Amplitudes

In this section we obtain the light-front (LF) amplitudes for Model II. The physical parameters are the constituent gluon mass of 0.469 GeV and an extended quark-gluon vertex scale $\Lambda = 0.1$ GeV. We present results for two different bound state masses, $M = 0.447$GeV and $M = 0.653\,$GeV.

The light-front amplitudes $\psi_i(\gamma, \xi)$ can be obtained by projecting the components of the BS amplitude $\phi_i(k, p)$ onto the light-front. Using the NIR of the scalar functions ϕ_i as given in equation (3.11), we obtain

$$\psi_i(\gamma, \xi) \;=\; \int \frac{dk^-}{2\pi}\phi_i(k,p) = -\frac{i}{M}\int_0^\infty \frac{g_i(\gamma', z)}{\left(\gamma' + \gamma + m_1^2 z^2 + (1-z^2)\kappa^2\right)^2}, \qquad (5.3)$$

where $\gamma = |\mathbf{k}_\perp|^2$ and $\xi = \frac{1}{2} + \frac{k^+}{p^+} = (1-z)/2$, with ξ belonging to [0,1]. Once we solve the BS equation, we have the Nakanishi weight functions and we can obtain the light-front amplitudes $\psi_i(\gamma, \xi)$, which are scalar functions that will be used to construct the valence component of the 0^- bound state system.

The LF amplitudes $\psi_i(\gamma, \xi)$ for the pseudoscalar system bound by a vector exchange are presented in Fig. 5.8 and 5.9. We compare the results using dressed quark propagator (Model II) against the fixed mass model, for two different binding energies, which correspond to bound state masses of $M = 0.653\,$GeV and $M = 0.447\,$GeV.

The motivation of this comparison is to understand the impact of using dressed quark propagator in the bound state analysis, as well as how the binding affects its inner struc-

ture. In Fig. 5.8, it is shown the dependence on ξ of the LF amplitudes. They present the expected maximum around 1/2, except for ψ_3, which is anti-symmetric in z.

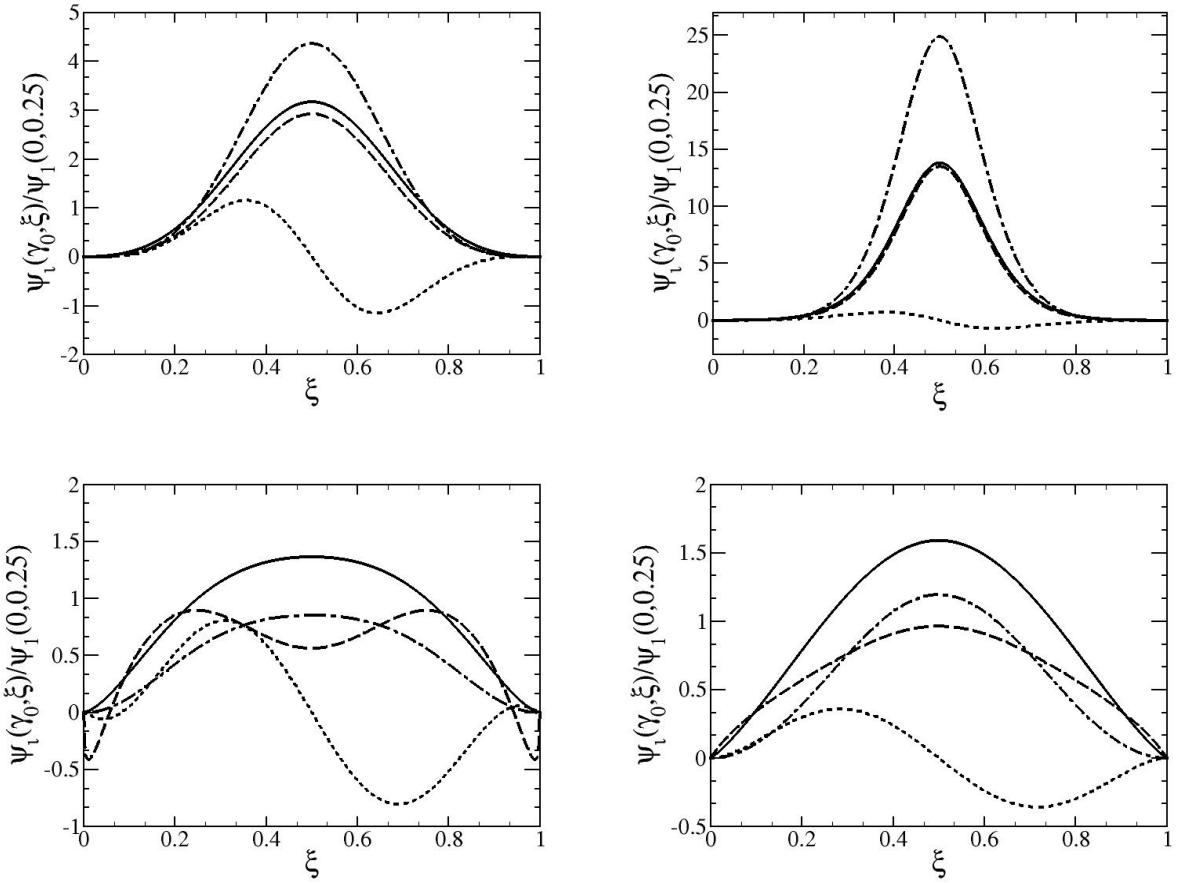

FIGURE 5.8 – Light-front amplitudes as a function of ξ. On the left are presented the LF amplitudes considering the running mass function. On the right are presented the amplitudes considering fixed quark mass of $m_q = 0.344$GeV. In the upper panel $M = 0.653\,$GeV. In the lower panel $M = 0.447\,$GeV. The other parameters are $\Lambda = 0.1\,$GeV and $\mu = 0.469\,$GeV. Solid line: ψ_1. Dashed line: ψ_2. Doted line: ψ_3. Doted-dashed line: ψ_4.

By increasing the binding, we obtain the expected behavior: the peak decreases and it starts to increase the value of ψ_i close to the end-points. The reason is that higher bindings imply more compact systems and therefore relativistic effects are more important, which are present in the end-points. In general, the effect of the dressing in ψ_i is also a broadening of the distribution. One can see that, with respect to ξ, the fixed mass cases present narrow peaks around 1/2.

The amplitudes ψ_1 and ψ_2 present similar behavior when considering their dependence on ξ, almost coinciding with each other in the fixed mass model and with little distance between them in the running mass case. The change in their behavior, when the binding is stronger, is a broadening distance amidst them in the fixed mass model. However, in the running mass propagator case, ψ_2 acquires two peaks while ψ_1 has a more flat curve in comparison with the fixed mass model.

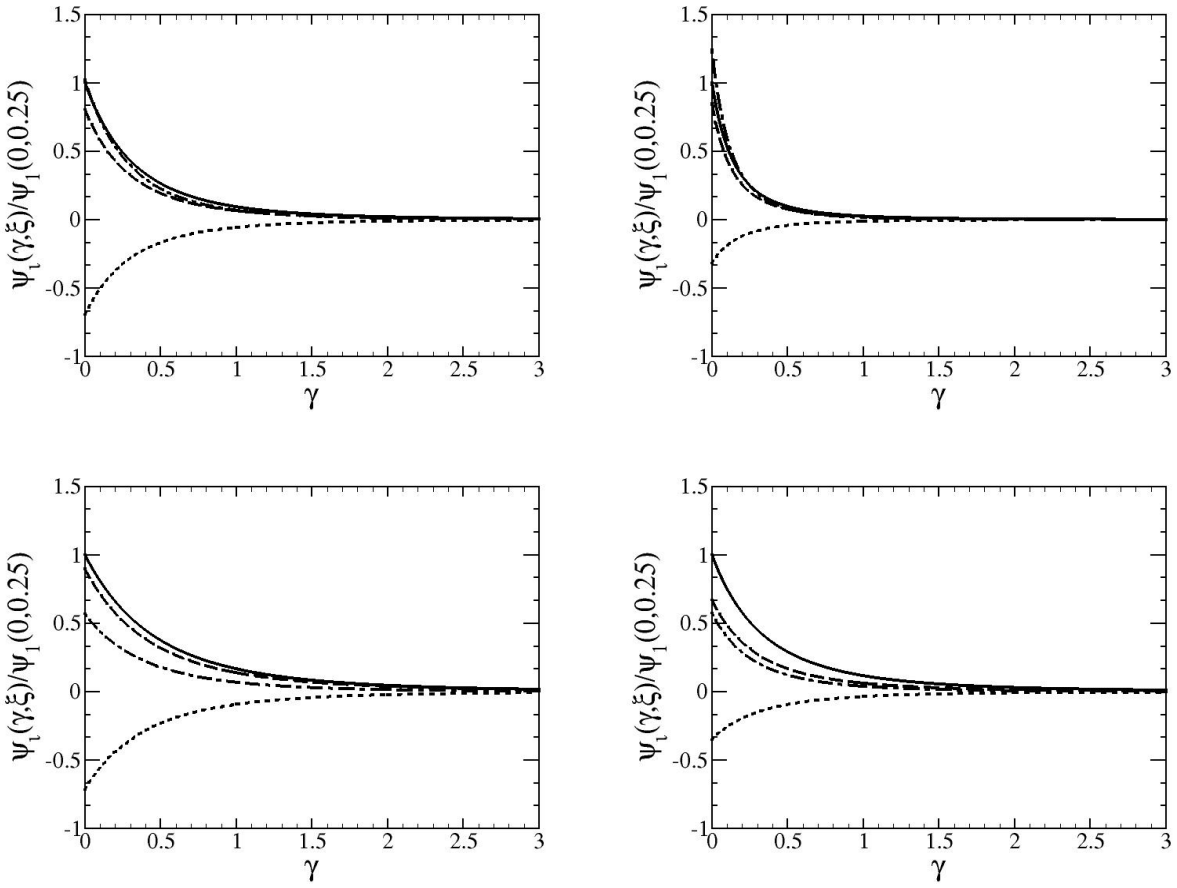

FIGURE 5.9 – Light-front amplitudes as a function of γ. On the left are presented the LF amplitudes considering the running mass function. On the right are presented the amplitudes considering fixed quark mass of $m_q = 0.344$GeV. In the upper panel $M = 0.653\,$GeV. In the lower panel $M = 0.447\,$GeV. The other parameters are $\Lambda = 0.1\,$GeV and $\mu = 0.469\,$GeV. Solid line: ψ_1. Dashed line: ψ_2. Doted line: ψ_3. Doted-dashed line: ψ_4.

In the Fig. 5.9, it is presented the dependence in γ of the LF-amplitudes. It is shown that the system explores a higher transverse momentum region when the binding increases. This is also explained by the fact that for higher binding, the system shrinks and therefore becomes more relativistic. The same effect is obtained by comparing the fixed mass case (right panels) against the model with dressed quark propagators (left panels).

The LF-amplitudes are the building blocks to construct hadronic observables. In the next section, we are going to discuss the valence momentum distributions, which give more information about the 0^- bound state structure under analysis.

5.4 Valence Momentum Distributions

In this section we use the mass function parameterized in Model II to calculate the valence momentum distributions. We considered a constituent gluon mass of 0.469 GeV

and quark-gluon vertex scale $\Lambda = 0.1$ GeV, exploring the mass of the bound system in the range $3m_\pi < M < 5m_\pi$ (cf. Table 5.4). The analysis of the coupling constant gives a

TABLE 5.4 – The chosen masses, M, of the 0^- bound-system (in unit of the IR mass $\mathcal{M}(0) = 0.344$ GeV) are presented along with the coupling constants $\alpha = g^2/4\pi$ and the percentages of the spin configurations in the valence wave function. Recall that in addition to M the set of model parameters is completed by: i) the gluon mass $\mu/\mathcal{M}(0) = 1.363$, ii) a the vertex parameter $\Lambda/\mathcal{M}(0) = 0.291$ and iii) $\lambda/\mathcal{M}(0) = 2.616$ (see equation (4.2)). For each M, the first line represents the dressed case, while the second line is the undressed one with a quark mass equal to 0.344 GeV.

$M/\mathcal{M}(0)$	g^2	α	$\mathcal{P}_{\uparrow\downarrow}(\%)$	$\mathcal{P}_{\uparrow\uparrow}(\%)$
1.9	7.62	0.61	93	7
	3.76	0.30	96	4
1.6	12.46	0.99	93	7
	11.29	0.90	93	7
1.5	14.13	1.12	93	7
	13.67	1.09	93	7
1.4	15.78	1.26	94	6
	15.93	1.27	93	7
1.3	17.38	1.38	94	6
	18.07	1.44	93	7

global information of the bound state formation. In general, the behavior for the running and fixed mass models is in accordance with the physical intuition: decreasing the mass of the bound state implies in higher values of the coupling constant.

For a fixed mass model, the binding energy B is defined as the difference between the bound-system mass M and the constituent mass m_q, $B = 2m_q - M$. Intuitively, one can generalize to the dressed quark propagator model by considering $B = 2m_{eff} - M$, being m_{eff} an effective quark mass. In Table 5.4, we compare the running mass model with the fixed mass case considering $m_q = \mathcal{M}(0)$. On the other hand, Fig. 5.5 shows that the effective mass should be smaller than the IR mass. For small M the coupling constant of the Model II is higher than the fixed mass case. When the binding energy increases, the effective mass decreases, because the system shrinks and the momentum-distribution tail grows, emphasizing the small mass region in $\mathcal{M}(p^2)$. Therefore, by increasing the binding, the coupling constant for the running mass case increases slower than the fixed mass model. In the limit, we expect that m_{eff} achieves an asymptotic value in the IR region. At some point, around $M = 0.48$, there is an inversion of the hierarchy with the coupling of the fixed mass case higher than the running mass model.

The valence wave function is obtained by LF-projecting the BS amplitude, and notably, it can be decomposed into its quark-spin configurations, $S = 0$ and $S = 1$, as demonstrated in Chapter 4, which is clear in equation (4.37). The amplitudes $\psi_i(\gamma, z)$ are obtained by integrating on k^- the scalar functions in equation (5.3), as we discussed in section 4.4.

In correspondence, we can write the valence probability density (cf. equation (4.42)) as follows

$$\mathcal{P}_{val}(\gamma, z) = \mathcal{P}_{\uparrow\downarrow}(\gamma, z) + \mathcal{P}_{\uparrow\uparrow}(\gamma, z)\,, \tag{5.4}$$

where one has the antialigned and the aligned probability densities given as

$$\mathcal{P}_{\uparrow\downarrow(\uparrow\uparrow)}(\gamma, z) = \frac{N_c}{16\pi^2}|\Psi_{\uparrow\downarrow(\uparrow\uparrow)}(\gamma, z)|^2\,. \tag{5.5}$$

Considering the normalization of $\mathcal{P}_{val} = 1$, we have calculated the percentage of each spin component, $\mathcal{P}_{\uparrow\downarrow}$ and $\mathcal{P}_{\uparrow\uparrow}$, as one can see in Table 5.4. We can define the longitudinal[1] and the transverse momentum distributions as follows

$$\phi(\xi) = \int_0^\infty d\gamma \left(\mathcal{P}_{\uparrow\downarrow}(\gamma, z) + \mathcal{P}_{\uparrow\uparrow}(\gamma, z)\right)\,, \tag{5.6}$$

$$P(\gamma) = \int_1^{-1} dz \left(\mathcal{P}_{\uparrow\downarrow}(\gamma, z) + \mathcal{P}_{\uparrow\uparrow}(\gamma, z)\right)\,, \tag{5.7}$$

with $\mathcal{P}_{\uparrow\downarrow}(\gamma, z)$ and $\mathcal{P}_{\uparrow\uparrow}(\gamma, z)$ defined in equation (5.5). Furthermore, we define the components of the longitudinal and transverse momentum distributions as:

$$\phi(\xi)_{\uparrow\downarrow(\uparrow\uparrow)} = \int_0^\infty d\gamma \mathcal{P}_{\uparrow\downarrow(\uparrow\uparrow)}(\gamma, z)\,, \tag{5.8}$$

$$P(\gamma)_{\uparrow\downarrow(\uparrow\uparrow)} = \int_{-1}^1 dz \mathcal{P}_{\uparrow\downarrow(\uparrow\uparrow)}(\gamma, z)\,. \tag{5.9}$$

The longitudinal and transverse momentum distributions are presented in Figs. 5.10 and 5.13, for bound state masses of $M = 0.653$ GeV and $M = 0.447$ GeV. It is also presented the spin components in Figs. 5.11, 5.12, 5.14 and 5.15. On the left panels of the above figures, it is used dressed quark propagator (Model II), while on the right panels, it is considered a constituent quark propagator model.

By looking at Fig. 5.10, for $M = 0.653$ GeV, the total longitudinal distribution for the fixed-mass model is narrower than the running-mass one, decreasing faster when approaching the end-points. That can be understood by a smaller value of the coupling constant (cf. the first two lines in Table 5.4) that leads to a larger size of the system and hence a smaller average relative momentum. While to $M = 0.447$GeV, we have the opposite behavior between them, which reflects the hierarchy's change of the coupling constant (c.f. Table 5.4).

The aligned component of the longitudinal momentum distribution (Fig. 5.11) is broader than the anti-aligned one (Fig. 5.12) whether in the dressing of the quarks or

[1]The longitudinal momentum distributions are represented by $\phi(\xi)$. On the other side, the Nakanishi amplitudes are also represented by $\phi(\gamma', z')$.

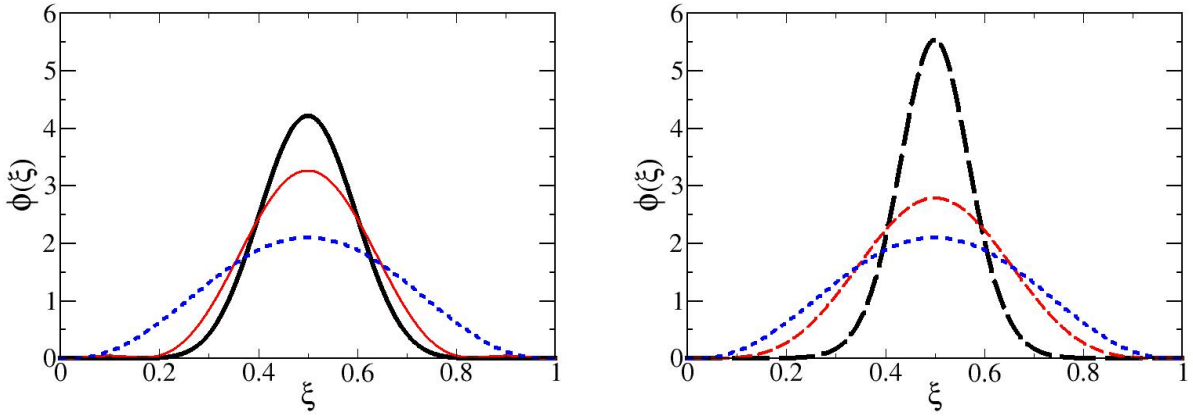

FIGURE 5.10 – The longitudinal momentum distribution defined in equation (5.6), with $\Lambda = 0.1\,\text{GeV}$ and $\mu = 0.469\,\text{GeV}$. Left panel: Thick solid line - running mass model for $M = 0.653\,\text{GeV}$. Thin solid line - the same as the thick one, but for $M = 0.447\,\text{GeV}$. Dotted line: fixed quark mass with bound state mass $M = m_\pi = 0.141\,\text{GeV}$. Right panel: Thick dashed Line - fixed quark mass equal to $0.344\,\text{GeV}$ and $M = 0.653\,\text{GeV}$. Thin dashed line - the same as the thick one, but for $M = 0.447\,\text{GeV}$. Dotted line - the same as the thick one, but for $M = m_\pi = 0.141\,\text{GeV}$.

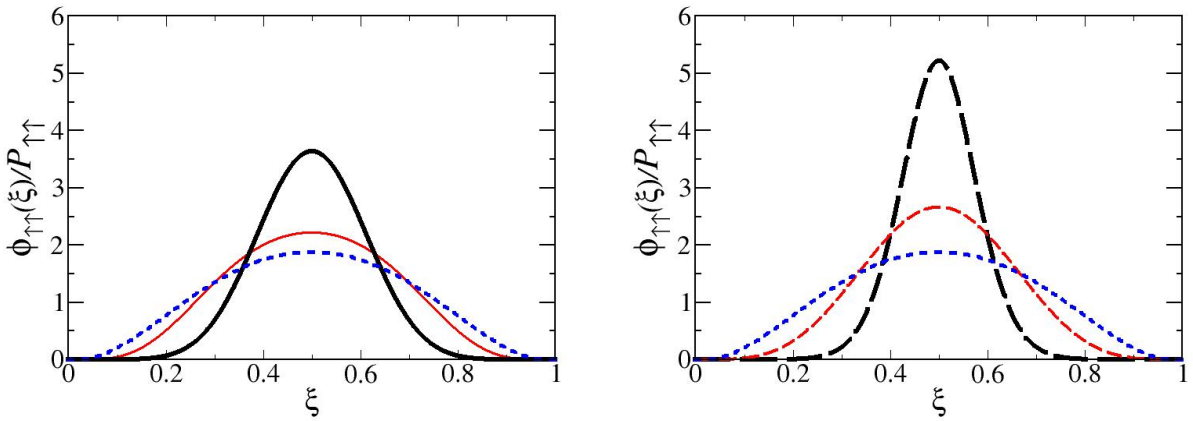

FIGURE 5.11 – Parallel component of the longitudinal momentum distributions defined in equation (5.8), with $\Lambda = 0.1\,\text{GeV}$ and $\mu = 0.469\,\text{GeV}$. Left panel: Thick solid line - running mass model for $M = 0.653\,\text{GeV}$. Thin solid line - the same as the thick one, but for $M = 0.447\,\text{GeV}$. Dotted line: fixed quark mass with bound state mass $M = m_\pi = 0.141\,\text{GeV}$. Right panel: Thick dashed Line - fixed quark mass equal to $0.344\,\text{GeV}$ and $M = 0.653\,\text{GeV}$. Thin dashed line - the same as the thick one, but for $M = 0.447\,\text{GeV}$. Dotted line - the same as the thick one, but for $M = m_\pi = 0.141\,\text{GeV}$.

fixed mass model, which can be explained due to the relativistic nature of the aligned component. For $M = 0.447$ GeV, the running mass-case and the fixed-mass one yield closer results than the one obtained for $M = 0.653$. This can be expected if one looks at the similar values of the corresponding coupling constants present in Table 5.4.

In Table 5.4 is shown the relative weight in the valence state between the anti-aligned and the aligned spin components. By varying M, both spin configurations keep almost the same percentage for both running and fixed quark masses. A possible explanation of this feature regards to adoption of the same interaction kernel in both the fixed mass

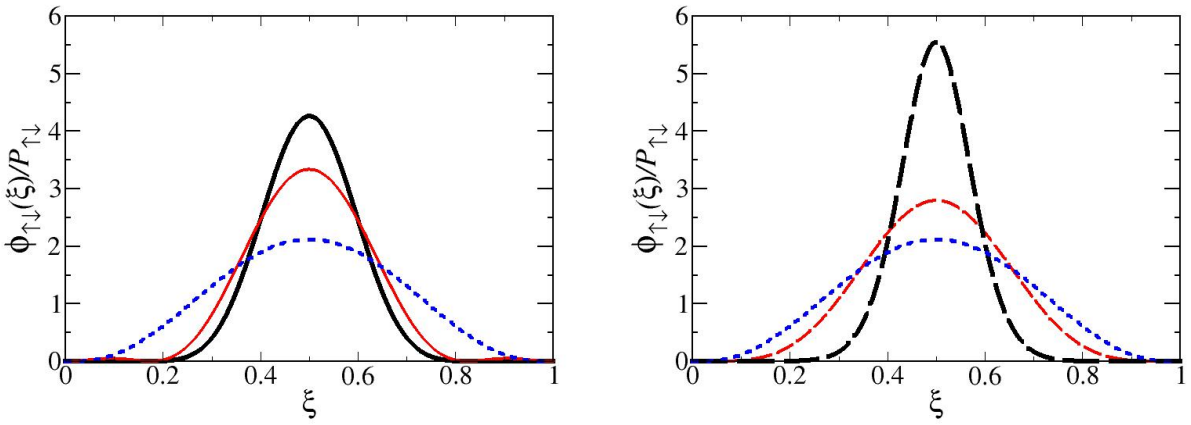

FIGURE 5.12 – Anti-Parallel component of the longitudinal momentum distributions defined in equation (5.8), with $\Lambda = 0.1\,\text{GeV}$ and $\mu = 0.469\,\text{GeV}$. Left panel: Thick solid line - running mass model for $M = 0.653\,\text{GeV}$. Thin solid line - the same as the thick one, but for $M = 0.447\,\text{GeV}$. Dotted line: fixed quark mass with bound state mass $M = m_\pi = 0.141\,\text{GeV}$. Right panel: Thick dashed Line - fixed quark mass equal to $0.344\,\text{GeV}$ and $M = 0.653\,\text{GeV}$. Thin dashed line - the same as the thick one, but for $M = 0.447\,\text{GeV}$. Dotted line - the same as the thick one, but for $M = m_\pi = 0.141\,\text{GeV}$.

model and dressed quark propagator model.

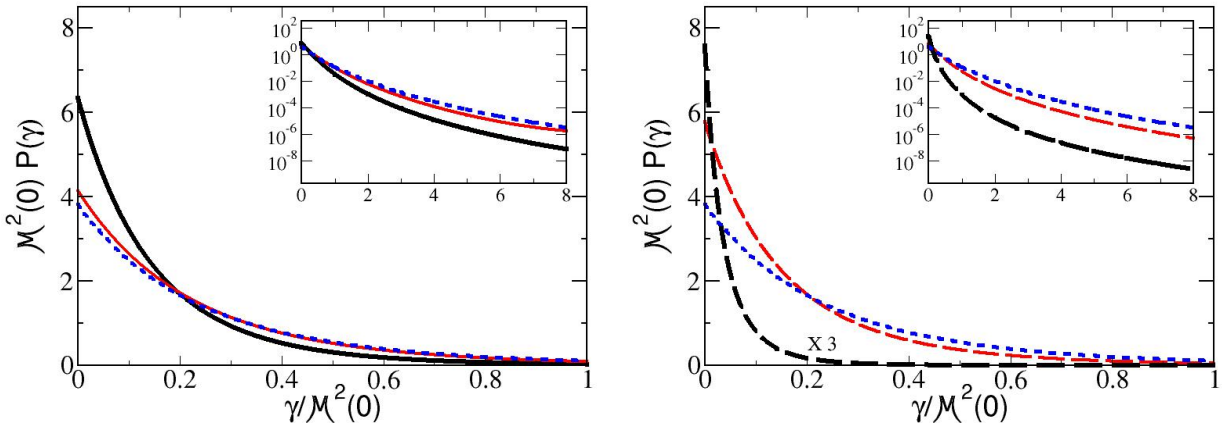

FIGURE 5.13 – Transverse momentum distribution defined in equation (5.7), with $\Lambda = 0.1\,\text{GeV}$ and $\mu = 0.469\,\text{GeV}$. Left panel: Thick solid line - running mass model for $M = 0.653\,\text{GeV}$. Thin solid line - the same as the thick one, but for $M = 0.447\,\text{GeV}$. Dotted line: fixed quark mass with bound state mass $M = m_\pi = 0.141\,\text{GeV}$. Right panel: Thick dashed Line - fixed quark mass equal to $0.344\,\text{GeV}$ and $M = 0.653\,\text{GeV}$. Thin dashed line - the same as the thick one, but for $M = 0.447\,\text{GeV}$. Dotted line - it is the same as the thick one, but for $M = m_\pi = 0.141\,\text{GeV}$.

The dressing of the quark-propagator generates a larger momentum tail than in the undressed case as one can see in the transverse momentum distribution presented in the inset of Fig. 5.13 [2]. Also, when analyzing the parallel (Fig. 5.14) and anti-parallel (Fig. 5.15) spin components, the same behavior is observed. Furthermore, the dressing of the quark-gluon vertex weakens the kernel at a scale of $\Lambda^2/\mathcal{M}^2(0) \sim \gamma/\mathcal{M}^2(0) \sim 0.1$, as

[2]The thick black dashed line, in the right panel, was divided by 3 in order to compare the behavior of the curves more easily. Thus in order to see the real curve one needs to multiply by 3.

shown in the plots for the larger binding corresponding to $M = 0.447$ in both dressed and undressed quark cases. Another point to remark is that the aligned transverse momentum distribution vanishes for $\gamma = 0$, as one can see in Fig. 5.14. This is expected for an orbital-angular momentum $L = 1$ component. The insets in Figs. 5.13-5.15 show that the tail of the transverse distributions has a power law on γ.

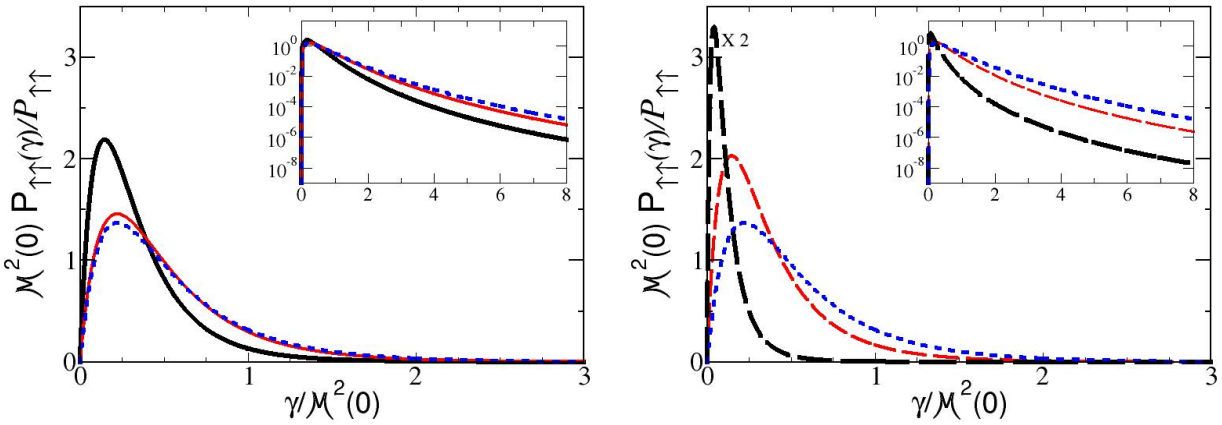

FIGURE 5.14 – Parallel component of the transverse momentum distribution defined in equation (5.9), with $\Lambda = 0.1\,\text{GeV}$ and $\mu = 0.469\,\text{GeV}$. Left panel: Thick solid line - running mass model for $M = 0.653\,\text{GeV}$. Thin solid line - the same as the thick one, but for $M = 0.447\,\text{GeV}$. Dotted line: fixed quark mass with bound state mass $M = m_\pi = 0.141\,\text{GeV}$. Right panel: Thick dashed Line - fixed quark mass equal to $0.344\,\text{GeV}$ and $M = 0.653\,\text{GeV}$. Thin dashed line - the same as the thick one, but for $M = 0.447\,\text{GeV}$. Dotted line - the same as the thick one, but for $M = m_\pi = 0.141\,\text{GeV}$.

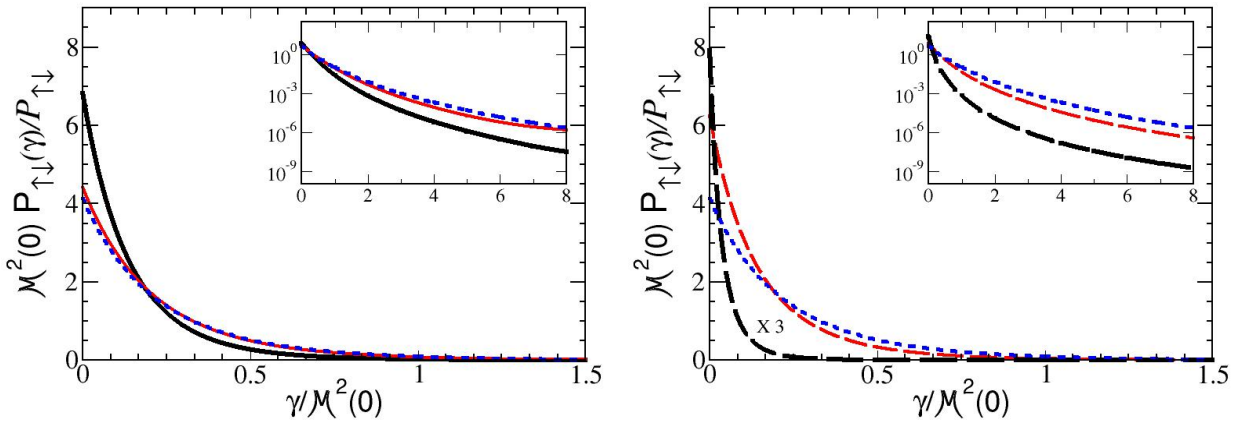

FIGURE 5.15 – Anti-parallel component of the transverse momentum distribution defined in equation (5.9), with $\Lambda = 0.1\,\text{GeV}$ and $\mu = 0.469\,\text{GeV}$. Left panel: Thick solid line - running mass model for $M = 0.653\,\text{GeV}$. Thin solid line - the same as the thick one, but for $M = 0.447\,\text{GeV}$. Dotted line: fixed quark mass with bound state mass $M = m_\pi = 0.141\,\text{GeV}$. Right panel: Thick dashed Line - fixed quark mass equal to $0.344\,\text{GeV}$ and $M = 0.653\,\text{GeV}$. Thin dashed line - the same as the thick one, but for $M = 0.447\,\text{GeV}$. Dotted line - the same as the thick one, but for $M = m_\pi = 0.141\,\text{GeV}$.

6 Conclusions

In this thesis, we calculated bound state static and dynamical quantities by solving the Bethe-Salpeter equation, in Minkowski space, for a pseudo-scalar system 0^-, considering a dressed quark propagator, a massive gluon exchange, in the ladder approximation, and extended quark-gluon vertex. The outcome of the model reflects the competition between three gluonic scales: the effective gluon mass around Λ_{QCD}, the size of the extended quark-gluon vertex ~ 2 fm and the dressing of the quark propagator. Thus, the impact of the dressing on the bound state structure depends on the binding scale.

The main tool to deal with Minkowski space dynamics is to make use of integral representations. In particular, we adopted the Nakanishi integral representation for the components of the Bethe-Salpeter amplitude and the Källen-Lehman spectral representation for the components of the fermionic propagators. The reason for their utility is due to the fact that they give an analytical structure in terms of the external momenta, allowing to perform the loop integration of the kernel of the BS equation. Also, in our framework, we project the BS equation onto the Light-Front. This mathematical step simplifies the coupled integral equations, which are solved numerically by using basis expansion.

The considered dressed quark propagator has a phenomenological mass function, in which parameters are fixed in order to reproduce LQCD calculations. We analyzed two cases: i) Model I - LQCD calculations for bare quark mass of 155 MeV; ii) Model II - LQCD calculations for bare quark mass of 8 MeV. For Model I, we studied the evolution of the coupling constant in terms of the parameter m, which interpolates between the fixed mass case and the fully dressed one. We observed a quadratically increasing of the eigenvalues (c.f Fig. 5.2).

Also, it was made an analysis of the coupling constant in terms of the lightest pole m_1, where we observed a detachment of the fixed mass model and dressed quark propagator only for $m > 0.06$ GeV (see Fig. 5.3). The reason for the discrepancy is due to the fact that for $m > 0.06$ GeV the other two poles of the running mass function have the same order of magnitude of the lightest one (see Table 5.2). Finally, by plotting the coupling constant against the IR mass $\mathcal{M}(0)$, it was observed a linear dependence and a small difference between the fixed quark mass calculation and the dressed one, which shows the

important role of the QCD IR dynamics in the hadronic structure (c.f. Fig. 5.4).

For Model II, we studied the difference between the constituent and the dressed quark propagator behavior (see Fig. 5.6), observing that in the limit $p_E \gg \mathcal{M}(0)$ the tails behave as expected for a massless quark propagator. In addition, the coupling constant dependence with the IR mass was shown, demonstrating a small variation ($\sim 10\%$) between the fixed mass case and the dressed quark model (c.f. Fig. 5.7), as already obtained for Model I. The analysis of the coupling constant behavior shows, in the case of the light quark mass, that depending on the value of M we have a change of hierarchy between the coupling constant of the running quark mass model and of the fixed mass case (see Table 5.4). Such effect happens because the running mass coupling constant increases slower than the one of the fixed mass model as the binding increases, reflecting the interplay between the three gluonic scales.

An important step for understanding the bound state internal structure is to determine the momentum distributions. In this thesis, we calculated the longitudinal and transverse valence momentum distributions in a dynamical model for two different bound state masses, $M = 653$ MeV and $M = 447$ MeV. We showed that, in the quark dressing model, the valence momentum distributions decay slower for high transverse momentum when compared to the case of an undressed one, with a fixed quark mass equal to the IR mass $\mathcal{M}(0) = 344$ MeV. In our analysis, we found that in whatever cases, fixed mass model or running mass function model, the aligned spin component of the valence wave function is suppressed with respect to the anti-aligned one, which could be explained by the fact that in both cases we used a ladder kernel approximation with the same gluon propagator and quark-gluon vertex.

The analyzed system that we discussed in this work is a first step to build a dynamical model with dressed quark propagators for the pion. We will implement an absolute normalization (c.f Appendix F), which is important to assure the predictability of the model when we construct observables that depend on the LF amplitudes. There are many observables that we intend to calculate in order to gain a better understanding of the pion structure. Firstly, we aim to implement the Electromagnetic Form Factor (c.f Appendix G) and the correspondent decay constant and charge radius. Furthermore, we intend to calculate the parton momentum distributions functions (PDFs), transverse momentum distributions (TMDs) and generalized parton distributions (GPDs), which are in line with the ongoing experimental efforts of JLAB (RADYUSHKIN, 2017) and CERN (ADOLPH *et al.*, 2013) in producing a three-dimensional (3D) tomographic image of the structure of hadrons. It is worth mentioning the planned accelerator "Electron-Ion Collider" (ACCARDI *et al.*, 2023; AGUILAR *et al.*, 2019), which will be dedicated to this purpose.

An important improvement for the model is to solve the BS equation for a dressed quark propagator which is an actual solution of the Dyson-Schwinger equation, in rainbow

ladder approximation. We stress that the expressions of the coefficients of the kernel in chapter 4 are suitable for using the spectral densities derived from the solution of the DS equation for the quark propagator. Furthermore, one can extend this framework to other hadrons, such as the kaon, by considering different quark propagators.

Bibliography

AAD, G. *et al.* Observation of a new particle in the search for the standard model higgs boson with the atlas detector at the lhc. **Physics Letters B**, v. 716, n. 1, p. 1–29, 2012. ISSN 0370-2693.

ACCARDI, A. *et al.* Strong Interaction Physics at the Luminosity Frontier with 22 GeV Electrons at Jefferson Lab. 6 2023.

ADOLPH, C. *et al.* Hadron Transverse Momentum Distributions in Muon Deep Inelastic Scattering at 160 GeV/c. **Eur. Phys. J. C**, v. 73, n. 8, p. 2531, [Erratum: Eur.Phys.J.C 75, 94 (2015)], 2013.

AGUILAR, A. C. *et al.* Pion and Kaon Structure at the Electron-Ion Collider. **Eur. Phys. J. A**, v. 55, n. 10, p. 190, 2019.

ARBUZOV, A. *et al.* On the physics potential to study the gluon content of proton and deuteron at NICA SPD. **Prog. Part. Nucl. Phys.**, v. 119, p. 103858, 2021.

BACCHETTA, A. Where do we stand with a 3-D picture of the proton? **Eur. Phys. J. A**, v. 52, n. 6, p. 163, 2016.

BAKKER, B. *et al.* Light-front quantum chromodynamics: A framework for the analysis of hadron physics. **Nuclear Physics B - Proceedings Supplements**, v. 251-252, p. 165–174, international Conference on Light-Cone Physics: Hadronic and Particle Physics, 2014. ISSN 0920-5632.

BELYAEV, A.; ROSS, D. **The Basics of Nuclear and Particle Physics**. Southampton: Springer Nature Switzerland, 2021.

BJORKLUND, R. *et al.* High Energy Photons from Proton-Nucleon Collisions. **Phys. Rev.**, v. 77, p. 213–218, 1950.

BOWMAN, P. O. *et al.* Unquenched quark propagator in landau gauge. **Phys. Rev. D**, American Physical Society, v. 71, p. 054507, Mar 2005.

BRAIBANT, S.; GIACOMELLI, G.; SPURIO, M. **Particles and Fundamental Interactions**. Berlin: Springer, 2012. (Undergraduate Lecture Notes in Physics).

BRODSKY, S. Quantum chromodynamics and other field theories on the light cone. **Physics Reports**, v. 301, n. 4-6, p. 299–486, aug 1998.

CAPRI, M. A. L.; SORELLA, S. P.; TERIN, R. C. All order renormalizable refined Gribov-Zwanziger model with BRST invariant fermionic horizon function in linear covariant gauges. **Phys. Rev. D**, v. 104, n. 5, p. 054048, 2021.

CARBONELL, J.; KARMANOV, V. A. Solving Bethe-Salpeter equation for two fermions in Minkowski space. **Eur. Phys. J. A**, v. 46, p. 387–397, 2010.

CARBONELL, J.; KARMANOV, V. A. Direct Bethe-Salpeter solutions in Minkowski space. **EPJ Web Conf.**, v. 113, p. 03012, 2016.

CASTRO, A. *et al.* The Bethe-Salpeter approach to bound states: from Euclidean to Minkowski space. **J. Phys. Conf. Ser.**, v. 1291, n. 1, p. 012006, 2019.

CASTRO, A. *et al.* Exploring the 0^- bound state with dressed quarks in Minkowski space. **arXiv**, v. 2305.12536, 2023.

CHAPON, E. *et al.* Prospects for quarkonium studies at the high-luminosity LHC. **Prog. Part. Nucl. Phys.**, v. 122, p. 103906, 2022.

CHATRCHYAN, S. *et al.* Observation of a new boson at a mass of 125 gev with the cms experiment at the lhc. **Physics Letters B**, v. 716, n. 1, p. 30–61, 2012. ISSN 0370-2693.

CHAVEZ, J. M. M. *et al.* Pion gpds: A path toward phenomenology. **arXiv**, n. 2110.06052v1, 2021. Available at: https://doi.org/10.48550/arXiv.2110.06052.

CHENG, T. **Gauge Theory Of Elementary Particle Physics**: Problems and solutions. Oxford: Oxford University Press, 1984. (Oxford science publications). ISBN 9780195693287.

DING, M. *et al.* Drawing insights from pion parton distributions. **Chin. Phys. C**, v. 44, n. 3, p. 031002, 2020.

DUDAL, D. *et al.* A Refinement of the Gribov-Zwanziger approach in the Landau gauge: Infrared propagators in harmony with the lattice results. **Phys. Rev. D**, v. 78, p. 065047, 2008.

DYSON, F. J. The s matrix in quantum electrodynamics. **Phys. Rev.**, American Physical Society, v. 75, p. 1736–1755, Jun 1949.

DYSON, F. J. The Radiation theories of Tomonaga, Schwinger, and Feynman. **Phys. Rev.**, v. 75, p. 486–502, 1949.

FANELLI, C. *et al.* Pion Generalized Parton Distributions within a fully covariant constituent quark model. **Eur. Phys. J. C**, v. 76, n. 5, p. 253, 2016.

FEYNMAN, R. P. Space-time approach to non-relativistic quantum mechanics. **Rev. Mod. Phys.**, American Physical Society, v. 20, p. 367–387, Apr 1948.

FEYNMAN, R. P. Space - time approach to quantum electrodynamics. **Phys. Rev.**, v. 76, p. 769–789, 1949.

FEYNMAN, R. P. The Theory of positrons. **Phys. Rev.**, v. 76, p. 749–759, 1949.

FISCHER, C. S.; ALKOFER, R. Nonperturbative propagators, running coupling, and the dynamical quark mass of landau gauge qcd. **Phys. Rev. D**, v. 67, p. 094020, May 2003.

FREDERICO, T.; SALME, G.; VIVIANI, M. Two-body Scattering States in Minkowski Space and the Nakanishi Integral Representation onto the Null Plane. **Phys. Rev.**, D85, p. 036009, 2012.

FREDERICO, T.; SALME, G.; VIVIANI, M. Nakanishi representation onto the null plane and the solution of the bethe-salpeter equation. **Acta Physica Polonica B, Proceedings Supplement**, v. 6, p. 303–309, 01 2013.

FREDERICO, T.; SALMè, G.; VIVIANI, M. Quantitative studies of the homogeneous Bethe-Salpeter Equation in Minkowski space. **Phys. Rev. D**, v. 89, p. 016010, 2014.

FRITZSCH, H.; GELL-MANN, M.; LEUTWYLER, H. Advantages of the Color Octet Gluon Picture. **Phys. Lett. B**, v. 47, p. 365–368, 1973.

GLASHOW, S. L. The Standard Model. **Interference**, v. 4, n. 1, May 2018.

GOLDSTONE, J. Field Theories with Superconductor Solutions. **Nuovo Cim.**, v. 19, p. 154–164, 1961.

GOLDSTONE, J.; SALAM, A.; WEINBERG, S. Broken Symmetries. **Phys. Rev.**, v. 127, p. 965–970, 1962.

GRASSBERGER, P. Classical charged particles with spin. **Journal of Physics A: Mathematical and General**, v. 11, n. 7, p. 1221, jul 1978.

GRIBOV, V. Quantization of non-abelian gauge theories. **Nuclear Physics B**, v. 139, n. 1, p. 1–19, 1978. ISSN 0550-3213.

GROSS, D. J.; WILCZEK, F. Ultraviolet behavior of non-abelian gauge theories. **Phys. Rev. Lett.**, v. 30, p. 1343–1346, Jun 1973.

GUTIERREZ, C. *et al.* Bethe–Salpeter bound-state structure in Minkowski space. **Phys. Lett. B**, v. 759, p. 131–137, 2016.

GóMEZ, C. L. G. **Minkowski space Bethe-Salpeter equation within Nakanishi representation**. Tese. (Doutorado em Física) — Instituto de Física Teórica, Universidade Estadual Paulista, São Paulo, 2016.

HORN, T.; ROBERTS, C. D. The pion: an enigma within the Standard Model. **J. Phys. G**, v. 43, n. 7, p. 073001, 2016.

ITZYKSON, C.; ZUBER, J. B. **Quantum field theory**. New York: McGraw-Hill, 1980. (International Series In Pure and Applied Physics). ISBN 978-0-486-44568-7.

KAUR, S. *et al.* Tomography of light mesons in the light-cone quark model. **Phys. Rev. D**, v. 102, n. 1, p. 014021, 2020.

KHALEK, R. A. *et al.* Science Requirements and Detector Concepts for the Electron-Ion Collider: EIC Yellow Report. 3 2022.

KUSAKA, K.; SIMPSON, K. M.; WILLIAMS, A. G. Solving the Bethe-Salpeter equation for bound states of scalar theories in Minkowski space. **Phys. Rev. D**, v. 56, p. 5071–5085, 1997.

KUSAKA, K.; WILLIAMS, A. G. Solving the Bethe-Salpeter Equation for Scalar Theories in Minkowski Space. **Phys. Rev.**, D51, p. 7026–7039, 1995.

LATTES, C. M. G. *et al.* Processes involving charged mesons. **Nature**, v. 159, p. 694–697, 1947.

LURIÉ, D.; MACFARLANE, A. J.; TAKAHASHI, Y. Normalization of bethe-salpeter wave functions. **Phys. Rev.**, American Physical Society, v. 140, p. B1091–B1099, Nov 1965.

MACKENZIE, R. Path integral methods and applications. **arXiv: quant-ph/0004090**, 2000.

MARCIANO, W. J.; PAGELS, H. Quantum Chromodynamics: A Review. **Phys. Rept.**, v. 36, p. 137, 1978.

MARTIN, B. R.; SHAW, G. **Nuclear and Particle Physics: an introduction**. 3. ed. West Sussex: John Wiley Sons, 2019.

MOITA, R. M. *et al.* Pion model with the Nakanishi integral representation. **Rev. Mex. Fis. Suppl.**, v. 3, n. 3, p. 0308089, 2022.

NAKANISHI, N. Partial-Wave Bethe-Salpeter Equation. **Phys. Rev.**, v. 130, p. 1230–1235, 1963.

NAKANISHI, N. Perturbation-theoretical integral representation and the high-energy behavior of the scattering amplitude. ii. **Phys. Rev.**, v. 133, p. B1224–B1231, Mar 1964.

NAKANISHI, N. A General survey of the theory of the Bethe-Salpeter equation. **Prog. Theor. Phys. Suppl.**, v. 43, p. 1–81, 1969.

NAKANISHI, N. **Graph Theory and Feynman Integrals**. [*S.l.*]: Gordon and Breach, 1971. (Mathematics and its applications : a series of monographs and texts). ISBN 9780677029504.

NAMBU, Y. Quasi-particles and gauge invariance in the theory of superconductivity. **Phys. Rev.**, American Physical Society, v. 117, p. 648–663, Feb 1960.

NORONHA, A. *et al.* Chiral limit of a fermion-scalar (1/2)+ system in covariant gauges. **Phys. Rev. D**, v. 107, n. 9, p. 096019, 2023.

OLIVEIRA, O. *et al.* Exploring the Quark-Gluon Vertex with Slavnov-Taylor Identities and Lattice Simulations. **Eur. Phys. J. C**, v. 78, n. 7, p. 553, 2018.

OLIVEIRA, O. *et al.* Quark propagator with two flavors of O(a)-improved Wilson fermions. **Phys. Rev. D**, v. 99, n. 9, p. 094506, 2019.

PARAPPILLY, M. B. *et al.* Scaling behavior of quark propagator in full QCD. **Phys. Rev. D**, v. 73, p. 054504, 2006.

PASQUINI, B. Imaging the Partonic Structure of the Nucleon. **Springer Proc. Phys.**, v. 238, p. 763–772, 2020.

PAULA, W. de *et al.* Advances in solving the two-fermion homogeneous Bethe-Salpeter equation in Minkowski space. **Phys. Rev. D**, v. 94, n. 7, p. 071901, 2016.

PAULA, W. de *et al.* Fermionic bound states in Minkowski-space: Light-cone singularities and structure. **Eur. Phys. J. C**, v. 77, n. 11, p. 764, 2017.

PAULA, W. de *et al.* Numerical studies of the Bethe–Salpeter equation for a two-fermion bound state. **J. Phys. Conf. Ser.**, v. 981, n. 1, p. 012020, 2018.

PAULA, W. de *et al.* Observing the Minkowskian dynamics of the pion on the null-plane. **Phys. Rev. D**, v. 103, n. 1, p. 014002, 2021.

PAULA, W. de *et al.* Parton distribution function in a pion with Minkowskian dynamics. **Phys. Rev. D**, v. 105, n. 7, p. L071505, 2022.

PESKIN, M. E.; SCHROEDER, D. V. **An Introduction to Quantum Field Theory**. [*S.l.*]: Westview Press, 1995. Reading, USA: Addison-Wesley (1995) 842 p.

PIMENTEL, R.; PAULA, W. de. Excited States of the Wick–Cutkosky Model with the Nakanishi Representation in the Light-Front Framework. **Few Body Syst.**, v. 57, n. 7, p. 491–496, 2016.

POLITZER, H. D. Reliable Perturbative Results for Strong Interactions? **Phys. Rev. Lett.**, v. 30, p. 1346–1349, 1973.

PRIZE, N. **Hideki Yukawa**: Facts. 2023. Available at: <https://www.nobelprize.org/prizes/physics/1949/yukawa/facts/> . Accessed: 2023-06-30.

RADYUSHKIN, A. Target mass effects in parton quasi-distributions. **Physics Letters B**, v. 770, p. 514–522, 2017. ISSN 0370-2693.

SALMÈ, G. *et al.* Two-Fermion Bethe–Salpeter Equation in Minkowski Space: The Nakanishi Way. **Few Body Syst.**, v. 58, n. 3, p. 118, 2017.

SALPETER, E. E.; BETHE, H. A. A Relativistic equation for bound state problems. **Phys. Rev.**, v. 84, p. 1232–1242, 1951.

SCHWEBER, S. S. **QED and the Men Who Made It**: Dyson, Feynman, Schwinger, and Tomonaga. Princeton: Princeton University Press, 1994. ISBN 9780691036854.

SCHWINGER, J. On quantum-electrodynamics and the magnetic moment of the electron. **Phys. Rev.**, v. 73, p. 416–417, Feb 1948.

SCHWINGER, J. Quantum electrodynamics. I. a covariant formulation. **Phys. Rev.**, v. 74, p. 1439–1461, Nov 1948.

SCHWINGER, J. S. On the Green's functions of quantized fields. 1. **Proc. Nat. Acad. Sci.**, v. 37, p. 452–455, 1951.

STEINBERGER, J.; PANOFSKY, W. K. H.; STELLER, J. Evidence for the production of neutral mesons by photons. **Phys. Rev.**, v. 78, p. 802–805, 1950.

TOMONAGA, S. On a relativistically invariant formulation of the quantum theory of wave fields. **Prog. Theor. Phys.**, v. 1, p. 27–42, 1946.

TOMONAGA, S.-I.; OPPENHEIMER, J. R. On infinite field reactions in quantum field theory. **Phys. Rev.**, v. 74, p. 224–225, 1948.

VANDERSICKEL, N.; ZWANZIGER, D. The Gribov problem and QCD dynamics. **Phys. Rept.**, v. 520, p. 175–251, 2012.

WEINBERG, S. **The Quantum theory of fields. Vol. 1: Foundations**. [*S.l.*]: Cambridge University Press, 2005. ISBN 978-0-521-67053-1, 978-0-511-25204-4.

WILLIAMS, R. **Schwinger-Dyson equations in QED and QCD**: The calculation of fermion-antifermion condensates. Thesis. (Doctor of Philosophy) — University of Durham, Durham, 2007.

WORKMAN, R. L. *et al.* Review of Particle Physics. **Progress of Theoretical and Experimental Physics**, v. 2022, n. 8, 083C01, 08 2022.

YAN, T.-M. Quantum field theories in the infinite momentum frame. 4. Scattering matrix of vector and Dirac fields and perturbation theory. **Phys. Rev. D**, v. 7, p. 1780–1800, 1973.

YDREFORS, E. *et al.* Pion electromagnetic form factor with Minkowskian dynamics. **Phys. Lett. B**, v. 820, p. 136494, 2021.

YDREFORS, E. *et al.* Unpolarized transverse-momentum dependent distribution functions of a quark in a pion with Minkowskian dynamics. **arXiv**, v. 2301.11599, 1 2023.

YUKAWA, H. On the interaction of elementary particles. I. **Proceedings of the Physico-Mathematical Society of Japan**, v. 17, p. 48–57, 1935.

Appendix A - Constant mass propagator

In this appendix we show how to map the constant mass propagator model (CARBONELL; KARMANOV, 2010; PAULA *et al.*, 2016)

$$S(k)_f = i\frac{\not{k} + m'}{k^2 - m'^2 + i\epsilon}\,, \tag{A.1}$$

with the dressed propagator model proposed in this thesis

$$S(k)_d = i\int_0^\infty \frac{\not{k}}{k^2 - s + i\epsilon}\rho_v(s)ds + i\int_0^\infty \frac{\rho_s(s)ds}{k^2 - s + i\epsilon}\,, \tag{A.2}$$

one has to apply, in equation (A.2), the following spectral densities

$$\rho_v(s) = \delta(s - m'^2) \quad \text{and} \quad \rho_s(s) = m'\ \delta(s - m'^2)\,. \tag{A.3}$$

which were obtained by considering the spectral densities residues in equation (4.6) written as

$$R_1^{(v)} = 1 \tag{A.4}$$

$$R_1^{(s)} = m', \tag{A.5}$$

with $R_2^{v,s} = R_3^{v,s} = 0$ and $\lambda = 0$. Besides it is necessary that $m_0 = m'$ and $m = 0$.

Appendix B - $C_{ij,a}$ Coefficients

In this appendix, we present the non-vanishing coefficients $C_{ij,l}(k,k',p)$ necessary for calculations in Chapter (3). The Bethe-Salpeter equation can be written as

$$\Phi(k,p) = S(k+p/2)\int \frac{d^4k'}{(2\pi)^4}\; i\;\mathcal{K}(k,k')\Gamma_1\;\Phi(k',p)\;\hat{\Gamma}_2\;S(k-p/2)\,, \tag{B.1}$$

where $S(k+p/2)$ and $S(k-p/2)$ are the quark propagators, and the quark-gluon vertex is represented by Γ_α. Those vertice structures the coupling can be scalar, pseudoscalar, or vectorial which means $\Gamma_\alpha = 1$, $\Gamma_\alpha = \gamma^5$ and $\Gamma_\alpha = \gamma^\mu$. In special, $\hat{\Gamma}_2 = C\,\Gamma_2^T\,C$.

To obtain the $C_{ij,l}(k,k',p)$ we have to take the equation (3.8) in comparison (3.9), thus we have that

$$\begin{aligned}\sum_l P_l(s,s')C_{ij,l}(k,k',p) = \frac{1}{N_i}Tr\Bigg[S_i(k,p)\left(\left(\not{k}+\frac{\not{p}}{2}\right)\rho_V(s)+\rho_S(s)\right)\\ \times\,\Gamma_1 S_j(k',p)\hat{\Gamma}_2\left(\left(\not{k}-\frac{\not{p}}{2}\right)\rho_V(s')+\rho_S(s')\right)\Bigg]\,,\end{aligned} \tag{B.2}$$

with $N_i = Tr[S_i^2(k,p)]$. By performing the trace operation, choosing the scalar coupling and defining that $P_l(s,s')$ as

$$\begin{aligned} P_1(s,s') &= \rho_V(s)\,\rho_V(s'),\\ P_2(s,s') &= \rho_V(s)\,\rho_S(s')\,,\\ P_3(s,s') &= \rho_S(s)\rho_V(s')\,,\\ P_4(s,s') &= \rho_S(s)\,\rho_S(s')\,, \end{aligned} \tag{B.3}$$

we have the non-vanishing scalar coefficients $C^S_{ij,a}$:

$$
\begin{aligned}
C^S_{11,1} &= -k^2 + M^2/4, \\
C^S_{14,1} &= -B'/M^2, \\
C^S_{22,1} &= -2(k\cdot p)^2/M^2 + k^2 + M^2/4, \\
C^S_{23,1} &= -2(k\cdot p)\ B'/M^4, \\
C^S_{32,1} &= 2(k\cdot p), \\
C^S_{33,1} &= -\frac{B'}{B}\left[-2\frac{(k\cdot p)^2}{M^2} + k^2 + M^2/4\right], \\
C^S_{41,1} &= M^2, \\
C^S_{44,1} &= -B'/B\left[M^2/4 - k^2\right], \\
C^S_{12,2} &= [2(k\cdot p) + M^2]/2M, \\
C^S_{13,2} &= \frac{B'}{M^3}, \\
C^S_{21,2} &= \left[2(k\cdot p) + M^2\right]/2M, \\
C^S_{24,2} &= -\,B'/M^3, \\
C^S_{31,2} &= -M, \\
C^S_{34,2} &= \frac{B'}{B}\frac{\left[2(k\cdot p) + M^2\right]}{2M} \\
C^S_{42,2} &= M, \\
C^S_{43,2} &= \frac{B'}{B}\frac{\left[2(k\cdot p) + M^2\right]}{2M}, \\
C^S_{12,3} &= -\left[2(k\cdot p) - M^2\right]/2M, \\
C^S_{13,3} &= -\frac{B'}{M^3}, \\
C^S_{21,3} &= -\left[2(k\cdot p) - M^2\right]/2M,
\end{aligned}
$$

$$
\begin{aligned}
C^S_{24,3} &= -B'/M^3, \\
C^S_{31,3} &= M, \\
C^S_{34,3} &= \frac{B'}{B}\frac{\left[2(k\cdot p)-M^2\right]}{2M}, \\
C^S_{42,3} &= M, \\
C^S_{43,3} &= \frac{B'}{B}\frac{\left[2(k\cdot p)-M^2\right]}{2M}, \\
C^S_{11,4} &= 1, \\
C^S_{22,4} &= 1, \\
C^S_{33,4} &= B'/B, \\
C^S_{44,4} &= B'/B,
\end{aligned}
$$

with

$$B = (p\cdot k)^2 - M^2k^2; B' = (p\cdot k)(p\cdot k'') - M^2(k\cdot k''). \tag{B.4}$$

The pseudoscalar and vector coefficients are obtained by the following relations

$$C^{PS}_{ik,l}(k,k',p) = C^S_{ij,l}(k,k',p)\ \zeta^{PS}_{jk}\ , \tag{B.5}$$

$$C^{V}_{ij,l}(k,k',p) = C^S_{ij,l}(k,k',p)\ \zeta^{V}_{jk}\,, \tag{B.6}$$

with

$$\zeta^{PS} = \begin{pmatrix} -1 & 0 & 0 & 0 \\ 0 & 1 & 0 & 0 \\ 0 & 0 & 1 & 0 \\ 0 & 0 & 0 & -1 \end{pmatrix}\ , \tag{B.7}$$

$$\zeta^{V} = \begin{pmatrix} 4 & 0 & 0 & 0 \\ 0 & -2 & 0 & 0 \\ 0 & 0 & -2 & 0 \\ 0 & 0 & 0 & 0 \end{pmatrix}. \tag{B.8}$$

In the chapter 3, in order to do the four-dimensional integration in k'', the coefficients are organized in terms of the dependence of k'', k and p:

$$
\begin{aligned}
C_{ij,l} = a^0_{ij,l} + a^1_{ij,l}(p\cdot k) + a^2_{ij,l}(p\cdot k)^2 + a^3_{ij,l}k^2 + \\
+ \frac{B'}{B}\left[b^0_{ij,l} + b^1_{ij,l}(p\cdot k) + b^2_{ij,l}(p\cdot k)^2 + b^3_{ij,l}k^2\right] + B'\left[d^0_{ij,l} + d^1_{ij,l}(p\cdot k)\right].
\end{aligned} \tag{B.9}
$$

In the case of the vectorial coupling the non-vanishing a^n, b^n e d^n are given by

$$
\begin{aligned}
a^0_{11,1} &= \frac{M^2}{4} \; ; \; a^3_{11,1} = -1 \; , \\
d^0_{14,1} &= -\frac{1}{M^2} \; , \\
a^0_{22,1} &= \frac{M^2}{4} \; ; \; a^2_{22,1} = -\frac{2}{M^2} \; ; \; a^3_{22,1} = 1 \; , \\
d^1_{23,1} &= -\frac{2}{M^4} \; , \\
a^1_{32,1} &= 2 \; , \\
b^0_{33,1} &= -\frac{M^2}{4} \; ; \; b^2_{33,1} = \frac{2}{M^2} \; ; \; b^3_{33,1} = -1 \; , \\
a^0_{41,1} &= M^2 \; , \\
b^0_{44,1} &= -\frac{M^2}{4} \; ; \; b^3_{44,1} = 1 \; , \\
a^0_{12,2} &= \frac{M}{2} \; ; \; a^1_{12,2} = \frac{1}{M} \; , \\
d^0_{13,2} &= \frac{1}{M^3} \; , \\
a^0_{21,2} &= \frac{M}{2} \; ; \; a^1_{21,2} = \frac{1}{M} \; , \\
d^0_{24,2} &= -\frac{1}{M^3} \; , \\
a^0_{31,2} &= -M \; , \\
b^0_{34,2} &= \frac{M}{2} \; ; \; b^1_{34,2} = \frac{1}{M} \; , \\
a^0_{42,2} &= M \; , \\
b^0_{43,2} &= \frac{M}{2} \; ; \; b^1_{43,2} = \frac{1}{M} \; , \\
a^0_{12,3} &= \frac{M}{2} \; , \\
a^1_{12,3} &= -\frac{1}{M} \; , \\
d^0_{13,3} &= \frac{-1}{M^3} \; , \\
a^0_{21,3} &= \frac{M}{2} \; ; \; a^1_{21,3} = -\frac{1}{M} \; , \\
d^0_{24,3} &= -\frac{1}{M^3} \; , \\
a^0_{31,3} &= M \; ,
\end{aligned}
$$

$$
\begin{aligned}
b^0_{34,3} &= -\frac{M}{2}\ ;\ b^1_{34,3} = \frac{1}{M}\ , \\
a^0_{42,3} &= M\ , \\
b^0_{43,3} &= -\frac{M}{2}\ ; b^1_{43,3} = \frac{1}{M}\ , \\
a^0_{11,4} &= 1\ ;\ a^0_{22,4} = 1\ ;\ b^0_{33,4} = 1\ ;\ b^0_{44,4} = 1\ .
\end{aligned}
$$

Appendix C - $\mathcal{F}_{n;ij,l}$ Coefficients

In Chapter 3, the $\mathcal{F}_{ij,l}(v,\gamma,z,k^-,p)$ coefficients appears on the right-hand side of Bethe-Salpeter equation (3.28). They were obtained by writing the $\mathcal{C}_{ij,l}(k,p)$, expressed in the equation below, in terms of the Light-Front (LF) variables.

$$\begin{aligned}\mathcal{C}_{ij,l}(k,p) &= a^0_{ij,l} + a^1_{ij,l}\ (p\cdot k) + a^2_{ij,l}\ (p\cdot k)^2 + a^3_{ij,l}\ k^2 + \\ &+ (1-v)\left[b^0_{ij,l} + b^1_{ij,l}\ (p\cdot k) + b^2_{ij,l}\ (p\cdot k)^2 + b^3_{ij,l}\ k^2\right] \\ &+ (1-v)\Big[(p\cdot k)^2 - M^2k^2\Big]\ \left[d^0_{ij,l} + d^1_{ij,l}\ (p\cdot k)\right]. \end{aligned} \tag{C.1}$$

In the LF framework we have a four-vector x^μ given by $x^\mu = (x^-, x^+, x^1, x^2)$, where $x^- = x^0 - x^3$ and $x^+ = x^0 + x^3$, which we can write as

$$k^2_\perp = \gamma \quad , \quad k^+ = \frac{-zM}{2}, \quad k^2 = k^-k^+ - k^2_\perp \quad , \quad p\cdot k = (k^- + k^+)\frac{M}{2}. \tag{C.2}$$

Therefore, by expressing the coefficients $\mathcal{C}_{ij,l}(k,p)$ in terms of their k dependence and applying the LF variables, we have $\mathcal{F}_{ij,l}(v,\gamma,z,k^-,p)$ expressed as

$$\begin{aligned}&\mathcal{F}_{ij,l}(v,\gamma,z,k^-,p) = \Big[a^0_{ij,l} + (1-v)b^0_{ij,l}\Big] - \Big\{z\frac{M^2}{4}\Big[a^1_{ij,l} \\ &+(1-v)b^1_{ij,l}\Big]\ + \gamma\Big[a^3_{ij,l} + (1-v)b^3_{ij,l} - (1-v)M^2d^0_{ij,l}\Big]\Big\} + \frac{M^4}{2^4}\Big\{z^2\Big[a^2_{ij,l} \\ &+(1-v)b^2_{ij,l} + (1-v)d^0_{ij,l}\Big] - (1-v)z4\gamma d^1_{ij,l}\Big\} - (1-v)\frac{M^6}{64}z^3d^1_{ij,l} \\ &+k^-\frac{M}{2}\Big\{\Big[a^1_{ij,l} + (1-v)b^1_{ij,l}\Big] - z\Big[a^3_{ij,l} + (1-v)b^3_{ij,l} - (1-v)M^2d^0_{ij,l}\Big]\Big\} \\ &+k^-\frac{M^3}{2^3}\Big\{-2z\Big[a^2_{ij,l} + (1-v)b^2_{ij,l} + (1-v)d^0_{ij,l}\Big] + (1-v)\left(4\gamma - z^2M^2\right)d^1_{ij,l}\Big\} \\ &+k^-(1-v)\ \frac{M^5}{32}\ 3z^2d^1_{ij,l} + (k^-)^2\frac{M^2}{4}\ \Big\{a^2_{ij} + (1-v)b^2_{ij,l} + (1-v)d^0_{ij,l} \\ &+(1-v)M^2z\ d^1_{ij,l}\Big\} - (k^-)^2(1-v)\frac{M^4}{16}3zd^1_{ij,l} + (k^-)^3(1-v)\frac{M^3}{8}d^1_{ij,l}\,. \end{aligned} \tag{C.3}$$

Another way of expressing $\mathcal{F}_{ij,l}(v,\gamma,z,k^-,p)$ is by defining new coefficients $F_{n;ij,l}$ that

doesn't have dependence in k^-, which mean to write $\mathcal{F}_{ij,l}(v,\gamma,z,k^-,p)$ as

$$\mathcal{F}_{ij,l}(v,\gamma,z,k^-,p) = F_{0;ij,l} + k^-\ F_{1;ij,l} + (k^-)^2\ F_{2;ij,l} + (k^-)^3\ F_{3;ij,l}\,, \tag{C.4}$$

where

$$\begin{aligned}
F_{0;ij,l} &= a^0_{ij,l} - z\frac{M^2}{4}a^1_{ij,l} + \frac{M^4}{2^4}z^2a^2_{ij,l} - \gamma a^3_{ij,l} + (1-v)\Bigg[b^0_{ij,l} - z\frac{M^2}{4}b^1_{ij,l} \\
&- \gamma b^3_{ij,l} + \frac{M^2}{4}\left(4\gamma + z^2\frac{M^2}{4}\right)d^0_{ij,l} + \frac{M^4}{2^4}\Big[z^2b^2_{ij,l} - z\left(4\gamma + z^2\frac{M^2}{4}\right)d^1_{ij,l}\Big]\Bigg], \qquad \text{(C.5)}\\
F_{1;ij,l} &= \frac{M}{2}\Bigg[a^1_{ij,l} - z\Big[a^3_{ij,l} + \frac{M^2}{2}a^2_{ij,l}\Big] + (1-v)\Big[b^1_{ij,l} - z\ b^3_{ij,l} - \frac{M^2}{2}zb^2_{ij,l}\Big] \\
&+ \frac{M^2}{4}(1-v)\Big[2zd^0_{ij,l} + \Big(4\gamma - z^2\frac{M^2}{4}\Big)d^1_{ij,l}\Big]\Bigg], \qquad \text{(C.6)}\\
F_{2;ij,l} &= \frac{M^2}{4}\ \Big\{a^2_{ij,l} + (1-v)b^2_{ij,l} + (1-v)d^0_{ij,l} + (1-v)\frac{M^2}{4}z\ d^1_{ij,l}\Big\}, \\
F_{3;ij,l} &= (1-v)\ \frac{M^3}{8}\ d^1_{ij,l}\ . \qquad \text{(C.7)}
\end{aligned}$$

The non-vanishing coefficients $F_{n;ij,l}$ are given explicitly in next sections of this appendix.

C.1 Coefficients $F_{0;ij,l}$

$$\begin{aligned}
F_{0;11,1} &= \frac{M^2}{4} + \gamma\ , \\
F_{0;14,1} &= -(1-v)(\gamma + \Big(z\frac{M}{4}\Big)^2)\ , \\
F_{0;22,1} &= \frac{M^2}{4} - \gamma - 2\Big(z\frac{M}{4}\Big)^2\ , \\
F_{0;23,1} &= \frac{z(1-v)}{2}\Big[\gamma + \Big(z\frac{M}{4}\Big)^2\Big]\ , \\
F_{0;32,1} &= -z\frac{M^2}{2}\ , \\
F_{0;33,1} &= (1-v)\Bigg[-\frac{M^2}{4} + \gamma + 2\Big(z\frac{M}{4}\Big)^2\Bigg]\ ,
\end{aligned}$$

$$
\begin{aligned}
F_{0;41,1} &= M^2 \ , \\
F_{0;44,1} &= -(1-v)\Big[\frac{M^2}{4}+\gamma\Big] \ , \\
F_{0;12,2} &= \frac{M}{4}(2-z) \ , \\
F_{0;13,2} &= \frac{1}{M}\Big[\gamma+\Big(z\frac{M}{4}\Big)^2\Big] \ , \\
F_{0;21,2} &= \frac{M}{4}(2-z) \ , \\
F_{0;24,2} &= -(1-v)\frac{1}{M}\Big[\gamma+\Big(z\frac{M}{4}\Big)^2\Big] \ , \\
F_{0;31,2} &= -M \ , \\
F_{0;34,2} &= (1-v)\frac{M}{4}(2-z) \ , \\
F_{0;42,2} &= M \ , \\
F_{0;43,2} &= (1-v)\frac{M}{4}(2-z) \ , \\
F_{0;12,3} &= \frac{M}{4}(2+z) \ , \\
F_{0;13,3} &= -\frac{1}{M}\Big[\gamma+\Big(z\frac{M}{4}\Big)^2\Big] \ , \\
F_{0;21,3} &= \frac{M}{4}(2+z) \ , \\
F_{0;24,3} &= -(1-v)\frac{1}{M}\Big[\gamma+\Big(z\frac{M}{4}\Big)^2\Big] \ , \\
F_{0;31,3} &= M \ , \\
F_{0;34,3} &= -(1-v)\frac{M}{4}(2+z) \ , \\
F_{0;42,3} &= M \ , \\
F_{0;43,3} &= -(1-v)\frac{M}{4}(2+z) \ , \\
F_{0;11,4} &= 1 \ , \\
F_{0;22,4} &= 1 \ , \\
F_{0;33,4} &= 1-v \ , \\
F_{0;44,4} &= 1-v \ .
\end{aligned}
$$

C.2 Coefficients $F_{1;ij,l}$

$$
\begin{aligned}
F_{1;11,1} &= \frac{zM}{2} \ , \\
F_{1;14,1} &= -z(1-v)\frac{M}{4} \ , \\
F_{1;23,1} &= -\frac{(1-v)}{M}\Big[\gamma - \Big(z\frac{M}{4}\Big)^2\Big] \ , \\
F_{1;32,1} &= M \ , \\
F_{1;44,1} &= -z(1-v)\frac{M}{2} \ , \\
F_{1;12,2} &= \frac{1}{2} \ , \\
F_{1;13,2} &= (1-v)\frac{z}{4} \ , \\
F_{1;21,2} &= \frac{1}{2} \ , \\
F_{1;24,2} &= -(1-v)\frac{z}{4} \ , \\
F_{1;34,2} &= \frac{(1-v)}{2} \ . \\
F_{1;43,2} &= \frac{(1-v)}{2} \ , \\
F_{1;12,3} &= -\frac{1}{2} \ , \\
F_{1;13,3} &= -(1-v)\frac{z}{4} \ , \\
F_{1;21,3} &= -\frac{1}{2} \ , \\
F_{1;24,3} &= -(1-v)\frac{z}{4} \ , \\
F_{1;34,3} &= \frac{(1-v)}{2} \ , \\
F_{1;43,3} &= \frac{(1-v)}{2} \ .
\end{aligned}
$$

C.3 Coefficients $F_{2;ij,l}$

$$
\begin{aligned}
F_{2;14,1} &= -\frac{(1-v)}{4} \ , \\
F_{2;22,1} &= -\frac{1}{2} \ , \\
F_{2;23,1} &= -\frac{z}{8}(1-v) \ , \\
F_{2;33,1} &= \frac{(1-v)}{2} \ , \\
F_{2;13,2} &= \frac{(1-v)}{4M} \ , \\
F_{2;24,2} &= -\frac{(1-v)}{4M} \ , \\
F_{2;13,3} &= -\frac{(1-v)}{4M} \ , \\
F_{2;24,3} &= -\frac{(1-v)}{4M} \ .
\end{aligned}
$$

C.4 Coefficients $F_{3;ij,l}$

$$F_{3;23,1} = -\frac{(1-v)}{4M} \ .$$

Appendix D - $\mathcal{F}_{ij,l}$ Coefficients

In this appendix, we present explicitly the $\mathcal{F}^{ns}_{ij,l}(v,\gamma,z,m_a)$ coefficients of $\mathcal{L}^{(ns,1)}_{ij}(\gamma,z,\gamma',z')$ contributions present in the Bethe-Salpeter equation (4.9), where it is already considered the phenomenological mass function given in equation (4.2). The non-vanishing $\mathcal{F}^{ns}_{ij,l}(v,\gamma,z,m_a)$ are

$$
\begin{aligned}
\mathcal{F}^{ns}_{11,1}(v,\gamma,z,m_a^2) &= (1-z)^3\Big[(zm_a^2+\gamma)+\frac{M^2}{4}(1-z)^2\Big]\ ,\\
\mathcal{F}^{ns}_{11,4}(v,\gamma,z,m_a^2) &= (1-z)^4\ ,\\
\mathcal{F}^{ns}_{12,2}(v,\gamma,z,m_a^2) &= (1-z)^3\Big[\frac{(m_a^2+\gamma)}{M}+\frac{M}{4}(1-z)^2\Big]\ ,\\
\mathcal{F}^{ns}_{12,3}(v,\gamma,z,m_a^2) &= -\mathcal{F}^{ns}_{12,2}+M(1-z)^4\ ,\\
\mathcal{F}^{ns}_{13,2}(v,\gamma,z,m_a^2) &= \frac{(1-z)^2}{16}\Bigg[(1-z)^2(z^2M+16\gamma/M)+(1-v)M(-(1-z)\\
&\quad +4(\gamma+m_a^2)/M^2)^2+2z(1-z)(1-v)(-(1-z)M\\
&\quad +4(\gamma+m_a^2)/M)\Bigg]\ ,\\
\mathcal{F}^{ns}_{13,3}(v,\gamma,z,m_a^2) &= -\mathcal{F}^{ns}_{13,2}\ ,\\
\mathcal{F}^{ns}_{14,1}(v,\gamma,z,m_a^2) &= -\tfrac{(1-v)(1-z)^2}{16}\Big[M^2(1-z)^4-8(1-z)^2(m_a^2-\gamma)\\
&\quad +16((\gamma+m_a^2)/M)^2\Big]\ ,\\
\mathcal{F}^{ns}_{21,2}(v,\gamma,z,m_a^2) &= \mathcal{F}^{ns}_{12,2}\ ,\\
\mathcal{F}^{ns}_{21,3}(v,\gamma,z,m_a^2) &= \mathcal{F}^{ns}_{12,3}\ ,\\
\mathcal{F}^{ns}_{22,1}(v,\gamma,z,m_a^2) &= -\tfrac{(1-z)^2}{8}\Big[-(1-z)^3(1+z)M^2-8(1-z)(m_a^2+\gamma z)\\
&\quad +16((m_a^2+\gamma)/M)^2\Big]\ ,\\
\mathcal{F}^{ns}_{22,4}(v,\gamma,z,m_a^2) &= \mathcal{F}^{ns}_{11,4}\\
\mathcal{F}^{ns}_{23,1}(v,\gamma,z,m_a^2) &= -\frac{(1-z)(1-v)}{32}\left(-(1-z^2)+4(m_a^2+\gamma)/M^2\right)\\
&\quad \times\Big(M^2(1-z)^4-8(1-z)^2(m_a^2-\gamma)\\
&\quad +16\left((m_a^2+\gamma)/M\right)^2\Big)\ ,
\end{aligned}
$$

$$
\begin{aligned}
\mathcal{F}^{ns}_{24,2}(v,\gamma,z,m_a^2) &= \frac{1}{M}\mathcal{F}^{ns}_{14,1} \ , \\
\mathcal{F}^{ns}_{24,3}(v,\gamma,z,m_a^2) &= \mathcal{F}^{ns}_{24,2} \ , \\
\mathcal{F}^{ns}_{31,2}(v,\gamma,z,m_a^2) &= -M\mathcal{F}^{ns}_{11,4} \ , \\
\mathcal{F}^{ns}_{31,3}(v,\gamma,z,m_a^2) &= M\mathcal{F}^{ns}_{11,4} \ , \\
\mathcal{F}^{ns}_{33,1}(v,\gamma,z,m_a) &= -(1-v)\mathcal{F}^{ns}_{22,1} \ , \\
\mathcal{F}^{ns}_{33,4}(v,\gamma,z,m_a^2) &= (1-v)\mathcal{F}^{ns}_{11,4} \ , \\
\mathcal{F}^{ns}_{34,2}(v,\gamma,z,m_a^2) &= (1-v)\mathcal{F}^{ns}_{12,2} \ , \\
\mathcal{F}^{ns}_{34,3}(v,\gamma,z,m_a^2) &= -(1-v)\mathcal{F}^{ns}_{12,3} \ , \\
\mathcal{F}^{ns}_{41,1}(v,\gamma,z,m_a^2) &= M^2\mathcal{F}^{ns}_{11,4} \ , \\
\mathcal{F}^{ns}_{42,2}(v,\gamma,z,m_a) &= M\mathcal{F}^{ns}_{11,4} \ , \\
\mathcal{F}^{ns}_{42,3}(v,\gamma,z,m_a) &= \mathcal{F}^{ns}_{42,2} \ , \\
\mathcal{F}^{ns}_{43,2}(v,\gamma,z,m_a) &= (1-v)\mathcal{F}^{ns}_{12,2} \ , \\
\mathcal{F}^{ns}_{43,3}(v,\gamma,z,m_a) &= -(1-v)\mathcal{F}^{ns}_{12,3} \ , \\
\mathcal{F}^{ns}_{44,1}(v,\gamma,z,m_a) &= -(1-v)\mathcal{F}^{ns}_{11,1} \ , \\
\mathcal{F}^{ns}_{44,4}(v,\gamma,z,m_a) &= (1-v)\mathcal{F}^{ns}_{11,4} \ .
\end{aligned}
$$

We can obtain the $\mathcal{F}^{ns}_{ij,l}(v,\gamma,-z,m_{a'})$ coefficients, which are the ones necessary to calculate the $\mathcal{L}^{(ns,2)}_{ij}(\gamma,z,\gamma',z')$ contributions to the BS equation, by using the $\mathcal{F}^{ns}_{ij,1}(v,\gamma,z,m_a)$. This means that one needs to exchange $z \to -z$ and $a \to a'$, thus obtaining

$$\mathcal{F}^{ns}_{ij,1}(v,\gamma,z,m_a) = \sigma_{ij}\ \mathcal{F}^{ns}_{ij,1}(v,\gamma,-z,m_{a'}) \ , \tag{D.1a}$$

$$\mathcal{F}^{ns}_{ij,2}(v,\gamma,z,m_a) = \sigma_{ij}\ \mathcal{F}^{ns}_{ij,3}(v,\gamma,-z,m_{a'}) \ , \tag{D.1b}$$

$$\mathcal{F}^{ns}_{ij,3}(v,\gamma,z,m_a) = \sigma_{ij}\ \mathcal{F}^{ns}_{ij,2}(v,\gamma,-z,m_{a'}) \ , \tag{D.1c}$$

$$\mathcal{F}^{ns}_{ij,4}(v,\gamma,z,m_a) = \sigma_{ij}\ \mathcal{F}^{ns}_{ij,4}(v,\gamma,-z,m_{a'}) \ . \tag{D.1d}$$

Furthermore, the matrix σ is defined as

$$\sigma = \begin{pmatrix} 1 & 1 & -1 & 1 \\ 1 & 1 & -1 & 1 \\ -1 & -1 & 1 & -1 \\ 1 & 1 & -1 & 1 \end{pmatrix} \ . \tag{D.2}$$

The coefficients $\mathcal{F}^{ns}_{ijl}$ also can be decomposed in terms of the v dependence as follow

$$\mathcal{F}^{ns}_{ijl} = \tilde{\mathcal{F}}^{(1)}_{ijl} + (1-v)\tilde{\mathcal{F}}^{(2)}_{ijl} \ , \tag{D.3}$$

with the non-zero coefficients being

$$
\begin{aligned}
\tilde{\mathcal{F}}^{(1)}_{11,1}(\gamma,z,m_a^2) &= (1-z)^3\Big[(zm_a^2+\gamma)+\frac{M^2}{4}(1-z)^2\Big]\ ,\\
\tilde{\mathcal{F}}^{(1)}_{11,4}(\gamma,z,m_a^2) &= (1-z)^4\ ,\\
\tilde{\mathcal{F}}^{(1)}_{12,2}(\gamma,z,m_a^2) &= (1-z)^3\Big[\frac{(m_a^2+\gamma)}{M}+\frac{M}{4}(1-z)^2\Big]\ ,\\
\tilde{\mathcal{F}}^{(1)}_{12,3}(\gamma,z,m_a^2) &= -\tilde{\mathcal{F}}^{(1)}_{12,2}+M(1-z)^4\ ,\\
\tilde{\mathcal{F}}^{(1)}_{13,2}(\gamma,z,m_a^2) &= \frac{(1-z)^4}{16}(z^2M+16\gamma/M)\ ,\\
\tilde{\mathcal{F}}^{(2)}_{13,2}(\gamma,z,m_a^2) &= \frac{(1-z)^2}{16}\Big\{M[-(1-z)+4(\gamma+m_a^2)/M^2]^2\\
&\quad +2z(1-z)[-(1-z)M+4(\gamma+m_a^2)/M]\Big\}\ ,\\
\tilde{\mathcal{F}}^{(1)}_{13,3}(\gamma,z,m_a^2) &= -\tilde{\mathcal{F}}^{(1)}_{13,2}\ ,\\
\tilde{\mathcal{F}}^{(2)}_{13,3}(\gamma,z,m_a^2) &= -\tilde{\mathcal{F}}^{(2)}_{13,2}\ ,\\
\tilde{\mathcal{F}}^{(2)}_{14,1}(\gamma,z,m_a^2) &= -\tfrac{(1-z)^2}{16}\big[M^2(1-z)^4-8(1-z)^2(m_a^2-\gamma)\\
&\quad +16((\gamma+m_a^2)/M)^2\big]\ ,\\
\tilde{\mathcal{F}}^{1)}_{21,2}(\gamma,z,m_a^2) &= \tilde{\mathcal{F}}^{(1)}_{12,2}\ ,\\
\tilde{\mathcal{F}}^{(1)}_{21,3}(\gamma,z,m_a^2) &= \tilde{\mathcal{F}}^{(1)}_{12,3}\ ,\\
\tilde{\mathcal{F}}^{(1)}_{22,1}(\gamma,z,m_a^2) &= -\tfrac{(1-z)^2}{8}\Big[-(1-z)^3(1+z)M^2-8(1-z)(m_a^2+\gamma z)\\
&\quad +16((m_a^2+\gamma)/M)^2\Big]\ ,\\
\tilde{\mathcal{F}}^{(1)}_{22,4}(\gamma,z,m_a^2) &= \tilde{\mathcal{F}}^{(1)}_{11,4}\ ,\\
\tilde{\mathcal{F}}^{(2)}_{23,1}(\gamma,z,m_a^2) &= -\frac{(1-z)}{32}\left[-(1-z^2)+4(m_a^2+\gamma)/M^2\right]\\
&\quad \times\Big[M^2(1-z)^4-8(1-z)^2(m_a^2-\gamma)+16\left((m_a^2+\gamma)/M\right)^2\Big]\ ,\\
\tilde{\mathcal{F}}^{(2)}_{24,2}(\gamma,z,m_a^2) &= \frac{1}{M}\tilde{\mathcal{F}}^{(2)}_{14,1}\ ,
\end{aligned}
$$

$$
\begin{aligned}
\tilde{\mathcal{F}}^{(2)}_{24,3}(\gamma,z,m_a^2) &= \tilde{\mathcal{F}}^{(2)}_{24,2}\ , \\
\tilde{\mathcal{F}}^{(1)}_{31,2}(\gamma,z,m_a^2) &= -M\tilde{\mathcal{F}}^{(1)}_{11,4}\ , \\
,\tilde{\mathcal{F}}^{(1)}_{31,3}(\gamma,z,m_a^2) &= M\tilde{\mathcal{F}}^{(1)}_{11,4}\ , \\
\tilde{\mathcal{F}}^{(2)}_{33,1}(\gamma,z,m_a) &= -\tilde{\mathcal{F}}^{(1)}_{22,1}\ , \\
\tilde{\mathcal{F}}^{(2)}_{33,4}(\gamma,z,m_a^2) &= \tilde{\mathcal{F}}^{(1)}_{11,4}\ , \\
\tilde{\mathcal{F}}^{(2)}_{34,2}(\gamma,z,m_a^2) &= \tilde{\mathcal{F}}^{(1)}_{12,2}\ , \\
\tilde{\mathcal{F}}^{(2)}_{34,3}(\gamma,z,m_a^2) &= -\tilde{\mathcal{F}}^{(1)}_{12,3}\ , \\
\tilde{\mathcal{F}}^{(1)}_{41,1}(\gamma,z,m_a^2) &= M^2\tilde{\mathcal{F}}^{(1)}_{11,4}\ , \\
\tilde{\mathcal{F}}^{(1)}_{42,2}(\gamma,z,m_a) &= M\tilde{\mathcal{F}}^{(1)}_{11,4}\ , \\
\tilde{\mathcal{F}}^{(1)}_{42,3}(\gamma,z,m_a) &= \tilde{\mathcal{F}}^{(1)}_{42,2}\ , \\
\tilde{\mathcal{F}}^{(2)}_{43,2}(\gamma,z,m_a) &= \tilde{\mathcal{F}}^{(1)}_{12,2}\ , \\
\tilde{\mathcal{F}}^{(2)}_{43,3}(\gamma,z,m_a) &= -\tilde{\mathcal{F}}^{(1)}_{12,3}\ , \\
\tilde{\mathcal{F}}^{(2)}_{44,1}(\gamma,z,m_a) &= -\tilde{\mathcal{F}}^{(1)}_{11,1}\ , \\
\tilde{\mathcal{F}}^{(2)}_{44,4}(\gamma,z,m_a) &= \tilde{\mathcal{F}}^{(1)}_{11,4}\ .
\end{aligned}
$$

Appendix E - Singular Integrals

In order to evaluate the $\mathcal{C}_n$ integrals, one has to carefully take care of the value of $k_D^+ = v(1-v)\frac{M}{2}(z'-z)$, if it is positive, negative or null. In particular, it is $z'-z$ that defines what signal k_D^+ will have. In particular, we have that in the case $z'=z$, i.e. $k_D^+=0$, singular contributions appear. In Chapter 3, it is presented the non-singular contributions of $\mathcal{C}_n$. In this appendix, a more explicit derivation of the singular contributions is made.

The $\mathcal{C}_n$ integrals are written as follow

$$\begin{aligned}
\mathcal{C}_n &= 3\int \frac{dk^-}{2\pi} \frac{(k^-)^n}{\Big[(1-z)k^- - (1-z)k_d^- + i\epsilon\Big]\,\Big[(1+z)k^- - (1+z)k_u^- - i\epsilon\Big]} \\
&\quad \times \frac{1}{\Big[k_D^+k^- + \ell_D + (1-v)\Big(\mu^2-\Lambda^2\Big) + i\epsilon\Big]^3\,\Big[k_D^+k^- + \ell_D + i\epsilon\Big]} \\
&\quad + \int \frac{dk^-}{2\pi} \frac{(k^-)^n}{\Big[(1-z)k^- - (1-z)k_d^- + i\epsilon\Big]\,\Big[(1+z)k^- - (1+z)k_u^- - i\epsilon\Big]} \\
&\quad \times \frac{(1-v)\Big(\mu^2-\Lambda^2\Big)}{\Big[k_D^+k^- + \ell_D + (1-v)\Big(\mu^2-\Lambda^2\Big) + i\epsilon\Big]^3\,\Big[k_D^+k^- + \ell_D + i\epsilon\Big]^2}\,.
\end{aligned} \tag{E.1}$$

If we define

$$\begin{aligned}
\mathcal{B}(n) &= \int \frac{dk^-}{2\pi} \frac{(k^-)^n}{\Big[(1-z)k^- - (1-z)k_d^- + i\epsilon\Big]\,\Big[(1+z)k^- - (1+z)k_u^- - i\epsilon\Big]} \\
&\quad \times \frac{1}{\Big[k_D^+k^- + C + i\epsilon\Big]^3\,\Big[k_D^+k^- + E + i\epsilon\Big]}
\end{aligned} \tag{E.2}$$

with $n=0,1,2$ and 3, $C = \ell_D + (1-v)\Big(\mu^2-\Lambda^2\Big)$ and $E=\ell_D$, we can write

$$\mathcal{C}_n = 3\mathcal{B}(n) - (1-v)\Big(\mu^2-\Lambda^2\Big)\frac{\partial}{\partial E}\mathcal{B}(n)\,, \tag{E.3}$$

since a derivative of the result with respect to E leads to the second integral in equation

(E.1). The singularities came from the difference between the power of k^- in the numerator and in the denominator of $\mathcal{C}_n$. To $n = 0, 1$ we don't have real issues with the poles. The singularities arise to $n = 2, 3$.

The first case that we have is to $n = 0$. If we consider the following integral

$$\begin{aligned} I_M^{(0)} &= \int \frac{dk^-}{2\pi} \frac{1}{\Big[(1-z)k^- - (1-z)k_d^- + i\epsilon\Big]\ \Big[(1+z)k^- - (1+z)k_u^- - i\epsilon\Big]} \\ &\times \frac{1}{\Big[k_D^+ k^- + C + i\epsilon\Big]\ \Big[k_D^+ k^- + E + i\epsilon\Big]}, \end{aligned} \tag{E.4}$$

we can express $\mathcal{B}(0)$ in terms of the derivative of $I_M^{(0)}$.

To integrate in dk^-, We apply the residue theorem considering the following poles:

1.$k_u^- + i\epsilon/(1+z) \in$ the upper plane

2.$k_d^- - i\epsilon/(1-z) \in$ the lower plane

3.$-C/k_D^+ - i\epsilon/k_D^+$

4.$-E/k_D^+ - i\epsilon/k_D^+$

Therefore, we have the term $I_M^{(0)}$ is given as

$$I_M^{(0)} = i\ \theta(k_D^+)\ \mathcal{R}es(k_u^-) - i\ \theta(-k_D^+)\ \mathcal{R}es(k_d^-) \tag{E.5}$$

or more explicitly,

$$\begin{aligned} I_M^{(0)} = \frac{i}{(1-z^2)} \Big\{ &\frac{\theta(k_D^+)}{\Big[k_u^- - k_d^-\Big]\ \Big[k_D^+ k_u^- + C + i\epsilon\Big]\ \Big[k_D^+ k_u^- + E + i\epsilon\Big]} \\ &- \frac{\theta(-k_D^+)}{\Big[k_d^- - k_u^-\Big]\ \Big[k_D^+ k_d^- + C + i\epsilon\Big]\ \Big[k_D^+ k_d^- + E + i\epsilon\Big]} \Big\}. \end{aligned} \tag{E.6}$$

Then one has

$$\begin{aligned} \mathcal{B}(0) &= \frac{1}{2}\frac{\partial^2}{\partial C^2}\ I_M^{(0)} \\ &= i\frac{1}{(1-z^2)}\ \frac{1}{\Big[k_u^- - k_d^-\Big]}\ \Big\{ \frac{\theta(k_D^+)}{\Big[k_D^+ k_u^- + C + i\epsilon\Big]^3\ \Big[k_D^+ k_u^- + E + i\epsilon\Big]} \\ &+ \frac{\theta(-k_D^+)}{\Big[k_D^+ k_d^- + C + i\epsilon\Big]^3\ \Big[k_D^+ k_d^- + E + i\epsilon\Big]} \Big\}. \end{aligned} \tag{E.7}$$

The function $\mathcal{B}(0)$ does not contain any delta function, thus at $z' = z$, the $\mathcal{C}_0$ has no singular contribution.

First power (n=1)

The integral with the first power of k^- is given by

$$\begin{aligned}
\mathcal{B}(1) &= \int \frac{dk^-}{2\pi} \frac{k^-}{\Big[(1-z)k^- - (1-z)k_d^- + i\epsilon\Big]\ \Big[(1+z)k^- - (1+z)k_u^- - i\epsilon\Big]} \\
&\quad \times \frac{1}{\Big[k_D^+ k^- + C + i\epsilon\Big]^3\ \Big[k_D^+ k^- + E + i\epsilon\Big]} \\
&= \int \frac{dk^-}{2\pi} \frac{k^- - k_u^- + k_u^-}{\Big[(1-z)k^- - (1-z)k_d^- + i\epsilon\Big]\ \Big[(1+z)k^- - (1+z)k_u^- - i\epsilon\Big]} \\
&\quad \times \frac{1}{\Big[k_D^+ k^- + C + i\epsilon\Big]^3\ \Big[k_D^+ k^- + E + i\epsilon\Big]} \\
&= \frac{1}{(1+z)} \frac{1}{2} \frac{\partial^2}{\partial C^2}\ I_M^{(1)} + k_u^-\ \mathcal{B}(0)\ ,
\end{aligned} \tag{E.8}$$

where

$$\begin{aligned}
I_M^{(1)} &= \int \frac{dk^-}{2\pi} \frac{1}{\Big[(1-z)k^- - (1-z)k_d^- + i\epsilon\Big]}\ \frac{1}{\Big[k_D^+ k^- + C + i\epsilon\Big]\ \Big[k_D^+ k^- + E + i\epsilon\Big]} \\
&= \frac{1}{C-E} \int \frac{dk^-}{2\pi} \frac{M}{\Big[(1-z)Mk^- - (1-z)Mk_d^- + i\epsilon\Big]} \\
&\quad \times \left[\frac{1}{\Big[k_D^+ k^- + E + i\epsilon\Big]} - \frac{1}{\Big[k_D^+ k^- + C + i\epsilon\Big]} \right] ,
\end{aligned} \tag{E.9}$$

where if one use the Feynman parametrization, the terms of the denominator can be

unified. Therefore one has

$$
\begin{aligned}
I_M^{(1)} &= \frac{M}{(C-E)(1-z)} \int \frac{dk^-}{2\pi} \int_0^1 d\xi \; \frac{1}{\Big[Mk^- - Mk_d^- + i\epsilon + \xi(k_D^+ k^- + E - Mk^- + Mk_d^-)\Big]^2} \\
&\quad - \frac{M}{(C-E)(1-z)} \int \frac{dk^-}{2\pi} \int_0^1 d\xi \; \frac{1}{\Big[Mk^- - Mk_d^- + i\epsilon + \xi(k_D^+ k^- + C - Mk^- + Mk_d^-)\Big]^2}, \\
&= -i \; \frac{M}{(C-E)(1-z)} \times \int_0^1 d\xi \; \delta\Big[M + \xi(k_D^+ - M)\Big] \; \Big[\frac{1}{-Mk_d^- + \xi(E + Mk_d^-)} \\
&\quad - \frac{1}{-Mk_d^- + \xi(C + Mk_d^-)}\Big], \\
&= -i \; \frac{M}{(1-z)} \int_0^1 d\xi \; \frac{\delta\Big[M + \xi(k_D^+ - M)\Big] \; \xi}{[Mk_d^- - \xi(E + Mk_d^-)] \; [Mk_d^- - \xi(C + Mk_d^-)]}, \\
&= -i \; \frac{1}{(1-z)} \; \frac{(M - k_D^+)}{|k_D^+ - M|} \; \frac{\theta(M - k_D^+) \; \theta(-k_D^+)}{[k_d^-(M - k_D^+) - E - Mk_d^-] \; [k_d^-(M - k_D^+) - C - Mk_d^-]}, \\
&= -i \; \frac{1}{(1-z)} \; \frac{\theta(-k_D^+)}{[k_d^- k_D^+ + E] \; [k_d^- k_D^+ + C]},
\end{aligned}
\tag{E.10}
$$

where we used the identity

$$
\int_{-\infty}^{\infty} dx \; \frac{1}{\Big[\beta \; x - y \mp i\epsilon\Big]^2} \;=\; \pm(2\pi)i \; \frac{\delta(\beta)}{\Big[-y \mp i\epsilon\Big]} \, . \tag{E.11}
$$

Then one gets

$$
\begin{aligned}
\mathcal{B}(1) &= -i \; \frac{1}{(1-z^2)} \; \frac{\theta(-k_D^+)[k_u^- - k_d^-]}{[k_u^- - k_d^-] \; [k_d^- k_D^+ + C]^3 \; [k_d^- k_D^+ + E]} + i \; \frac{1}{(1-z^2)} \; \frac{k_u^-}{[k_u^- - k_d^-]} \\
&\quad \times \Big\{ \frac{\theta(k_D^+)}{\Big[k_D^+ k_u^- + C + i\epsilon\Big]^3 \; \Big[k_D^+ k_u^- + E + i\epsilon\Big]} + \frac{\theta(-k_D^+)}{\Big[k_D^+ k_d^- + C + i\epsilon\Big]^3 \; \Big[k_D^+ k_d^- + E + i\epsilon\Big]} \Big\}, \\
&= i \; \frac{1}{(1-z^2)} \; \frac{1}{(k_u^- - k_d^-)} \; \Bigg[\frac{k_u^- \; \theta(k_D^+)}{\Big[k_D^+ k_u^- + C + i\epsilon\Big]^3 \; \Big[k_D^+ k_u^- + E + i\epsilon\Big]} \\
&\quad + \frac{k_d^- \; \theta(-k_D^+)}{[k_d^- k_D^+ + C]^3 \; [k_d^- k_D^+ + E]} \Bigg] \, .
\end{aligned}
\tag{E.12}
$$

In conclusion, no singular correction for $\mathcal{C}_1$ at $k_D^+ = 0$.

Second power (n=2)

To $n = 2$, we have $\mathcal{B}(2)$ given by

$$\begin{aligned}
\mathcal{B}(2) &= \int \frac{dk^-}{2\pi} \frac{(k^-)^2}{\Big[(1-z)k^- - (1-z)k_d^- + i\epsilon\Big]\ \Big[(1+z)k^- - (1+z)k_u^- - i\epsilon\Big]} \\
&\quad \times \frac{1}{\Big[k_D^+ k^- + C + i\epsilon\Big]^3\ \Big[k_D^+ k^- + E + i\epsilon\Big]}, \\
&= \int \frac{dk^-}{2\pi} \frac{(k^- - k_u^-)\ (k^- - k_d^-) + (k_u^- + k_d^-)\ k^- - k_u^-\ k_d^-}{\Big[(1-z)k^- - (1-z)k_d^- + i\epsilon\Big]\ \Big[(1+z)k^- - (1+z)k_u^- - i\epsilon\Big]} \\
&\quad \times \frac{1}{\Big[k_D^+ k^- + C + i\epsilon\Big]^3\ \Big[k_D^+ k^- + E + i\epsilon\Big]}, \\
&= \frac{1}{2}\ \frac{1}{(1-z^2)}\ \frac{\partial^2}{\partial C^2} I_M^{(2)} + (k_u^- + k_d^-)\ \mathcal{B}(1) - k_u^-\ k_d^-\ \mathcal{B}(0)\ . \qquad \text{(E.13)}
\end{aligned}$$

where we have that $I_M^{(2)}$ is written as

$$\begin{aligned}
I_M^{(2)} &= \int \frac{dk^-}{2\pi}\ \frac{1}{\Big[k_D^+ k^- + C + i\epsilon\Big]\ \Big[k_D^+ k^- + E + i\epsilon\Big]}\ , \\
&= \int \frac{dk^-}{2\pi}\ \int_0^1 d\xi\ \frac{1}{\Big[k_D^+ k^- + C + \xi(E-C) + i\epsilon\Big]^2}\ , \\
&= i \int_0^1 d\xi\ \frac{\delta(k_D^+)}{C + \xi(E-C) + i\epsilon}\ , \\
&= -i \frac{\delta(k_D^+)}{(E-C)}\ \ln\left(\frac{E}{C}\right)\ . \qquad \text{(E.14)}
\end{aligned}$$

Therefore the second derivative of $I_M^{(2)}$

$$\frac{1}{2}\ \frac{\partial^2}{\partial C^2} I_M^{(2)} = -i \frac{\delta(k_D^+)}{(E-C)^2}\ \left[\frac{1}{(E-C)} \ln\left(\frac{E}{C}\right) + \frac{(E-3C)}{2C^2}\right] \qquad \text{(E.15)}$$

Then one can rewrite the expression of $\mathcal{B}(2)$ as

$$\mathcal{B}(2) = -\frac{i}{(1-z^2)}\ \delta(k_D^+)\ \mathcal{S}_2(C,E) + \mathcal{B}^{NS}(2)\ , \qquad \text{(E.16)}$$

with

$$\mathcal{B}^{NS}(2) = \frac{i}{(1-z^2)}\,\frac{1}{(k_u^- - k_d^-)}\,\frac{(k_u^-)^2\;\theta(k_D^+)}{\left[k_D^+k_u^- + C + i\epsilon\right]^3\,\left[k_D^+k_u^- + E + i\epsilon\right]} + \frac{i}{(1-z^2)}\,\frac{1}{(k_u^- - k_d^-)}\,\frac{(k_d^-)^2\;\theta(-k_D^+)}{[k_d^-k_D^+ + C]^3\;[k_d^-k_D^+ + E]}\Bigg], \tag{E.17}$$

$$\mathcal{S}_2(C,E) = \frac{1}{(E-C)^2}\,\left[\frac{1}{(E-C)}\ln\left(\frac{E}{C}\right) + \frac{(E-3C)}{2C^2}\right]. \tag{E.18}$$

The first term of $\mathcal{B}(2)$ presents a delta function in terms of k_D^+, thus is responsible for the singular contribution of $\mathcal{C}_2$ at $z' = z$, which is given by

$$\mathcal{C}_2^S = -\frac{i}{(1-z^2)}\;\delta(k_D^+)\;\left[3\;\mathcal{S}_2(C,E) + (E-C)\;\frac{\partial}{\partial E}\mathcal{S}_2(C,E)\right], \tag{E.19}$$

with $E - C = -(1-v)\;(\mu^2 - \Lambda^2)$. In special, by performing the derivative related to E we obtain

$$\begin{aligned}\frac{\partial}{\partial E}\mathcal{S}_2(C,E) &= -\frac{3}{(E-C)^4}\;\ln\left(\frac{E}{C}\right) + \frac{1}{E(E-C)^3} + \frac{5C-E}{2C^2(E-C)^3}\;,\\ &= -\frac{3}{(E-C)^4}\;\ln\left(\frac{E}{C}\right) - \frac{1}{2EC^2(E-C)} + \frac{3}{2EC}\;\frac{E+C}{(E-C)^3}\;,\end{aligned} \tag{E.20}$$

then we can write

$$\begin{aligned}3\;\mathcal{S}_2(C,E) + (E-C)\;\frac{\partial}{\partial E}\mathcal{S}_2(C,E) &= \frac{3}{(E-C)^3}\;\ln\left(\frac{E}{C}\right) + \frac{3(E-3C)}{2C^2(E-C)^2}\\ &\quad -\frac{3}{(E-C)^3}\;\ln\left(\frac{E}{C}\right) - \frac{1}{2EC^2} + \frac{3}{2EC}\;\frac{E+C}{(E-C)^2}\;,\\ &= \frac{3(E-3C)}{2C^2(E-C)^2} - \frac{1}{2EC^2} + \frac{3}{2EC}\;\frac{E+C}{(E-C)^2}\;,\\ &= \frac{1}{EC^2}\;.\end{aligned} \tag{E.21}$$

Therefore, by using that

$$\delta(k_D^+) = \frac{2\;\delta(z'-z)}{M\;v(1-v)}\,,$$

the singular contribution to $\mathcal{C}_2$ can be expressed as

$$\begin{aligned}\mathcal{C}_2^S &= -\frac{i}{(1-z^2)}\;\delta(k_D^+)\;\frac{1}{EC^2}\\ &= -\frac{i}{1-z^2}\frac{2}{EC^2}\frac{1}{v(1-v)M}\delta(z'-z)\,.\end{aligned} \tag{E.22}$$

Third power (n=3)

The last integral is $\mathcal{B}(3)$, given by

$$\begin{aligned}
\mathcal{B}(3) &= \int \frac{dk^-}{2\pi} \frac{(k^-)^3}{\Big[(1-z)k^- - (1-z)k_d^- + i\epsilon\Big]\ \Big[(1+z)k^- - (1+z)k_u^- - i\epsilon\Big]} \\
&\quad \times \frac{1}{\Big[k_D^+ k^- + C + i\epsilon\Big]^3\ \Big[k_D^+ k^- + E + i\epsilon\Big]}\ , \\
&= \int \frac{dk^-}{2\pi} \frac{k^-\ \Big[(k^- - k_u^-)\ (k^- - k_d^-) + (k_u^- + k_d^-)\ k^- - k_u^-\ k_d^-\Big]}{\Big[(1-z)k^- - (1-z)k_d^- + i\epsilon\Big]\ \Big[(1+z)k^- - (1+z)k_u^- - i\epsilon\Big]} \\
&\quad \times \frac{1}{\Big[k_D^+ k^- + C + i\epsilon\Big]^3\ \Big[k_D^+ k^- + E + i\epsilon\Big]}\ , \\
&= \int \frac{dk^-}{2\pi} \frac{k_D^+ k^- + E - E}{k_D^+(1-z^2)\Big[k_D^+ k^- + C + i\epsilon\Big]^3\ \Big[k_D^+ k^- + E + i\epsilon\Big]} + (k_u^- + k_d^-)\ \mathcal{B}(2) \\
&\quad -k_u^-\ k_d^- \mathcal{B}(1)\ , \\
&= \frac{1}{(1-z^2)} I_M^{(3)} - \frac{1}{2}\ \frac{E}{k_D^+(1-z^2)}\ \frac{\partial^2}{\partial C^2} I_M^{(2)} + (k_u^- + k_d^-)\ \mathcal{B}(2) - k_u^-\ k_d^- \mathcal{B}(1). \qquad \text{(E.23)}
\end{aligned}$$

where

$$\begin{aligned}
I_M^{(3)} &= \frac{1}{k_D^+} \int \frac{dk^-}{2\pi} \frac{1}{\Big[k_D^+ k^- + C + i\epsilon\Big]^3}\ , \\
&= -\frac{i}{2}\ \frac{\delta(k_D^+)}{k_D^+\ [C + i\epsilon]^2} \\
&= \frac{i}{2}\ \frac{\delta'(k_D^+)}{[C + i\epsilon]^2}\ , \qquad \text{(E.24)}
\end{aligned}$$

with $\frac{\delta(x)}{x} = -\delta'(x)$. Then one gets

$$\mathcal{B}(3) = \frac{i}{2(1-z^2)} \frac{\delta'(k_D^+)}{C^2} - \frac{1}{2} \frac{E}{k_D^+(1-z^2)} \frac{\partial^2}{\partial C^2} I_M^{(2)} + (k_u^- + k_d^-)\mathcal{B}(2) - k_u^-\ k_d^- \mathcal{B}(1)\,. \qquad \text{(E.25)}$$

In conclusion, the singular part of $\mathcal{C}_3$ is (cf equation (E.21))

$$\begin{aligned}
\mathcal{C}_3^S &= 3\ \mathcal{B}(3) - (1-v)\Big(\mu^2 - \Lambda^2\Big)\ \frac{\partial}{\partial E} \mathcal{B}(3) \\
&= \frac{i}{2(1-z^2)}\ \delta'(k_D^+)\ \Big\{3\ \Big[\frac{1}{C^2} - 2E\ \mathcal{S}_2(C,E)\Big] - 2(E-C)\Big[\mathcal{S}_2(C,E) + E\frac{\partial}{\partial E}\mathcal{S}_2(C,E)\Big]\Big\} \\
&\quad -\frac{i}{(1-z^2)}\ (k_u^- + k_d^-)\ \delta(k_D^+)\ \Big[3\mathcal{S}_2(C,E) - (1-v)(\mu^2 - \Lambda^2)\ \frac{\partial}{\partial E}\mathcal{S}_2(C,E)\Big\}\,, \qquad \text{(E.26)}
\end{aligned}$$

$$
\begin{aligned}
\mathcal{C}_3^S &= \frac{i}{2(1-z^2)}\,\delta'(k_D^+)\,\Big\{\frac{3}{C^2} - 2E\,\Big[3\mathcal{S}_2(C,E) + (E-C)\frac{\partial}{\partial E}\mathcal{S}_2(C,E)\Big] - 2(E-C)\mathcal{S}_2(C,E)\Big\} \\
&\quad +(k_u^- + k_d^-)\,\mathcal{C}_2^S \\
&= \frac{i}{2(1-z^2)}\,\delta'(k_D^+)\,\Big[\frac{3}{C^2} - \frac{2}{C^2} - 2(E-C)\mathcal{S}_2(C,E)\Big] + (k_u^- + k_d^-)\,\mathcal{C}_2^S \\
&= \frac{i}{2(1-z^2)}\,\delta'(k_D^+)\,\Big\{\frac{1}{C^2} - 2\frac{1}{(E-C)}\,\Big[\frac{1}{(E-C)}\,\ln\Big(\frac{E}{C}\Big) + \frac{(E-3C)}{2C^2}\Big]\Big\} \\
&\quad +\frac{2}{M}\,\frac{2z\gamma - s' + s + z(s'+s)}{(1-z^2)}\mathcal{C}_2^S \\
&= \frac{i}{(1-z^2)}\delta'(k_D^+)\frac{1}{(E-C)}\,\Big[\frac{1}{C} - \frac{1}{(E-C)}\ln\Big(\frac{E}{C}\Big)\Big] + \frac{2}{M}\frac{2z\gamma - s' + s + z(s'+s)}{(1-z^2)}\mathcal{C}_2^S \\
&= \frac{i}{(1-z^2)}\,\frac{4}{(v(1-v)M)^2}\,\frac{1}{(E-C)^2}\,\Big[\frac{(E-C)}{C} - \ln\Big(\frac{E}{C}\Big)\Big]\,\delta'(z'-z) \\
&\quad +2\,\frac{2z\gamma - s' + s + z(s'+s)}{(1-z^2)M}\,\mathcal{C}_2^S\,, \qquad \text{(E.27)}
\end{aligned}
$$

with

$$
\begin{aligned}
C &= \ell_D + (1-v)\Big(\mu^2 - \Lambda^2\Big)\,, \\
E &= \ell_D = -v(1-v)\Big(\gamma + zz'\frac{M^2}{4}\Big) - v^2 z' M^2/2 - v(\gamma' + \kappa^2) - (1-v)\mu^2\,, \\
\frac{\partial}{\partial k_D^+}\delta(k_D^+) &= \frac{4}{[M\ v(1-v)]^2}\,\Big[\frac{\partial}{\partial z'}\delta(z'-z)\Big]\,. \qquad \text{(E.28)}
\end{aligned}
$$

The singular functions $\mathcal{C}_2^S$ and $\mathcal{C}_3^S$,that are proportional to distributions such as $\delta(z'-z)$ or $\delta'(z'-z)$, are given in equation (E.22) and (E.27), respectively. It should be pointed out that ℓ_D, $\delta(k_D^+)$ and $\delta'(k_D^+)$ are even for the exchanges $z \to -z$ and $z' \to -z'$. Then by defining that

$$
\begin{aligned}
D_\ell &= \Big[\tilde{\ell}_D + (1-v)\Big(\mu^2 - \Lambda^2\Big)\Big]^2\,\tilde{\ell}_D\,, \\
\tilde{\ell}_D &= -v(1-v)\Big(\gamma + zz'\frac{M^2}{4}\Big) - v^2 z' M^2/2 - v(\gamma' + \kappa^2) - (1-v)\mu^2\Big|_{z'=z}\,, \\
&= -v(1-v)\Big(\gamma + z^2\frac{M^2}{4}\Big) - v^2 z M^2/2 - v(\gamma' + \kappa^2) - (1-v)\mu^2\,, \qquad \text{(E.29)} \\
\mathcal{D}_3^S &= \frac{1}{\Big[(1-v)\Big(\mu^2 - \Lambda^2\Big)\Big]^2}\,\Big[\frac{\partial}{\partial z'}\delta(z'-z)\Big] \\
&\quad \times \Big[\frac{(1-v)\Big(\mu^2 - \Lambda^2\Big)}{\Big[\ell_D + (1-v)\Big(\mu^2 - \Lambda^2\Big)\Big]} + \ln\Big\{\frac{\ell_D}{\Big[\ell_D + (1-v)\Big(\mu^2 - \Lambda^2\Big)\Big]}\Big\}\Big]\,. \qquad \text{(E.30)}
\end{aligned}
$$

we have the expression to the singular contribution that appears at $z' = z$ to $\mathcal{C}_2$ and $\mathcal{C}_3$:

$$\mathcal{C}_2^S = -\frac{i}{M}\,\frac{\delta(z'-z)}{v(1-v)(1-z^2)}\frac{2}{D_\ell} \tag{E.31}$$

$$\mathcal{C}_3^S = -\frac{i}{M}\frac{4}{M\ v(1-v)(1-z^2)}\left[\frac{\mathcal{D}_3^S}{v(1-v)} + \frac{\delta(z'-z)(2z\gamma - s' + s + z(s'+s))}{(1-z^2)\ D_\ell}\right] \tag{E.32}$$

In conclusion one has

$$\begin{aligned}\mathcal{L}_{ij}^S &= \frac{2}{M^2}\frac{(\mu^2-\Lambda^2)^2}{(1-z^2)}\int_0^1 dv\ v\ (1-v)\sum_l\ P_l \\ &\times \left\{\delta(z'-z)\ \frac{1}{D_\ell}\Big[F_{2;ij,l}(v,\gamma,z) + 2\frac{(2z\gamma - s' + s + z(s'+s))}{M\ (1-z^2)}F_{3;ij,l}(v,\gamma,z)\Big]\right. \\ &+ \left.\frac{2}{v(1-v)M}\ F_{3;ij,l}(v,\gamma,z)\ \mathcal{D}_3^S\right\}\,,\end{aligned} \tag{E.33}$$

with

$$\begin{aligned}F_{2;ij,l} &= \frac{M^2}{4}\left\{a_{ij,l}^2 + (1-v)b_{ij,l}^2 + (1-v)d_{ij,l}^0 + (1-v)\frac{M^2}{4}z\ d_{ij,l}^1\right\}\,, \\ F_{3;ij,l} &= (1-v)\ \frac{M^3}{8}\ d_{ij,l}^1\ .\end{aligned} \tag{E.34}$$

Appendix F - Normalization Condition

In this section, we obtain the normalization of the BS amplitude for a Fermion and anti-Fermion interacting system with a given Mass Function. The normalization condition to a bound-state is given by (LURIÉ *et al.*, 1965)

$$Tr\left(\left[\frac{\partial}{\partial p'^{\mu}}\int\frac{d^4k}{(2\pi)^4}\Big(S^{-1}(k-p'/2)\bar{\Psi}(k,p)S^{-1}(k+p'/2)\Psi(k,p)\Big)\right]_{p'=p}\right) = -i\ 2p_{\mu}\ , \tag{F.1}$$

where we should consider in our case that

$$\begin{aligned}
S^{-1}(k-p'/2) &= -i\Big((\not{k}-\not{p}'/2) - M(k_{\bar{q}}^2)\Big)\ ,\\
S^{-1}(k+p'/2) &= -i\Big((\not{k}+\not{p}'/2) - M(k_{q}^2)\Big)\ ,\\
\Psi(k,p) &= \sum_{i=1}^{4} S_i(k,p)\phi_i(k,p)\ ,\\
\bar{\Psi}(k,p) &= -S_1(k,p)\phi_1(k,p) + \sum_{i=2}^{4} S_i(k,p)\phi_i(k,p)\ ,
\end{aligned} \tag{F.2}$$

where ϕ_i are the Nakanishi functions, scalar functions of $(k^2, p^2, k\cdot p)$ with well-defined properties under the exchange $k\to -k$: even for $i=1,2,4$ and odd for $i=3$.

$$\begin{aligned}
\phi_i &= \int_{-1}^{1}\int_{0}^{\gamma'_f} dz'd\gamma' \frac{g_i(\gamma',z')}{[k^2+z'(k\cdot p)-\gamma'+i\epsilon]^3}\ ,\\
M(k_{\bar{q}}^2) &= m_0 - \frac{m^3}{(k-p'/2)^2-\lambda^2+i\epsilon}\ ,\\
M(k_{q}^2) &= m_0 - \frac{m^3}{(k+p'/2)^2-\lambda^2+i\epsilon}\ ,\\
S_1(k,p) &= \gamma^5\ ;\ S_2(k,p) = \frac{\not{p}}{M}\gamma^5\ ,\\
S_3(k,p) &= \frac{k\cdot p}{M^3}\not{p}\gamma^5 - \frac{\not{k}}{M}\gamma_5\ ,\ ;\ S_4(k,p) = \frac{i\sigma^{\mu\nu}p_{\mu}k_{\nu}}{M^2}\gamma^5\ .
\end{aligned} \tag{F.3}$$

After doing the derivative operation in equation (F.1) and multiplying p^μ in both sides of that equation, we will have

$$Tr\ A + Tr\ B = -i\ 2M_\pi^2, \tag{F.4}$$

with

$$\begin{aligned} Tr\ A = (-i)Tr\Bigg(\int \frac{d^4k}{(2\pi)^4}\Bigg(&-\not{p}/2 + \frac{m^3\big(k\cdot p - p^2/2\big)}{\big[(k-p/2)^2-\lambda^2+i\epsilon\big]^2}\Bigg) \\ &\times \bar{\Psi}(k,p)S^{-1}(k+p/2)\Psi(k,p)\Bigg), \\ Tr\ B = (-i)Tr\Bigg(\int \frac{d^4k}{(2\pi)^4}&S^{-1}(k-p/2)\bar{\Psi}(k,p) \\ &\times\left(\not{p}/2 - \frac{m^3\big(k\cdot p + p^2/2\big)}{\big[(k+p/2)^2-\lambda^2+i\epsilon\big]^2}\right)\Psi(k,p)\Bigg). \end{aligned} \tag{F.5}$$

In other to do the trace operation, we need to introduce in equation (F.4) the expression of the propagators and amplitudes present in equations (F.2) and (F.3). Then we have two ways of proceeding: do the trace operation considering or not the symmetry present when do exchange $k \to -k$. If we chose to calculate the trace without considering it we will to do the trace of the four parts present in equation (F.5). This will give us more work and more complicated terms to perform the integration in d^4k. The equation (F.4) will turn to be after the traces operation:

$$i\int \frac{d^4k}{(2\pi)^4}\left[\sum_{ij} a_{ij}^1\,(\phi_i\phi_j) + \sum_{ij} a_{ij}^2\,(\phi_i\phi_j)\right] = 1\ . \tag{F.6}$$

with the a_{ij}^1 and a_{ij}^2 coefficients being

$$\begin{aligned} &a_{11}^1 = 1\ ;\ a_{12}^1 = -\frac{\big[M(k_{\bar{q}}^2)+M(k_q^2)\big]}{M_\pi}\ ;\ a_{14}^1 = -4\mathcal{B}\ ;\ a_{22}^1 = 1\ ;\ a_{33}^1 = \mathcal{B}, \\ &a_{34}^1 = \frac{\big[M(k_{\bar{q}}^2)-M(k_q^2)\big]}{M_\pi}\mathcal{B}\ ;\ a_{44}^1 = \mathcal{B}\ \ ;\ a_{11}^2 = \frac{2}{M_\pi^2}(\mathcal{A}_pM(k_{\bar{q}}^2) - \mathcal{A}_mM(k_q^2)), \\ &a_{12}^2 = \frac{4(k\cdot p)}{M_\pi^3}\left(\mathcal{A}_m+\mathcal{A}_p\right) + \frac{2}{M_\pi}\left(\mathcal{A}_m-\mathcal{A}_p\right)\ ;\ a_{13}^2 = \frac{4\mathcal{B}}{M_\pi}\left(\mathcal{A}_m+\mathcal{A}_p\right), \\ &a_{22}^2 = \frac{2}{M_\pi^2}(\mathcal{A}_pM(k_{\bar{q}}^2) - \mathcal{A}_mM(k_q^2))\ ;\ a_{24}^2 = \frac{4\mathcal{B}}{M_\pi}\left(\mathcal{A}_p-\mathcal{A}_m\right), \\ &a_{33}^2 = -\frac{2\mathcal{B}}{M_\pi^2}(\mathcal{A}_pM(k_{\bar{q}}^2) - \mathcal{A}_mM(k_q^2))\ ;\ a_{34}^2 = \frac{4(k\cdot p)\mathcal{B}}{M_\pi^3}\left(\mathcal{A}_p-\mathcal{A}_m\right) - \frac{2\mathcal{B}}{M_\pi}\left(\mathcal{A}_m+\mathcal{A}_p\right), \\ &a_{44}^2 = -\frac{2\mathcal{B}}{M_\pi^2}(\mathcal{A}_pM(k_{\bar{q}}^2) - \mathcal{A}_mM(k_q^2)), \end{aligned} \tag{F.7}$$

where

$$\mathcal{B}(k^2) = \frac{1}{M_\pi^4}\left[(k\cdot p)^2 - M_\pi^2 k^2\right] , \tag{F.8}$$

$$\mathcal{A}_p(k,p) = \frac{m^3\left(k\cdot p + \frac{M_\pi^2}{2}\right)}{[(k+p/2)^2-\lambda^2+i\epsilon]^2} , \tag{F.9}$$

$$\mathcal{A}_m(k,p) = -\frac{m^3\left(k\cdot p - \frac{M_\pi^2}{2}\right)}{[(k-p/2)^2-\lambda^2+i\epsilon]^2} . \tag{F.10}$$

Now if chose the other way, from the four traces

$$\begin{aligned}
\mathcal{I}_1 =& \frac{i}{2}\, Tr\left(\not{p}\bar{\Psi}(k,p)S^{-1}(k+p/2)\Psi(k,p)\right)\\
\mathcal{I}_2 =& -\frac{i}{2}\, Tr\left(S^{-1}(k-p/2)\bar{\Psi}(k,p)\not{p}\Psi(k,p)\right)\\
\mathcal{I}_3 =& i\,\mathcal{A}_m\, Tr\left(\bar{\Psi}(k,p)S^{-1}(k+p/2)\Psi(k,p)\right)\\
\mathcal{I}_4 =& i\,\mathcal{A}_p\, Tr\left(S^{-1}(k-p/2)\bar{\Psi}(k,p)\Psi(k,p)\right)
\end{aligned}$$

we will have to truly calculate two of them, because if do the exchange $k \to -k$ in the traces $\mathcal{I}_2$ and $\mathcal{I}_4$ we obtain $\mathcal{I}_2(-k,p) = \mathcal{I}_1$ and $\mathcal{I}_4(-k,p) = \mathcal{I}_3$. Thus, after doing the trace operation we will have

$$\mathcal{I}_1 = M_\pi^2 \int \frac{d^4k}{(2\pi)^4} \sum_{ij} a_{ij}^1 \left(\phi_i\phi_j\right) , \tag{F.11}$$

$$\mathcal{I}_3 = M_\pi \int \frac{d^4k}{(2\pi)^4} \mathcal{A}_m \sum_{ij} a_{ij}^3 \left(\phi_i\phi_j\right) , \tag{F.12}$$

with

$$\begin{aligned}
&a_{11}^1 = 1 + 2\frac{k\cdot p}{M_\pi^2}\,;\, a_{12}^1 = a_{21}^1 = -2\frac{M(k_q^2)}{M_\pi}\,;\, a_{14}^1 = a_{41}^1 = -2\mathcal{B}\ ,\\
&a_{22}^1 = a_{11}^1\,;\, a_{23}^1 = a_{32}^1 = -a_{14}^1\,;\, a_{33}^1 = \left(1 + 2\frac{k\cdot p}{M_\pi^2}\right)\mathcal{B}\ ,\\
&a_{34}^1 = a_{43}^1 = -2\frac{M(k_q^2)}{M_\pi}\mathcal{B}\,;\, a_{44}^1 = a_{33}^1\ ,\\
&a_{11}^3 = 4\frac{M(k_q^2)}{M_\pi}\,;\, a_{12}^3 = \ a_{21}^3 = -2\left(1 + 2\frac{k\cdot p}{M_\pi^2}\right)\,;\, a_{13}^3 = \ a_{31}^3 = -4\mathcal{B}\ ,\\
&a_{22}^3 = a_{11}^3\,;\, a_{24}^3 = \ a_{42}^3 = -a_{13}^3\,;\, a_{33}^3 = -4\frac{M(k_q^2)}{M_\pi}\mathcal{B}\ ,\\
&a_{34}^3 = a_{43}^3 = 2\left(1 + 2\frac{k\cdot p}{M_\pi^2}\right)\mathcal{B}\,;\, a_{44}^3 = \ a_{33}^3\ ,
\end{aligned} \tag{F.13}$$

Therefore the normalization reads

$$i\int\frac{d^4k}{(2\pi)^4}\sum_{ij}a^1_{ij}\phi_i\phi_j+i\int\frac{d^4k}{(2\pi)^4}\frac{\mathcal{A}_m}{M_\pi}\sum_{ij}a^3_{ij}\phi_i\phi_j=1\ , \tag{F.14}$$

that is a easier expression to calculate than equation (F.6). To obtain an expression ready to be numerically implemented we need to do the Feynman parametrization and after do the four-dimensional integration in dk^-. Thus, after doing the mentioned steps we have the following expression to the normalization:

$$\begin{aligned}1 &= -\frac{3N_c}{32\,\pi^2}\int_{-1}^{1}dz'\int_0^\infty d\gamma'\int_{-1}^{1}dz\int_0^\infty d\gamma\int_0^1 dv\,v^2\\ &\quad\times\left\{T_1+\frac{8\,m^3}{M}\int_0^{1-v}du\,u^2\Big[T_2+30\,m^3\,M\int_0^{1-v-u}w\,dw\,T_3\Big]\right\}\end{aligned} \tag{F.15}$$

with

$$\begin{aligned}T_1 &= \frac{(1-v)^2}{t_1^3}\left(\frac{G(1;2)-4(m_0/M)\mathcal{G}_{12}}{t_1}+\frac{G(3;4)-4\,\mathcal{G}_{14}}{2\,M^2}\right),\\ T_2 &= \frac{1}{t_2^4}\Bigg(\frac{3(2-v-u)}{4\,M^2}\,\mathcal{G}_{34}-\frac{4(2-v-u)\,\mathcal{G}_{12}}{2\,t_2}\\ &\quad-\frac{3(1-v-u)}{2\,t_2}\big(2(1+\lambda_2)(\mathcal{G}_{13}-\mathcal{G}_{24})+(m_0/M)(1+\lambda_2)G(3;4)-(1-\lambda_2^2)\mathcal{G}_{34}\big)\\ &\quad+\frac{5\,M^2}{t_2^2}(1-v-u)\Big((m_0/M)\,(1+\lambda_2)\,G(1;2)-(1-\lambda_2^2)\,\mathcal{G}_{12})\Big)\Bigg),\\ T_3 &= \frac{(1+\lambda_3)}{t_3^6}\left(\frac{G(1;2)}{t_3}-\frac{G(3;4)}{4\,M^2}\right),\end{aligned} \tag{F.16}$$

where we have

$$\begin{aligned}&\lambda_1=v\,z'+(1-v)\,z\\ &\lambda_2=-1+u\,(1+z)+v\,(1+z')\\ &\lambda_3=1-2\,w-u\,(1-z)-v\,(1-z')\\ &t_1=(1-v)\,\gamma+v\,\gamma'+\kappa^2+\frac{M^2}{4}\,\lambda_1^2\\ &t_2=u\,\gamma+v\,\gamma'+(u+v)\,\kappa^2+(1-u-v)\left(\lambda^2-\frac{M^2}{4}\right)+\frac{M^2}{4}\,\lambda_2^2\\ &t_3=u\,\gamma+v\,\gamma'+(u+v)\,\kappa^2+(1-u-v)\left(\lambda^2-\frac{M^2}{4}\right)+\frac{M^2}{4}\,\lambda_3^2\\ &\mathcal{G}_{ij}(\gamma,z,\gamma',z')=g_i(\gamma,z)\,g_j(\gamma',z')\\ &G(1;2)=\mathcal{G}_{11}(\gamma,z,\gamma',z')+\mathcal{G}_{22}(\gamma,z,\gamma',z')\\ &G(3;4)=\mathcal{G}_{33}(\gamma,z,\gamma',z')+\mathcal{G}_{44}(\gamma,z,\gamma',z')\end{aligned} \tag{F.17}$$

Appendix G - Electromagnetic Form Factor

In order to calculate the Electromagnetic Form Factor of the pion, we will consider the quark-photon vertex where the quark propagator is given by the following expression

$$S^{-1}(k) = -i\Big(\not{k} - M(k^2)\Big) \tag{G.1}$$

$$M(k^2) = m_0 - \frac{m^3}{k^2 - \lambda^2 + i\epsilon}, \tag{G.2}$$

with $M(k^2)$ is a running mass fitted to lattice QCD calculations.

The pion-photon vertex is given by

$$-i\Gamma^{\mu}_{\pi}(P, P'; q) \equiv < \pi(P')|J^{\mu}|\pi(P) >= (P + P')^{\mu} F_{\pi}(Q^2) \tag{G.3}$$

where $Q^2 = -q^2$, $|\pi(P) >$ is the pion state and J^{μ} the electromagnetic current operator. Besides, in the impulse approximation, the meson-photon vertex is written as

$$\Gamma^{\mu}_{\pi^+}(P, P'; q) = \tilde{Q}_u \Gamma^{\mu}_{\pi^+,u}(P, P'; q) + \tilde{Q}_{\bar{d}} \Gamma^{\mu}_{\pi^+,\bar{d}}(P, P'; q) \tag{G.4}$$

with $\tilde{Q}_u$ and $\tilde{Q}_{\bar{d}}$ are the electromagnetic charges. One important detail is to have Γ^{μ}_{π} which satisfies the Ward-Takahashi identity

$$q_{\mu}\Gamma^{\mu}_{\pi}(p', p, q) = S_F^{-1}(p') - S_F^{-1}(p) \tag{G.5}$$

considering the expression to the propagator given in ((G.1)). It is important to take in consideration the equation (7.69) of Peskin (PESKIN; SCHROEDER, 1995), where the Ward-Takahashi identity have a $\Gamma^{\mu} \to -i\Gamma^{\mu}$. Thus, considering the income photon momenta $q_{\mu} = p'_{\mu} - p_{\mu}$, we will have

$$\Gamma^{\mu}_{\pi}(p_f, p_i, q) = i\left[\gamma^{\mu} - \left(\frac{m^3(p_f + p_i)^{\mu}}{(p_f^2 - \lambda^2 + i\epsilon)(p_i^2 - \lambda^2 + i\epsilon)}\right)\right]. \tag{G.6}$$

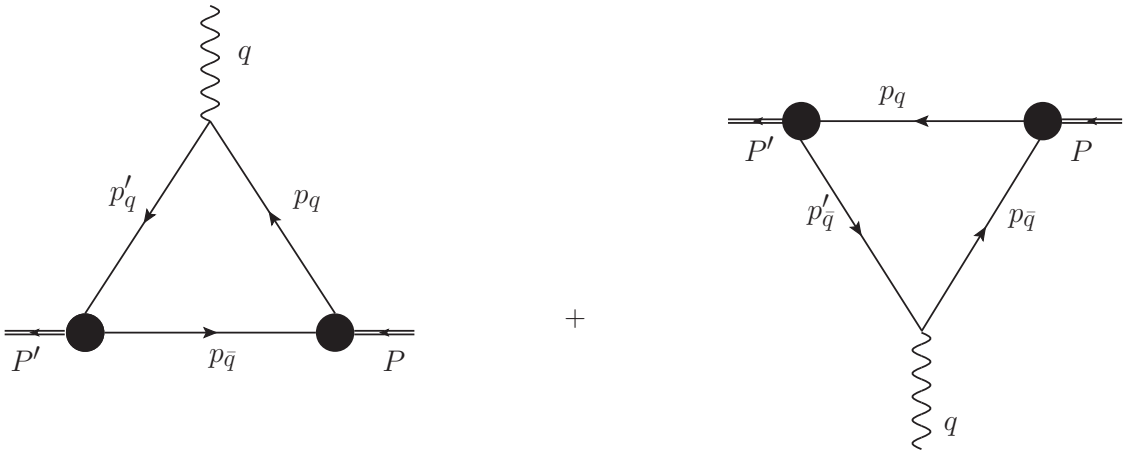

FIGURE G.1 – Pictorial representation of the pion electromagnetic form factor, in one-loop approximation. The full dots represents the vertex functions for the initial and final bound states, respectively.

One can write

$$< qq|J^{\mu}(x)|qq > = i \int d^4y_1 \int d^4y_2 \int d^4x_1 \int d^4x_2 \times \bar{\chi}(y_1, y_2)\ K^{\mu}(x; y_1, y_2, x_1, x_2)\ \chi(x_1, x_2) \tag{G.7}$$

where χ and $\bar{\chi}$ are the BS amplitude of the bound state. Where $K^{\mu}(x; y_1, y_2, x_1, x_2)$ in terms of the he photon-fermion vertex $\Gamma^{\mu}_{(i)}(x)$:

$$K^{\mu}(x; y_1, y_2, x_1, x_2) = \Gamma^{\mu}_{(1)}(x) S^{-1}_{(2)}(y_2 - x_2) + \Gamma^{\mu}_{(2)}(x) S^{-1}_{(1)}(y_1 - x_1)\,. \tag{G.8}$$

By looking at Fig. G.1, in the first graph the relations of 4-momentum conservation given by

$$P' = P + q\ , \quad k' = k + \frac{q}{2} \quad p_q = \frac{P}{2} + k\ , \quad p_{\bar{q}} = k - \frac{P}{2}\ , \quad p'_{\bar{q}} = k + q + \frac{P}{2} \tag{G.9}$$

In the second contribution we have

$$P' = P + q\ , \quad k'' = k - \frac{q}{2}\ , \quad p_q = k'' + \frac{P'}{2}\ , \quad p_{\bar{q}} = k - \frac{P}{2}\ , \quad p'_{\bar{q}} = k'' - \frac{P'}{2} \tag{G.10}$$

Then the *fermion-antifermion* matrix elements are given by the following expression

$$
\begin{aligned}
< q\bar{q}|J^{\mu}(q)|q\bar{q} > &= i\int \frac{d^4k}{(2\pi)^4}\left\{ Tr\Big[C\ S^{-1}(k-P/2)\ \bar{\Phi}(k',P')\ \Gamma^{\mu}_{u}(q)\Psi(k,P)\Big]\right. \\
&\left. +Tr\Big[[\Gamma^{\mu}_{\bar{d}}(q)]^{T}\ C\ \bar{\Phi}(k'',P')\ S^{-1}(k+P/2)\Psi(k,P)C^{-1}C\Big]\right\} = \\
&= i\int \frac{d^4k}{(2\pi)^4}\left\{ Tr\Big[S^{-1}(k-P/2)\ \bar{\Phi}(k',P')\ \Gamma^{\mu}_{u}(q)\ \Phi(k,P)\ C^{2}\Big]\right. \\
&\left. +\ Tr\Big[C^{2}\ \widehat{\Gamma}^{\mu}_{\bar{d}}(q)\ \bar{\Phi}(k'',P')\ S^{-1}(k+P/2)\ \Phi(k,P)\Big]\right\} = \\
&= -i\int \frac{d^4k}{(2\pi)^4}\left\{ Tr\Big[S^{-1}(k-P/2)\ \bar{\Phi}(k',P')\ \Gamma^{\mu}_{u}(q)\Phi(k,P)\Big]\right. \\
&\left. +Tr\Big[\ \widehat{\Gamma}^{\mu}_{\bar{d}}(q)\ \bar{\Phi}(k'',P')\ S^{-1}(k+P/2)\Phi(k,P)\Big]\right\}, \qquad \text{(G.11)}
\end{aligned}
$$

where $C = i\gamma^2\gamma^0$ and $C^2 = -\mathrm{I}$ has been used. We also have considered the following relations

$$
\begin{aligned}
\widehat{\Gamma}^{\mu}(q) &= C^{-1}\,[\Gamma^{\mu}(q)]^{T}\ C\ ;\ S^{T}(p) = C\ S(-p)\ C^{-1} \\
C^{-1}\bar{\Psi}(k',P') &= \bar{\Phi}(k',P')\ ;\ \Psi(k,P)\ C^{-1} = \Phi(k,P)\,.
\end{aligned}
$$

Furthermore, the expressions of the photon-fermion vertex are

$$
\Gamma^{\mu}_{u}(q) = i\ e_u\ \left(\gamma^{\mu} - \frac{m^3(2k+q+P)^{\mu}}{((k+q+\frac{P}{2})^2-\lambda^2+i\epsilon)((k+\frac{P}{2})^2-\lambda^2+i\epsilon)}\right), \qquad \text{(G.12)}
$$

$$
\Gamma^{\mu}_{\bar{d}}(q) = i\ e_{\bar{d}}\ \left(\gamma^{\mu} - \frac{m^3(k''-\frac{P'}{2}+k-\frac{P}{2})^{\mu}}{((k''-\frac{P'}{2})^2-\lambda^2+i\epsilon)((k-\frac{P}{2})^2-\lambda^2+i\epsilon)}\right). \qquad \text{(G.13)}
$$

In the last to $\widehat{\Gamma}^{\mu}$ one has

$$
\widehat{\Gamma}^{\mu}_{u(\bar{d})} = -i\ e_{u(\bar{d})}\left(\gamma^{\mu} + \frac{m^3(p_f+p_i)^{\mu}}{(p_f^2-\lambda^2+i\epsilon)(p_i^2-\lambda^2+i\epsilon)}\right) \qquad \text{(G.14)}
$$

Therefore the matrix element for the elastic case is

$$
\begin{aligned}
< q\bar{q}|J^{\mu}(q)|q\bar{q} > \;\; = \;\; & -iN_c \int \frac{d^4k}{(2\pi)^4} \left\{ \frac{2}{3}\, Tr\Bigg[(\not{k} - \not{P}/2 - M(k_{\bar{q}}^2))\; \bar{\Phi}(k', P') \right. \\
& \times \left(\gamma^{\mu} - \frac{m^3 (2k+q+P)^{\mu}}{((k+q+\frac{P}{2})^2 - \lambda^2 + i\epsilon)((k+\frac{P}{2})^2 - \lambda^2 + i\epsilon)} \right) \Phi(k,P) \Bigg] \\
& -\frac{1}{3}\; Tr\Bigg[\left(\gamma^{\mu} + \frac{m^3 (k'' - \frac{P'}{2} + k - \frac{P}{2})^{\mu}}{((k'' - \frac{P'}{2})^2 - \lambda^2 + i\epsilon)((k - \frac{P}{2})^2 - \lambda^2 + i\epsilon)} \right) \\
& \left. \times \bar{\Phi}(k'', P')\; (\not{k} + \not{P}/2 - M(k_q^2)) \Phi(k,P) \Bigg] \right\}, \qquad \text{(G.15)}
\end{aligned}
$$

which can also be expressed in terms of a form factor

$$
< q\bar{q}|J^{\mu}(q)|q\bar{q} >= (P' + P)^{\mu} F(Q^2)\,, \qquad \text{(G.16)}
$$

with $Q^2 = -q^2$. Hence, by using the equations (G.15) and (G.16) and multiplying $(P' + P)_{\mu}$ we have

$$
\begin{aligned}
(P'+P)^2 F(Q^2) \;\; = \;\; & -iN_c \int \frac{d^4k}{(2\pi)^4} \left\{ \frac{2}{3}\, Tr\Bigg[(\not{k} - \not{P}/2 - M(k_{\bar{q}}^2))\; \bar{\Phi}(k', P') \right. \\
& \times \left((P'+P)_{\mu}\gamma^{\mu} - \frac{m^3 (P'+P)_{\mu}(2k+q+P)^{\mu}}{((k+q+\frac{P}{2})^2 - \lambda^2 + i\epsilon)((k+\frac{P}{2})^2 - \lambda^2 + i\epsilon)} \right) \Phi(k,P) \Bigg] \\
& -\frac{1}{3} Tr\Bigg[\left((P'+P)_{\mu}\gamma^{\mu} + \frac{m^3 (P'+P)_{\mu}(k'' - \frac{P'}{2} + k - \frac{P}{2})^{\mu}}{((k'' - \frac{P'}{2})^2 - \lambda^2 + i\epsilon)((k - \frac{P}{2})^2 - \lambda^2 + i\epsilon)} \right) \\
& \left. \times \bar{\Phi}(k'', P')\; (\not{k} + \not{P}/2 - M(k_q^2)) \Phi(k,P) \Bigg] \right\} \qquad \text{(G.17)}
\end{aligned}
$$

where $(P'+P)^2 = 4M^2\;(1+\tau)$ with $\tau = \frac{Q^2}{4M^2}$. The Form Factor expression that we obtain is

$$
\begin{aligned}
F(Q^2) \;\; = \;\; & \frac{-iN_c}{4M^2\;(1+\tau)} \int \frac{d^4k}{(2\pi)^4} \left\{ \frac{2}{3}\, Tr\Bigg[(\not{k} - \not{P}/2 - M(k_{\bar{q}}^2))\; \bar{\Phi}(k', P') \right. \\
& \times \left((P'+P)_{\mu}\gamma^{\mu} - \frac{m^3 (P'+P)_{\mu}(2k+q+P)^{\mu}}{((k+q+\frac{P}{2})^2 - \lambda^2 + i\epsilon)((k+\frac{P}{2})^2 - \lambda^2 + i\epsilon)} \right) \Phi(k,P) \Bigg] \\
& -\frac{1}{3} Tr\Bigg[\left((P'+P)_{\mu}\gamma^{\mu} + \frac{m^3 (P'+P)_{\mu}(k'' - \frac{P'}{2} + k - \frac{P}{2})^{\mu}}{((k'' - \frac{P'}{2})^2 - \lambda^2 + i\epsilon)((k - \frac{P}{2})^2 - \lambda^2 + i\epsilon)} \right) \\
& \left. \times \bar{\Phi}(k'', P')\; (\not{k} + \not{P}/2 - M(k_q^2)) \Phi(k,P) \Bigg] \right\}. \qquad \text{(G.18)}
\end{aligned}
$$

Where we have then two traces to calculate:

$$\begin{aligned}
\mathcal{I}_1 &= \int \frac{d^4k}{(2\pi)^4} Tr\Bigg[(\not{k} - \not{P}/2 - M(k_{\bar{q}}^2))\ \bar{\Phi}(k', P') \\
&\quad \times \left((P'+P)_\mu \gamma^\mu - \frac{m^3 (P'+P)_\mu (2k+q+P)^\mu}{((k+q+\frac{P}{2})^2 - \lambda^2 + i\epsilon)((k+\frac{P}{2})^2 - \lambda^2 + i\epsilon)} \right) \Phi(k,P) \Bigg] \\
\mathcal{I}_2 &= \int \frac{d^4k}{(2\pi)^4} Tr\Bigg[\left((P'+P)_\mu \gamma^\mu + \frac{m^3 (P'+P)_\mu (k'' - \frac{P'}{2} + k - \frac{P}{2})^\mu}{((k''-\frac{P'}{2})^2 - \lambda^2 + i\epsilon)((k-\frac{P}{2})^2 - \lambda^2 + i\epsilon)} \right) \\
&\quad \times \bar{\Phi}(k'', P')\ (\not{k} + \not{P}/2 - M(k_q^2)) \Phi(k,P) \Bigg]
\end{aligned} \tag{G.19}$$

We can demonstrate that if do $k \to -k$ one has $k' \to -k''$, the result of calculating $\mathcal{I}_2$ will be equal to $-\mathcal{I}_1$. To demonstrate that we should consider how each term of the Form Factor expression in equation (G.18) reacts to that changes. First let us consider the BS amplitudes. To a 0^+ state they are written as (CARBONELL; KARMANOV, 2010)

$$\begin{aligned}
\Phi(k,p) &= S_1\phi_1 + S_2\phi_2 + S_3\phi_3 + S_4\phi_4\,, \\
\bar{\Phi}(k,p) &= \gamma^0 \Phi^\dagger(k,p;+i\epsilon)\gamma^0 = -S_1\phi_1 + S_2\phi_2 + S_3\phi_3 + S_4\phi_4\,.
\end{aligned} \tag{G.20}$$

where

$$S_1 = \gamma_5 \quad ; \quad S_2 = \frac{\not{p}}{M}\ \gamma_5 \quad ; \quad S_3 = \frac{k\cdot p}{M^3}\not{p}\ \gamma_5 - \frac{\not{k}}{M}\gamma_5 \quad ; \quad S_4 = \frac{i}{M^2}\sigma^{\mu\nu} p_\mu k_\nu\ \gamma_5 \tag{G.21}$$

with $\sigma_{\mu\nu} = \frac{i}{2}(\gamma_\mu\gamma_\nu - \gamma_\nu\gamma_\mu)$. Regarding to the basis, note that S_1 and S_2 does not depend on k. But if we do $k \to -k$, the others one that has k dependence behave as:

$$S_3(-k,p) = -S_3(k,p) \quad , \quad S_4(-k,p) = -S_4(k,p)\,. \tag{G.22}$$

The antisymmetry of the BS amplitude with respect to permutation of two fermions implies:

$$\begin{aligned}
\phi_i(-k,p) &= \phi_i(k,p) \quad \text{for i =1,2,4} \\
\phi_3(-k,p) &= -\phi_3(k,p)\,.
\end{aligned} \tag{G.23}$$

We can relate $M(k_{\bar{q}}^2)$ and $M(k_q^2)$ as:

$$M(k_{\bar{q}}^2)_{k\to -k} = M(k_q^2)\,. \tag{G.24}$$

The relations present in equation (G.9) and (G.10) give us that when we do $k \to -k$

it is equal to do $k' \to -k''$. Thus we have that by doing $k \to -k$ we obtain

$$\left.\frac{m^3(P'+P)_\mu(-2k+q+P)^\mu}{((-k+q+\frac{P}{2})^2-\lambda^2+i\epsilon)((-k+\frac{P}{2})^2-\lambda^2+i\epsilon)}\right|_{k\to -k} = \frac{m^3(P'+P)_\mu(k''-\frac{P'}{2}+k-\frac{P}{2})^\mu}{((k''-\frac{P'}{2})^2-\lambda^2+i\epsilon)((k-\frac{P}{2})^2-\lambda^2+i\epsilon)}$$

Furthermore, considering that

$$\begin{aligned}\Phi^{J^\pi}(-k,p) &= C\ \left[\Phi^{J^\pi}(k,p)\right]^T\ C^{-1}\\ \bar{\Phi}^{J^\pi}(-k,p) &= C\left[\bar{\Phi}^{J^\pi}(k,p)\right]^T C^{-1}\end{aligned} \tag{G.25}$$

one has

$$\begin{aligned}\mathcal{I}_2 &= \int \frac{d^4k}{(2\pi)^4} Tr\Bigg[\left((P'+P)_\mu\gamma^\mu + \frac{m^3(P'+P)_\mu(2k+q+P)^\mu}{((k+q+\frac{P}{2})^2-\lambda^2+i\epsilon)((k+\frac{P}{2})^2-\lambda^2+i\epsilon)}\right)\\ &\quad\times\bar{\Phi}(-k',P')\ (-\not{k}+\not{P}/2-M(k_{\bar{q}}^2))\Phi(-k,P)\Bigg]\\ &= \int \frac{d^4k}{(2\pi)^4} Tr\Bigg[\left((P'+P)_\mu\gamma^\mu + \frac{m^3(P'+P)_\mu(2k+q+P)^\mu}{((k+q+\frac{P}{2})^2-\lambda^2+i\epsilon)((k+\frac{P}{2})^2-\lambda^2+i\epsilon)}\right)\\ &\quad\times\bar{\Phi}(-k',P')\ (-\not{k}+\not{P}/2-M(k_{\bar{q}}^2))C\ \ [\Phi(k,p)]^T\ C^{-1}\Bigg]\\ &= -\int \frac{d^4k}{(2\pi)^4} Tr\Bigg[\left((P'+P)_\mu\gamma^\mu - \frac{m^3(P'+P)_\mu(2k+q+P)^\mu}{((k+q+\frac{P}{2})^2-\lambda^2+i\epsilon)((k+\frac{P}{2})^2-\lambda^2+i\epsilon)}\right)\\ &\quad\times\bar{\Phi}(k',P')(\not{k}-\not{P}/2-M(k_{\bar{q}}^2))\Phi(k,p)\Bigg],\end{aligned} \tag{G.26}$$

Thus, we can write the Form Factor expression as

$$\begin{aligned}F(Q^2) &= \frac{-iN_c}{4M^2\ (1+\tau)}\int\frac{d^4k}{(2\pi)^4}\ Tr\Bigg[(\not{k}-\not{P}/2-M(k_{\bar{q}}^2))\ \bar{\Phi}(k',P')\Bigg((P'+P)_\mu\gamma^\mu\\ &\quad-\frac{m^3(P'+P)_\mu(2k+q+P)^\mu}{((k+q+\frac{P}{2})^2-\lambda^2+i\epsilon)((k+\frac{P}{2})^2-\lambda^2+i\epsilon)}\Bigg)\Phi(k,P)\Bigg].\end{aligned} \tag{G.27}$$

FOLHA DE REGISTRO DO DOCUMENTO

1. CLASSIFICAÇÃO/TIPO	2. DATA	3. DOCUMENTO Nº	4. Nº DE PÁGINAS
TD	31 de Julho de 2023	DCTA/ITA/TD-027/2023	135

5. TÍTULO E SUBTÍTULO:

0^- BOUND STATE WITH DRESSED QUARK PROPAGATORS IN MINKOWSKI SPACE

6. AUTORA(ES):

Abigail Rodrigues Castro

7. INSTITUIÇÃO(ÕES)/ÓRGÃO(S) INTERNO(S)/DIVISÃO(ÕES):

Instituto Tecnológico de Aeronáutica – ITA

8. PALAVRAS-CHAVE SUGERIDAS PELA AUTORA:

Dressed Quark Propagator; Bound-State; Bethe-Salpeter Equation; Valence Momentum Distributions.

9. PALAVRAS-CHAVE RESULTANTES DE INDEXAÇÃO:

Matéria de Quark; Espaço de Minkowski; Propagadores; Equação de Bethe-Salpeter; Cronodinâmica quântica; Física de partículas; Física.

10. APRESENTAÇÃO: (X) **Nacional** ( ) **Internacional**

ITA, São José dos Campos. Curso de Doutorado. Programa de Pós-Graduação em Física. Área de Física Nuclear. Orientador: Prof. Dr. Wayne Leonardo de Paula. Defesa em 28/07/2023. Publicada em 2023.

11. RESUMO:

This work analyzes the effect of dressing the quark propagator in the bound state formation in Minkowski space. The Bethe-Salpeter equation is solved, for a 0^- fermion-antifermion bound state interacting through a vector boson exchange in the ladder approximation, using a dressed quark propagator with a phenomenological running mass function fitted to Lattice QCD calculations. The developed model contains three gluonic scales: the effective gluon mass $\sim \Lambda_{QCD}$, the size of the extended quark-gluon vertex ~ 2 fm, and the dressing of the quark propagator. Static and dynamical quantities that characterize the bound state are calculated and the effects of those scales in the dynamics of the bound system are discussed. In special, for the light quark mass case, a change of hierarchy between the coupling constant of the running quark mass model and of the fixed mass case is seen as the value of bound state mass M varies. The running mass coupling constant slower increase when compared with the increase of the fixed mass model coupling constant with the binding growth reflects the interplay between the three gluonic scales. The light-front amplitudes and the longitudinal and transverse valence momentum distributions are analyzed for two different bound state masses, $M = 653$ MeV and $M = 447$ MeV, with or without dressing effects. It is shown that, in the quark dressing model, those momentum distributions decay slower for high transverse momentum when compared to the case of an undressed one with a fixed quark mass equal to the Infrared mass of 344 MeV. In particular, either for the fixed mass model or running mass function model, the aligned spin component of the valence wave function is suppressed with respect to the anti-aligned one.

12. GRAU DE SIGILO:

(**X**) **OSTENSIVO** ( ) **RESERVADO** ( ) **SECRETO**